Investigation of Demand Response Potential in Smart Grids

A DISSERTATION SUBMITTED
TO THE GRADUATE DIVISION OF THE
UNIVERSITY OF HAWAIʻI AT MĀNOA IN PARTIAL FULFILLMENT OF
THE REQUIREMENTS FOR THE DEGREE OF

DOCTOR OF PHILOSOPHY
IN
ELECTRICAL ENGINEERING

June 2022

By

Foad Najafi

Dissertation Committee:
Matthias Fripp, Chairperson
Reza Ghorbani
Olga Borić-Lubecke
Michael J. Roberts
June Zhang

Keywords: Market Bidding, Electric Water Heater, MILP, PV, Optimization

To my parents for their never-ending support

ACKNOWLEDGMENT

I would like to express my gratitude to my advisor, Dr. Matthias Fripp, that I have been his Ph.D. throughout my studies at UH Manoa. I gained invaluable knowledge in these years that will help me in my future endeavors. One of the most remarkable experiences I had working with Matthias was being free to explore the unknown and new possibilities and moving forward at my own pace. I was free to cooperate with other entities and gain new experiences with them.

A special thank you to Dr. Lubecke. I had the honor of having Olga throughout all of my Ph.D. exams. Her comment helped me improve this work and develop new methodologies. Chapter two of this work was formed initially based on a suggestion from Dr. Lubecke on my comprehensive exam.

I would like to give a special thanks to Dr. Ghorbani. Reza was present throughout this journey with me. His ability to listen and find new and creative solutions amazes me every time. His vision of the future, alongside his creativity and deep understanding of the problems, make him an exceptional researcher.

I want to thank Dr. Roberts. Being a great economist, I was lucky that I could benefit from his point of view and comments to improve my research.

Dr. Zhang was on this committee on concise notice in the comprehensive exam. Given that her field of work is close to the works in this thesis, her judgment is critical for this work.

I would like to thank the folks in East-West Center. The staffs here are super friendly and supportive. Being a resident of EWC was one of the most incredible experiences that I had. Meeting new people from different cultures and different parts of the world and finding lifelong friends.

Also, I would like to thank my mom (Eshrat) and dad (Daryoush), who has been with me throughout every step. They encourage me to move forward and do my best to succeed in what I love to do.

Also, I would like to thank my brother Farshad who is always beside me in any direction that I move into.

I would like to thank my friends, who I could count on this journey. The last two years were very hard for all of us. Being able to connect with friends was a blessing, even remotely. Especially Saman, my study partner, camping buddy, roommate, and a great friend. Last but not least, I was lucky to have Meysam, a great friend who was always for me and a great human.

ABSTRACT

21st-century power systems are being exposed to many new challenges and opportunities at the same time. Climate change and the increasing cost of fossil fuels force us to replace our primary source of energy with renewables. At the same time, new communication technologies such as 5G paves the way for two-way communication between the generation side and the demand side. The two-way communication between two sides provides numerous advantages for the modern power systems to tackle the environmental and economic challenges with new and creative innovations.

One of the new ideas that are conceptualized after the emergence of two-way communication between generation and consumption is the demand response (DR). The DR can help us to overcome these challenges in parallel with other technologies such as energy storage systems. The DR program can help improve any objective that we pursue in the power systems. They can help to reduce the operation cost of power systems by redistributing their consumption plans to the times that less energy consumption is expected. They can help to incorporate more renewable energy sources into power systems. Since renewables are not dispatchable, the current power systems structure has difficulty incorporating a larger share of renewables into power systems due to their unpredictable nature. However, demand-responsive loads can alleviate this problem by adapting their consumption plans based on the generation side with a large share of renewables. The DR program can help reduce the capital cost of power system expansion. Each year, governments are forced to build new infrastructure so only to accommodate the annual peak increase that just happens for a couple of days each year. However, with the adaptive demand that could be used to curb the

peak load, millions could be saved by reducing the need to build new infrastructures that are built to meet the peak demand. The DR program can help to improve power quality and operational costs. The unit commitment problems are armed with demand-responsive loads, much lower operational cost, and better power quality at the same time.

While there are various types of demand control, such as direct load control (DLC), the focus of this research is on price responsive demand (PRD). The PRDs are more advantageous to DLC for various reasons. One reason is the possible discomfort that DLC approaches could bring. I.e., the service could cut off for the user when the user needs energy. However, with the PRD, the user simply pays the higher cost for using the service. Another main advantage that PRD control has over the DLC is the possibility of creating a market. With the two-way communication that is available, the loads can participate in the markets. E.g., currently, there is a surplus of solar production at midday. However, the PRDs could be used to increase their consumption in the middle of the day by responding to the low cost of electricity in those times. They can participate in ancillary services such as frequency and voltage provisioning based on the needs of the market (operator here) and reduce the cost for the user.

Given these opportunities the PRDs have, this thesis is focused on exploring the new opportunities that this program can bring to reality. In the literature, appliances are categorized roughly into three main categories: non-shiftable such as TVs, shiftable such EVs, and thermostatically controller appliances TCAs) such as Electric Water Heaters (EWH).

There have been many studies to evaluate the potential of shiftable appliances such as EVs. However, due to temperature drop of TCAs, and the relationship between working

temperature and the ambient temperatures, the potentials of TCAs as a reliable PRD is not investigated. Among the TCAs, the EWH have the most potentials to be successfully used in DR programming. They have relatively good insulation and can keep the energy for hours. In contrast, HVAC appliances (heating, ventilation, and air conditioning) cannot maintain their temperature for a long time and need to be fed by energy in short periods of time. At the same time, EWH are a large consumer of energy (some sources report up to 40 percent of daily energy usage). These characteristics makes EWHs a good choice for DR programming. The first two section of this thesis is focused on the potential of EWH as a PRD.

First capture investigates the effect unpredictability of energy usage for scheduling the EWHs. alongside that, a new approach to model the concept of comfort is introduced. Accurate Scheduling of appliances needs accurate estimation of environmental inputs. However, a 100 accurate prediction is not feasible. To tackle the uncertainty in prediction of variables, researchers proposed to main approaches to deal with uncertainly. One of them is robust optimization and the other stochastic optimization. In the first chapter of the thesis, a stochastic optimization model is proposed to deal with the randomness of user hot water withdrawal. Alongside that, a dual objective model where one of the objectives is the newly conceptualized discomfort cost. Together, the dual objective comfort-based approach combined with stochastic approach, improves the decision-making procedure by a large margin. The propose model proves that is more accurate at prediction user consumption and at the same time, it incurs less discomfort to the user.

Chapter two investigates the potential of EWH as solar energy self-absorbing unit. As mentioned before, solar energy production is concentrated mostly on the middle of the day and no production on other times. However, until now, no effective mechanism is used to

absorb this excess energy to the grid. An alternative method is the use of batteries as a storage. However, batteries are expensive as of today. An alternative method is increasing solar energy absorption by inducing demand in appliances. One of the best appliances for this matter is the EWHs. due to their large working temperature range, they can behave as a virtual energy storage unit. I.e., they can absorb energy when solar energy production is high and then gives back this energy to the user when they needed it. In chapter two, a new price-responsive EWH model with solar-absorption capacity is introduced. This model which is based on a modified version of the model that has been proposed in chapter one, can optimally schedule EWH. it can take advantage of using free solar energy and increase the PV self-absorption capacity. This price-responsive approach reduces the operational cost by reducing the dependency on the energy from the grid. At the same time, since it can absorb a large chunk for solar energy, it can reduce the need for a large capacity energy storage unit.

Thirst chapter investigates the possibility of market bidding mechanism with the presence of PRDs. a market for energy where the energy generators and users bid for the amount of energy that are willing to buy for a given price would be an ideal mechanism than can bring the energy section close to a free market where ha numerous advantages. However, this ideal model did not happen due to numerous reason such as lack of communication infrastructure, inelastic loads and many other reasons. Aside from these physical obstacles, the lack of an effective method to coordinate the PRD is another challenge. One of the main challenges for coordination of PRDs is creating a balance or equilibrium. In chapter three, a new market-based coordination algorithm for PRDs based on Dantzig-Wolfe decomposition is proposed. The aforementioned method can find an optimal solution (Nash Equilibrium) where no appliance is willing to change their consumption plan. At the same time, as this algorithm

progresses, the generation cost for the generation cost and correspondingly, the user payment is decreased. This procedure is continuing until to a point where no PRD is willing to change their behavior since they reached to their global minimum of their payments.

Contents

List of Figures

List of Tables

Chapter 1

1 Stochastic Optimization of Comfort-Centered Model of Electric Water Heater (EWH)

1.1 Literature Review

Historically, power systems have balanced supply and demand by scheduling generation and reserves to meet a fixed load forecast. However, power systems are moving toward scheduling both generation and consumption as peak loads rise each year, the need for reliability increases, and renewable energy is added [1].

With improved communication technology, the opportunity to make home appliances smarter is now available. Since 2010, millions of smart meters and sensors have been deployed. They can provide a two-way communication bridge to the power systems which will lead to a responsive demand side. Demand response (DR) refers to end-user customers that react to electricity grid needs through communications links. The U.S. Federal Energy Regulatory Commission and U.S. Department of Energy presented the advantages of DR in [2], [3].

DR can alleviate some problems in power systems such as high peak demand by scheduling the demand to avoid peak times. It can also help to incorporate more renewable energy by making appliances use energy at the times when renewable energy is abundant. It can also help support transient frequency and voltage stability, although those are not a subject of this work.

1.1.1 Demand Response Approaches

DR methods can be divided into two main approaches: direct load control (DLC) and price-based control (PBC) [4]. In the DLC method, the power system operator sheds loads during peak hours to decrease total power generation cost or when a power shortfall happens in the system to stabilize the power system [5]–[7]. However, DLC doesn't consider user preferences. The user might encounter power loss when they need electricity urgently which will make customers not to opt to remain in the DR program in the long term. e.g., turning off air conditioners during peak hours. To mitigate this problem, DLC programs usually restrict their impact to a small fraction of the year. As a result, they are unable to shift power consumption for multiple hours every day to minimize peaks or help integrate renewable energy, even if the customer would be willing to do so [8].

1.1.2 Pricing Method on Demand Response

On the other hand, with price-based methods, the goal is to incentivize a change in consumption patterns based on dynamic pricing. Under price-based control, a power company propagates time-varying price signals to customers to incentivize them to change their consumption pattern, so that the total cost to the customer is decreased, and the goals of the network operator such as peak shedding, decreasing total operating cost and increasing system stability are met [9]–[14].

Dynamic pricing methods include day-ahead pricing (DAP), real-time pricing (RTP), critical-peak pricing (CPP) and time-of-use (TOU) rates. In the DAP and RTP methods, prices vary

every market interval (5 minutes to 1 hour). With DAP, prices are announced one day in advance; with RTP, they are calculated based on real-time conditions [14]. In TOU rates, the week is typically broken into fixed time blocks identified as "peak", "shoulder" and "off-peak" periods, and fixed prices are set for each of these blocks, which do not vary with day-to-day market conditions [15]. The CPP method is similar to TOU, but sets much higher prices during "critical peak" periods which are usually announced one day in advance [15].

Ref. [16] proposed using RTP-based DR to change the temperature set point of HVAC based on a price signal every 15 minutes. Ref. [17] proposed a demand response for residential appliances for every 5 minutes' interval. The authors in [18], [19] proposed a load management program for HVAC and water heaters based on RTP to minimize the total cost. In this project, we use DAP method for scheduling a smart water heater. This allows the water heater to schedule thermal flows over the course of the whole day in a coherent manner. (In regions with RTP tariffs, DAP schedules are also generally available as a forecast of the real-time prices.)

1.1.3 **Advantages of Water Heaters**

An electric water heater (EWH) is considered an interruptible appliance since it can be turned on or off at any time. EWH is an important load, featuring several advantages for demand response. It is a relatively large consumer of household energy, consuming around 30 percent of total household energy usage, most of which occurs during peak hour periods [20]. It is a resistive load. Therefore, there is no inrush current when it is switched on or flyback voltage when it turns off. Consequently, switching on and off imposes less wear on controllers than motor loads such as HVAC. It has a large thermal storage capacity which could be used as virtual electricity storage. The working temperature of an EWH can be anywhere between 40 and 85 degrees Celsius without affecting user comfort. Furthermore, it has good insulation, enabling it to preserve and shift energy usage more than other appliances. In contrast, air conditioners which are another large consumer of energy have a working range of 18 to 25 degrees Celsius. Further, since users are located within the thermal store, they will be inconvenienced by any deviation from their preferred temperature. Considering the reasons above, the focus of this project is on controlling EWH as a residential appliance in demand response.

1.1.4 Control Strategies for Water Heater

As noted previously, EWH control strategies divide into two main groups: DLC and PBC. DLC strategies deal with controlling aggregated EWH for peak-load shedding, balancing and regulation services. DLC strategies were investigated in ref. [5]. From this category, direct regulation of temperature setting [21] and direct on/off switching [22] could be mentioned. In all the DLC strategies, all control parameters are set by the power system operator. Ref. [23] studied the potential of EWH to be used as a household demand response agent.

In contrast, PBC is a customer-centered strategy in which individual EWHs aim to minimize total energy cost of the end user. To shift the consumption pattern from times of peak demand to times of lower demand, ref. [24] investigated several control strategies including

load shedding, preheating and coasting while keeping tank temperature above a minimum temperature.

A number of studies have investigated scheduling EWH in response to dynamic pricing [25]–[30]. However, the concept of comfort is rarely discussed in the DR literature [31]. Minimizing the total cost should not be the only goal of scheduling an appliance in a DR program. PBC algorithms that do not consider user preferences face the same problems as DLC strategies: they must minimize their intervention to avoid driving people out of the program; but if their interventions are limited to unnoticeable levels, they may miss the opportunity to take advantage of all the customer's flexibility. So, an effective PBC algorithm must consider both the cost of electricity and the customer's willingness to pay for good service.

Minimizing operation cost considering temperature comfort was proposed in [31]. Ref. [32] proposed an algorithm to optimally schedule a WH considering user-adjusted thermal constraints. In [18], the author introduces a joint scheduling program for HVAC and an electric vehicle considering user preferences and thermal comfort constraints. In [33], the author modeled EWH using a physical model and considered user comfort as a set of linear constraints. Ref. [34] proposed an algorithm to control both the heating and mixing element of WH while considering user comfort preferences as thermal constraints. In [8], the preference is modeled through a cost function which constitutes a linear function of deviation from the desired temperature [15]. The proposed optimization model in [35] tries to find a trade-off between electric cost and thermal comfort. To minimize the electricity bill for the next 24 hours, [18] presented a linear-sequential-optimization algorithm to schedule thermostatic appliances, subject to comfort constraint of the thermal deadband.

Ref. [32] proposed a control strategy for air conditioners and EWH under real-time pricing. the strategy simply set the thermal set point relative to price, within a thermal-comfort deadband. Ref. [36] presented a model for household hot water withdrawal and presented a linear programming (LP) approach to find the optimal set point aiming to minimize the cost using a thermal deadband constraint to represent of comfort.

Almost all the work that has been done on EWH considers user comfort as a set of hard thermal constraints. In contrast, in this work we treat user comfort as an element of the objective function: the amount the customer is willing to pay to avoid discomfort. This allows us to model user preferences more directly, and is also more compatible with the stochastic framework we introduce below; e.g., the water heater can turn off when prices are high and there is low risk of hot water usage. This approach will have more flexibility in selecting temperature setpoints and is expected to provide better value than treating user comfort as a hard temperature constraint [37]. (In other words, previous work has treated users as being completely unwilling to accept any risk of water being delivered below the desired temperature; we model the fact that they may be willing to take on some risk if the financial savings are high enough.)

Another factor that is important for a successful control of water heater is considering the random behavior of hot water withdrawal. In any successful EWH control strategy the user

withdrawal pattern should be considered [29]. However, most of the approaches described above don't consider the uncertainty and variability of hot water withdrawal [15], [35]. Instead they assume perfect foresight [34] using a Load Profile Generator [38] or use heuristic methods that only need simple point forecasts [39] or no forecast at all [40]–[42]. Some previous models used independent probabilistic forecasts for hot water usage in different hours [43]. However, as will be discussed below, optimal control of EWH requires a stochastic model that can optimize setpoints based on a probabilistic forecast of the *joint* distribution of hot water withdrawals in all hours of the day. In this work, we introduce the first water heater optimization model of this type.

We also note that the combination of a stochastic model with an objective-based approach to user preferences is a qualitative improvement on previous work which only includes one of these elements. This is because the cost-vs-comfort tradeoff for water heating is primarily driven by uncertainty about water withdrawals. If the customer always uses hot water at a particular time each day, then they will almost certainly want hot water to be kept available at that time. However, if they rarely use hot water at a particular time of day, then they may be willing to accept lower temperatures at that time in exchange for large cost savings (e.g., by heating at a cheaper time and/or keeping the tank cool to reduce losses). To address these effects, a controller must use both a cost-based treatment of user preferences (not simple temperature constraints) and also a stochastic treatment of withdrawals.

1.1.5 Probabilistic Forecasting of Hot Water Withdrawals

One of the main issues for scheduling appliances for a DR program is their unpredictable nature of energy consumption. In case of an EWH, it shows itself in the random behavior of

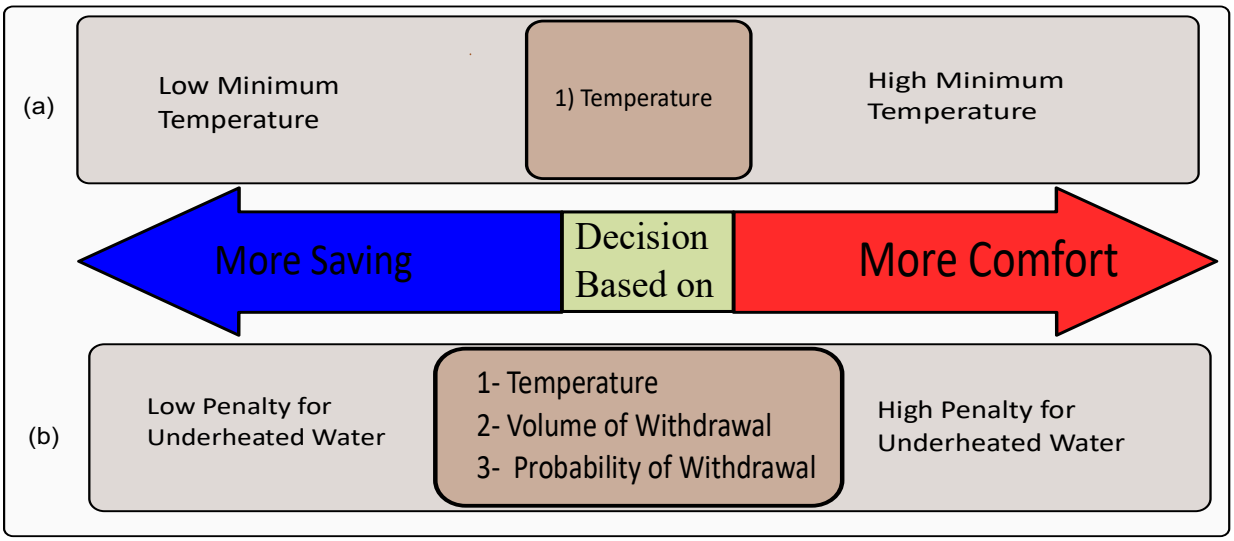

Figure 1: (a) treatment of other works to change the level of user comfort. (b) criteria to change comfort level in this paper

hot water withdrawals. For an HVAC it is related to the outside temperature. To deal with this randomness, stochastic optimization is proposed as a useful method to deal with the randomness of price (some pricing methods change every interval), withdrawal of hot water and outside temperature in case of HVAC [44]–[46].

Ref. [47] proposed a two-step optimization for scheduling EWH based on a single forecast. The algorithm optimizes the model based on the deterministic forecast in effect with the DA-pricing method. The second step optimization happens when the forecast was different from real-time consumption.

The authors in [37] modeled the scheduling problem of EWH as a single-source shortest path problem of a weighted acyclic graph which is solved by Dijkstra's algorithm. They used a typical simple expected-value forecast as presented in [48].

The problem with the single expected forecast method is that it will neglect extreme cases. If the forecast minimizes RMSE, it will use the average of the withdrawal distribution as the single point forecast for each interval. This approach neglects extreme cases that might need to be served. For example, if there is a 10% chance of a 4 kWh withdrawal, then the system may need to keep either 4 kWh or 0 kWh available, depending on user preferences. Keeping 0.4 kWh would be a poor choice. Therefore, it is necessary to use a probabilistic forecast which provides multiple possible usage levels for each interval.

Ref. [49] present a probabilistic forecast for water consumption (not just hot water) based on weather condition, time of year and socio-economic condition of the user. It applies Monte Carlo sampling on historical data to find a triangular probability density function for each interval based on statistical data (min, medium, max) of each interval.

Ref. [50] estimates the marginal expected value of the withdrawal vector under a limited range of conditions (day/weekend, different numbers of people in the house); however, they do not consider combinations of these conditions, omit other explanatory information such as weather, and do not estimate the probability density for this vector.

To deal with forecasting errors, [51] proposed a fuzzy algorithm which is applied on HVAC but the author claims it could be used for EWH. The algorithm "fuzzifies" the price and outdoor temperature and solves the corresponding problem with an immunity-based algorithm which is based on genetic algorithms. The more the error, the fuzzier the variable would be.

Ref. [35] proposed a probabilistic forecast method for electricity prices based on a seven-level discretized normal distribution defined in [52]. Then they optimize the schedule for a building heater with thermal storage based on these forecasts.

Ref. [43] proposed scheduling EWH using approximate dynamic programming. To simplify the problem, it assumes that hot water demand at any given time is independent of the previous demand.

The approaches in refs.[43], [49]–[51] use an independent probabilistic forecast for each individual hour. However, in real households the probability of withdrawal for each hour is correlated with the previous hours. For example, in a single-person household, if the user takes a shower at 7 a.m., the probability of another shower at 8 a.m. is nearly zero. However, when a method uses independent forecasts for each hour (including independent probabilistic forecasts), it doesn't include this fact for decision making. To accurately model water heater withdrawals, it is necessary to produce a probabilistic forecast for the joint usage in all hours of the day (forecast the distribution of a 24-dimensional random variable), rather than producing separate probabilistic forecasts for each hour (24 forecasts of independent 1-dimensional random variables).

In the main body of this paper, we present a simple probabilistic forecasting method for the joint distribution of hot water withdrawals in all hours of the coming day. This is the first model of its type for EWH withdrawals, and should be sufficient for developing and testing the stochastic water heater optimization model. In section 0, We then discuss future extensions which will investigate to improve the speed and accuracy of the model using machine learning techniques and alternative problem-solving algorithms such as heuristic algorithms. These alternative methods help to incorporate this method with traditional power systems networks and the future technology of the internet of things.

1.2 Problem Framing

1.2.1 Introduction

In this project, we develop methods for a water heater to schedule its temperature setpoint to minimize electricity cost and maximize user comfort, in the face of time-varying electricity prices and uncertain water withdrawals by the customer. This could, for example, maximize utility for a household connected to a next-generation "smart grid," where hourly prices are generated in a day-ahead market, reflecting the marginal cost of electricity production as supply and demand vary in the region.

The basic problem is given by:

$$\min_{\boldsymbol{T}^{\text{set}} \in \mathbb{R}^{24}} \mathbb{E}_{\boldsymbol{E}^{\text{des}}}\left[C\left(\boldsymbol{T}^{\text{set}}, \boldsymbol{E}^{\text{des}}\right)\right] \quad (1)$$

In this problem, $\boldsymbol{T}^{\text{set}}$ is a vector of hourly thermostat setpoints (°C) for the next day. These setpoints are the main decision variables of the problem, i.e., the values to be found via optimization. The random vector $\boldsymbol{E}^{\text{des}}$ represents hourly withdrawals of hot water**,** measured by the amount of heat added to the water prior to withdrawal (kWh). The function $C\left(\boldsymbol{T}^{\text{set}}, \boldsymbol{e}^{\text{des}}\right)$ shows the cost of operating the water heater for the next day if setpoints $\boldsymbol{T}^{\text{set}}$ are used and conditions $\boldsymbol{e}^{\text{des}}$ occur. This includes both the direct cost of purchasing electricity to heat the tank to meet the setpoints, and also a penalty factor indicating the amount the customer would be willing to pay to avoid discomfort experienced due to delivery of underheated water (if any). This cost function is discussed further in section 1.3.1. The term $\mathbb{E}_{\boldsymbol{E}^{\text{des}}}[\,]$ indicates the expected value of the cost function over all possible values of the random vector $\boldsymbol{E}^{\text{des}}$. This problem considers costs for the next day, but not beyond.

Table 1. comparison of published methods for EWH control

Paper	**Goal**	**Comfort**	**Uncertainty (in Input)**	**Main Inputs**	**Method**
CC-WH	Reduce Cost Vs Discomfort	Cost Based	Water usage	Water usage, Price	MILP
44	Minimize electric and Thermal deviation costs	Temperature Dead-Band	price, ambient temperature, water usage	price, ambient temperature, water usage	MILP
43	Increase PV Self-consumption and Reduce Cost	Temperature Dead-Band	water usage, ambient temperature	water usage, ambient temperature, PV radiation, Price	Stochastic DP
41-43	Variable Tolerance Vs electric Bill	Temperature Dead-Band	water usage, ambient temperature, price	water usage, ambient temperature, price	Interval analysis
40	Minimize Electric Cost	Temperature Dead-Band	water usage	water usage, Price	Approximate DP
36 (Du& Lu)	Minimize Electric Cost	Temperature Dead-Band	None	Water usage, Price	Recursive algorithm
15-17	Increase PV Self-consumption	Temperature Dead-Band	Energy Consumption	water usage, PV radiation, Price, energy	DP, LP
13-14	Reduce Battery Size, consumption shifting	Temperature Dead-Band & Time of use comfort	Energy Consumption, PV radiation	Energy Consumption, PV radiation	Approximate DP
11 (Apt&Goh)	Reduce Cost	Temperature Dead-Band	None	Price	Single input function

1.2.2 Probabilistic Forecasting of Hot Water Withdrawals

When scheduling the water heater, the next day's consumption is uncertain. A key advance in this work is that we treat consumption as a random vector drawn from a joint distribution of withdrawals in all hours of the day. This enables us to implicitly model dependencies between hourly withdrawals, e.g., a large withdrawal at 7 am for a shower may imply that no shower will be taken at 8 am.

Formally, we assume that the desired hourly withdrawals tomorrow are represented by a random vector $\boldsymbol{E}^{\mathrm{des}}$, which has an unknown distribution. We also assume that the known withdrawal vectors on some collection of recent days are independent samples from the same distribution as $\boldsymbol{E}^{\mathrm{des}}$. The known withdrawals are designated by $\boldsymbol{e}_d^{\mathrm{des}}$, $d \in D$, where D is a list of recent days with conditions similar to tomorrow. Then the available samples constitute an empirical probability distribution for $\boldsymbol{E}^{\mathrm{des}}$:

$$P\left(\boldsymbol{E}^{\mathrm{des}} = \boldsymbol{e}\right) \approx \begin{cases} w_d & \text{if } \boldsymbol{e} \in \left\{\boldsymbol{e}_d^{\mathrm{des}} : d \in D\right\} \\ 0 & \text{otherwise} \end{cases}, \quad \forall \boldsymbol{e} \in \mathbb{R}^{24}, \tag{2}$$

with

$$w_d = \frac{1}{|D|}, \quad \forall d \in D. \tag{3}$$

If the random withdrawal process is stationary, the empirical distribution converges to the true distribution by the Glivenko–Cantelli theorem [53], so it can be used directly as a probabilistic forecast for tomorrow's withdrawals. The set D is the last n days of withdrawal pattern. We need the value for n to be as big as possible to represent more possible withdrawal samples. However, choosing a big value for n will make the model computationally heavy. Therefore, the is a trade-off between speed and accuracy for selecting the right value for n.

Once the probabilistic forecast is constructed based on past D days of withdrawal pattern, we then estimate the expected cost of using any particular setpoints tomorrow:

$$\mathbb{E}_{\boldsymbol{E}^{\mathrm{des}}}\left[C\left(\boldsymbol{T}^{\mathrm{set}}, \boldsymbol{E}^{\mathrm{des}}\right)\right] \approx \sum_{d \in D} w_d \cdot C\left(\boldsymbol{T}^{\mathrm{set}}, \boldsymbol{e}_d^{\mathrm{des}}\right). \tag{4}$$

This gives the following deterministic problem:

$$\min_{\boldsymbol{T}^{\mathrm{set}} \in \mathbb{R}^{24}} \sum_{d \in D} w_d \cdot C\left(\boldsymbol{T}^{\mathrm{set}}, \boldsymbol{e}_d^{\mathrm{des}}\right). \tag{5}$$

This approach has a simple, intuitive explanation: we seek the setpoints $\boldsymbol{T}^{\mathrm{set}}$ that minimize expected costs if tomorrow's withdrawal pattern could match the withdrawals on any historical day $d \in D$ with probability w_d.

This technique takes advantage of the fact that the predictive probability density function for withdrawals is discrete (defined only for values $\boldsymbol{e}_d^{\mathrm{des}}$, for $d \in D$). However, the same

technique could be used with a continuous distribution via the Sample Average Approximation (SAA) method [54], which estimates expected values based on random samples from a continuous predictive distribution. In fact, the model shown here can be interpreted as an application of SAA already, where the previous withdrawals $\boldsymbol{e}_d^{\text{des}}$ are random samples from the true distribution of $\boldsymbol{E}^{\text{des}}$.

1.3 Water Heater Model

1.3.1 Introduction

The cost function $C\left(\boldsymbol{T}^{\text{set}}, \boldsymbol{e}_d^{\text{des}}\right)$ is deterministic; however writing it in closed form would require extensive use of branching statements to represent different outcomes depending on several "if/then" cases: water heater temperature above/below the acceptable level; setpoint attainable/not attainable when heater runs at maximum power; setpoints below/not below the "coasting" temperature for the heater. Further, if this function were written in closed from, using numerous case statements, there would be no easy way to solve the resulting non-convex problem.

To address these difficulties, we write the cost function $C\left(\boldsymbol{T}^{\text{set}}, \boldsymbol{e}_d^{\text{des}}\right)$ as a discrete-time simulation model, expressed as a mixed-integer linear program (MILP). (In this framework, the branching logic is represented by constraints (12)-(16) below.) With this approach, as we show next, the cost functions for all sample days $d \in D$ can be aggregated into a single MILP. This makes it possible to solve problem (5) quickly and reliably using standard MILP solver software.

We model $C\left(\boldsymbol{T}^{\text{set}}, \boldsymbol{e}_d^{\text{des}}\right)$ as follows:

$$C\left(\boldsymbol{T}^{\text{set}}, \boldsymbol{e}_d^{\text{des}}\right) = \begin{bmatrix} \min\limits_{\boldsymbol{x}_d \in \mathbb{R}^n} \boldsymbol{c}^T \boldsymbol{x}_d \\ \text{such that } \boldsymbol{x}_d \in \boldsymbol{X}\left(\boldsymbol{T}^{\text{set}}, \boldsymbol{e}_d^{\text{des}}\right) \end{bmatrix}. \tag{6}$$

In this formulation, $\boldsymbol{x}_d$ is a vector of decision variables that indicate how the water heater would be operated if tomorrow's withdrawals match the pattern $\boldsymbol{e}_d^{\text{des}}$ from day *d*. The vector $\boldsymbol{x}_d$ is a concatenation of all the variables listed in section 1.3.4 except $\boldsymbol{T}^{\text{set}}$ (i.e., the operational details for the water heater if setpoints $\boldsymbol{T}^{\text{set}}$ were used with the day-*d* withdrawals, $\boldsymbol{e}_d^{\text{des}}$). The parameter *n* is the dimensionality of the $\boldsymbol{x}_d$ vector. The decision variables $\boldsymbol{x}_d$ are restricted to a domain $\boldsymbol{X}\left(\boldsymbol{T}^{\text{set}}, \boldsymbol{e}_d^{\text{des}}\right)$ by a number of linear constraints that reflect the water heater's behavior in response to the setpoints $\boldsymbol{T}^{\text{set}}$ and conditions $\boldsymbol{e}_d^{\text{des}}$. Those constraints are described in section 1.3.5. In addition, $\boldsymbol{X}\left(\boldsymbol{T}^{\text{set}}, \boldsymbol{e}_d^{\text{des}}\right)$ encompasses binary requirements for some variables, and nonnegativity requirements for most variables, as discussed in section 1.3.4.

With equation (6), problem (5) becomes

$$\begin{aligned}\min_{\boldsymbol{T}^{\text{set}}\in\mathbb{R}^{24}} \sum_{d\in D} w_d C\left(\boldsymbol{T}^{\text{set}}, \boldsymbol{e}_d^{\text{des}}\right) &= \min_{\boldsymbol{T}^{\text{set}}\in\mathbb{R}^{24}} \sum_{d\in D} w_d \begin{bmatrix} \min\limits_{\boldsymbol{x}_d\in\mathbb{R}^n} \boldsymbol{c}^T\boldsymbol{x}_d \\ \text{s.t.}\ \ \boldsymbol{x}_d \in \boldsymbol{X}\left(\boldsymbol{T}^{\text{set}}, \boldsymbol{e}_d^{\text{des}}\right) \end{bmatrix} \\ &= \min_{\boldsymbol{T}^{\text{set}}\in\mathbb{R}^{24}} \begin{bmatrix} \min\limits_{\boldsymbol{x}_d\in\mathbb{R}^n, \forall d\in D} \sum\limits_{d\in D} w_d \boldsymbol{c}^T\boldsymbol{x}_d \\ \text{s.t.}\ \ \boldsymbol{x}_d \in \boldsymbol{X}_d(\boldsymbol{T}^{\text{set}}) \end{bmatrix} \\ &= \begin{bmatrix} \min\limits_{\substack{\boldsymbol{T}^{\text{set}}\in\mathbb{R}^{24} \\ \boldsymbol{x}_d\in\mathbb{R}^n, \forall d\in D}} \sum\limits_{d\in D} w_d \boldsymbol{c}^T\boldsymbol{x}_d \\ \text{s.t.}\ \ \boldsymbol{x}_d \in \boldsymbol{X}\left(\boldsymbol{T}^{\text{set}}, \boldsymbol{e}_d^{\text{des}}\right), \forall d \in D \end{bmatrix}. \end{aligned} \tag{7}$$

We can now simplify equation (7) and make it more specific. We first note that hourly electricity consumption and energy shortfalls are elements of $\boldsymbol{x}_d$, i.e.,

$$\boldsymbol{x}_d = \begin{bmatrix} \vdots \\ \boldsymbol{E}_d^{\text{in}} \\ \vdots \\ \boldsymbol{E}_d^{\text{short}} \\ \vdots \end{bmatrix}, \tag{8}$$

where $\boldsymbol{E}_d^{\text{in}}$ and $\boldsymbol{E}_d^{\text{short}}$ are vectors of hourly electricity consumption and hourly heating shortfalls (both measured in kWh). These vectors have one element per hour, $E_{d,h}^{\text{in}}$ and $E_{d,h}^{\text{short}}$. $E_{d,h}^{\text{short}}$ is the amount of extra heat that would need to be added to water delivered during hour h (if any) in order to reach a satisfactory temperature (when using setpoints $\boldsymbol{T}^{\text{set}}$ with withdrawal pattern $\boldsymbol{e}_d^{\text{des}}$).

In our model, direct costs only arise from electricity consumption and heating shortfalls. All other decision variables have coefficients of 0 in the cost vector $\boldsymbol{c}$ (though they may indirectly affect costs via their effect on the allowed values of $E_{d,h}^{\text{in}}$ and $E_{d,h}^{\text{short}}$). So the final form of (7) can be rewritten as

$$\begin{aligned} \min_{\substack{\boldsymbol{T}^{\text{set}}\in\mathbb{R}^{24} \\ \boldsymbol{x}_d\in\mathbb{R}^n, \forall d\in D}} & \sum_{d\in D} w_d \sum_{h\in I} p_h^{\text{p}} E_{d,h}^{\text{in}} + p^{\text{s}} E_{d,h}^{\text{short}} \\ \text{s.t.}\ \ & \boldsymbol{x}_d \in \boldsymbol{X}\left(\boldsymbol{T}^{\text{set}}, \boldsymbol{e}_d^{\text{des}}\right), \forall d \in D \end{aligned}. \tag{9}$$

Here, p_h^{p} is the cost of electricity during hour h of the coming day (\$/kWh) and p^{s} is a penalty factor (also in \$/kWh) which will be assigned to any heating shortfall in water delivered to the customer, i.e., p^{s} is the amount the customer would be willing to pay per kWh of heat to have water heated to a satisfactory temperature (generally greater than p_h^{p}). The term $p^{\text{s}}E_{d,h}^{\text{short}}$ is a simple representation of the customer's economic demand function for hot water, but it has the attractive properties of being linear and scaling in a logical way with both the temperature shortfall and the volume of water desired. We have found no existing literature showing a research-based form or parameters for this function. So in this work, we have tested a variety of values for p^{s} to evaluate the performance of the algorithm for

customers who prefer various balances between comfort and financial savings. (In future work we may represent the customer's willingness to pay for comfort via more complex functions of $\boldsymbol{E}_d^{\text{short}}$, possibly derived from customer usage tests). Note that usually $p^{\text{s}} > p_h^{\text{p}}$ all day. However, thermal losses are incurred whenever the tank is kept hot, so the heater may need to consume more than one kWh of electricity in order to deliver one additional kWh of hot water (i.e., avoid one kWh of shortfall). Consequently, the cost of avoiding a shortfall may be greater than p^{s}. In this case the algorithm may (correctly) choose to incur a shortfall.

The following subsections provide more information about each of the elements of problem (9). Section 1.3.2 describes the indexing sets used for the model (*D* and *I*) and section 1.3.3 describes parameters (input data). Then section 1.3.4 presents all the model's decision variables: $\boldsymbol{T}^{\text{set}}$, $\boldsymbol{E}_d^{\text{in}}$ and $\boldsymbol{E}_d^{\text{short}}$, as well as additional helper variables included in $\boldsymbol{x}_d$ in equation (8). Section 1.3.4 also introduces non-negativity and binary requirements that partly describe the feasible domain shown in the last line of equation (9). Finally, section 1.3.5 presents the remaining constraints corresponding to the last line of equation (9). These constraints force $\boldsymbol{E}_d^{\text{in}}$ and $\boldsymbol{E}_d^{\text{short}}$ to take physically correct values based on the values of $\boldsymbol{T}^{\text{set}}$ and $\boldsymbol{e}_d^{\text{des}}$.

Note that all input parameters are identified by lower-case letters and decision variables and sets use capital letters. Bold identifiers indicate vectors (not used in later sections).

1.3.2 Nomenclature: Indexing Sets

The optimization is done over historical days, and each day is divided into several intervals. Most variables are indexed over days and intervals, except $\boldsymbol{T}^{\text{set}}$, which is only indexed over intervals (corresponding to hourly setpoints for tomorrow).

D: set of historical days considered in the optimization, usually indexed by *d*. For our initial work we will use all weekdays or weekend days in the previous 60 days to do the optimization. However, any number of past days can be selected.

I: set of standard intervals used to divide up each day, usually indexed by *h*. In this work, we assume each interval is one hour long, giving 24 intervals in each day; that could be changed in later work.

Any variables, parameters and constraints in the following sections that use *h* or *d* subscripts are defined for all values of $d \in D$ and/or $h \in I$.

1.3.3 Nomenclature: Input Parameters (Data)

This section introduces the model's input parameters. These are values that are known before running the model, and are used to configure the model.

c^{liter}: specific heat of water, 0.001148 kWh/kg·deg C.

$t^{\min}$: minimum usable temperature. This is the minimum acceptable temperature for the user that he/she doesn't feel discomfort. In our model, the discomfort cost is zero unless the temperature of withdrawn water is less than $t^{\min}$.

$t^{\max}$: the maximum temperature that hot water is allowed to reach. The maximum temperature is restricted due to safety reasons.

T^{big}: an arbitrarily big temperature e.g., 200 degrees Celsius. This constant helps define the working condition of water heater (working at max, coasting or neither of these two).

r^{loss}: heat loss rate. This is a constant which is related to the thermodynamic properties of the water heater. It shows the fraction of heat that will be lost to the surrounding environment during each interval, depending on the temperature difference between the water heater tank and the ambient air. We use a simple model of losses similar to [55], which assumes equal temperatures throughout the tank, that heat loss is proportional to the temperature difference between the tank and the surrounding environment, and ignores changes in tank temperature over the course of each interval. Under these assumptions, the tank temperature moves toward the ambient air temperature by an amount equal to $r^{\text{loss}} \cdot (T_{d,h}^{\text{tank}} - t_{d,h}^{\text{amb}})$ during interval h on day d. In future work, we will investigate use of shorter timesteps and/or more detailed, nonlinear water heater models.

v^{tank}: volume of the water heater tank (liters).

c^{tank}: the number of degrees that temperature of the water heater would be raised for each kWh of input energy (°C/kWh); given by $c^{\text{tank}} = v^{\text{tank}} c^{\text{liter}}$.

p^{s}: shortfall penalty ($/kWh). Constant by which the discomfort cost is balanced against energy usage cost. The more the penalty factor is, the higher the discomfort cost will be.

$e^{\max}$: maximum energy input. The maximum energy that the water heater can inject from the electric element to water in each interval, e.g., if the power of water heater is 2 kW, it can give 2 kW · 1 h of energy which equals to 2 kWh of energy.

w_d: weight of historical day d in optimization. In our initial work, this will just be $1/|D|$ for all days, where $|D|$ is the number of sample days used for the optimization. In later extensions, we will seek to construct a better probabilistic forecast for the random withdrawal vectors by adjusting the weight for each sample day based on the similarity of that day to the conditions expected for tomorrow.

p_h^{p}: power price for interval h of the coming day ($/kWh). In our initial work we assume this is known in advance, e.g., from a day-ahead market that provides fixed prices for each hour of the next day. In future extensions, we may investigate the effect of differences between day-ahead and real-time prices, or incorporate price forecasting into the algorithm, or negotiate an equilibrium between the water heater and the rest of the market.

t_h^{amb}: ambient temperature (°C). Air temperature expected around the water heater during interval *h* of the coming day (assumed known in advance).

$t_{d,h}^{\text{out}}$: historical outlet temperature (°C). Temperature of outlet water during interval h on historical day d, i.e., the temperature of the water that goes into hot water tap. This is obtained by logging historical data.

$t_{d,h}^{\text{in}}$: historical inlet temperature. Temperature of cold-water supply to the water heater during interval h on historical day d. Obtained by logging historical data.

t_h^{in}: future inlet temperature. Temperature of cold-water supply to the water heater during interval h on the coming day. Assumed to be known in advance (may be forecasted as average temperature from prior day).

$v_{d,h}^{\text{hist}}$: historical volume withdrawn (liters). The volume of hot water that was used during interval h on day d.

$e_{d,h}^{\text{des}}$: desired energy withdrawal. The amount of heat that would need to be added to water withdrawn during interval h on the coming day to satisfy users, if household water usage follows the pattern from historical day d. This is calculated from logged data $t_{h,d}^{\text{in}}$, $t_{h,d}^{\text{out}}$ and $v_{d,h}^{\text{hist}}$ as

$$e_{d,h}^{\text{des}} = c^{\text{liter}} v_{d,h}^{\text{hist}} \left[\max\left(t_{d,h}^{\text{out}}, t^{\min}\right) - t_{d,h}^{\text{in}}\right] \left(1 + \frac{t_{d,h}^{\text{in}} - t_h^{\text{in}}}{t^{\min} - t_{d,h}^{\text{in}}}\right). \quad (10)$$

See equation (54) in the Appendix for the derivation of this equation.

1.3.4 Nomenclature: Decision Variables (Values Calculated During Optimization)

This section introduces the model's decision variables. These are values optimized or calculated by the model. The most important decision variables are the thermostat setpoints T_h^{set} for the coming day. Other variables are used to simulate how the water heater will behave tomorrow if the water usage pattern matches historical day d (but with tomorrow's setpoints and weather conditions, T_h^{set}, t_h^{in} and t_h^{amb}). For example, we know the historical tank temperature $t_{d,h}^{\text{out}}$, but we introduce the variable $T_{d,h}^{\text{tank}}$ to show the tank temperature that would occur during hour h if new setpoints T_h^{set} are used with the water usage pattern from day d. These variables are forced to take specific values by constraints representing the water heater's thermodynamic behavior and built-in thermostatic control in response to the setpoints T_h^{set}. Those constraints are described later, in section 1.3.5.

Every variable that uses a d and/or h subscript is indexed over every member of the corresponding set(s). So there is one T_h^{set} variable for every hour $h \in I$ of the coming day, and all other variables have one value for every hour $h \in I$ of every sample day (withdrawal pattern) $d \in D$.

T_h^{set}: thermostat setpoint for hour $h \in I$ of the coming day. Note: this variable is not indexed over historical days, only the intervals of the coming day. This is because we are not seeking

separate thermostat setpoints for each of the past days; we are seeking one vector (length 24) of thermostat setpoints that would have worked well for *all* past days of water usage, i.e., minimizing the expected cost, with tomorrow's electricity prices.

$E_{d,h}^{\text{in}}$: the amount of heating energy that would be used for interval *h* of each past day *d*, if the new thermostat setpoints T_h^{set} had been used.

$T_{d,h}^{\text{tank}}$: temperature of the water heater during interval *h* on simulated day *d*. This may differ from the setpoint for hour *h*, e.g., if the setpoint is far below the water heater's temperature the previous hour (heater will "coast" above the setpoint), or if the setpoint is raised quickly (or large volumes of hot water are used) and the water heater cannot heat quickly enough to reach the setpoint.

Note: this model assumes uniform temperatures throughout the tank, i.e., it doesn't take advantage of thermal stratification (concentration of hot water at the top of the tank, near the outlet). We also assume the tank is at a constant temperature during the period, i.e., heat additions and removals are concentrated at the start of the intervals, which is when the setpoint changes.

$E_{d,h}^{\text{w}}$: amount of energy (in kWh) withdrawn from the tank during interval *h* on simulated day *d*, due to hot water usage.

$T_{d,h}^{\text{short}}$: temperature shortfall (°C) during interval *h* on simulated day *d*. This is the amount by which the tank temperature would fall short of minimum usable temperature (if any), if the setpoints T_h^{set} were used with hot water usage from day *d*.

$E_{d,h}^{\text{short}}$: energy shortfall (kWh) during interval *h* on simulated day *d*. This is the amount of additional heat that would need to be added to hot water used by the household in order to correct the temperature shortfall (if any), i.e., the amount of heat that is "missing" from the hot water supply.

$C_{d,h}$: binary variable indicating whether the water heater is in "coasting" mode during interval *h* on simulated day *d*. This occurs if the setpoint is so low that it will be exceeded even if no heat is added to the tank.

$M_{d,h}$: binary variable indicating whether the water heater is in "maximum power" mode during interval *h* on simulated day *d*. This occurs if the setpoint is so high that it cannot be reached even if the heater runs at its maximum power for the whole interval.

$B_{d,h}$: binary variable indicating whether a temperature shortfall exists ($T_{d,h}^{\text{short}} = t^{\min} - T_{d,h}^{\text{tank}}$) or not ($T_{d,h}^{\text{short}} = 0$) during interval *h* on simulated day *d.*

1.3.5 Constraints

The model uses a number of constraints to represent the physical behavior of the water heater, as described in this subsection. These constraints force all decision variables to take deterministic values based on the temperature setpoints. In addition to the constraints below, all decision variables are constrained to be non-negative (≥0).

The tank temperature changes from one interval to the next depending on how much energy is added and how much is lost or withdrawn. This is shown by the following equation for the tank temperature at the end of each interval (derived as equation 58 in the Appendix):

$$T_{d,h}^{\text{tank}} = T_{d,(h-1)}^{\text{tank}} + \frac{\left(E_{d,h}^{\text{in}} - E_{d,h}^{\text{w}}\right)}{c^{\text{tank}}} - r^{\text{loss}} \cdot \left(T_{d,h}^{\text{tank}} - t_h^{\text{amb}}\right) \tag{11}$$

Note that this formulation assumes uniform temperatures throughout the tank, that all energy is added or removed at the start of the interval, and that losses don't cause a large temperature change over the interval.

Under standard thermostatic control, a water heater can be in one of three modes over the course of an interval: coasting (setpoint above tank temperature, no heat needed, $C_{d,h} = 1$, $M_{d,h} = 0$), running at maximum power (setpoint below tank temperature, applying full heat but unable to reach setpoint, $C_{d,h} = 0,\ M_{d,h} = 1$) or normal mode (just enough power used to reach setpoint, $C_{h,d} = 0,\ M_{h,d} = 0$). These behaviors are modeled via several constraints:

$$T_{d,h}^{\text{tank}} + M_{d,h} \cdot t^{\text{big}} \geq T_h^{\text{set}} \tag{12}$$

$$T_{d,h}^{\text{tank}} \leq T_h^{\text{set}} + C_{d,h} \cdot t^{\text{big}} \tag{13}$$

$$E_{d,h}^{\text{in}} \geq M_{h,d} \cdot e^{\max} \tag{14}$$

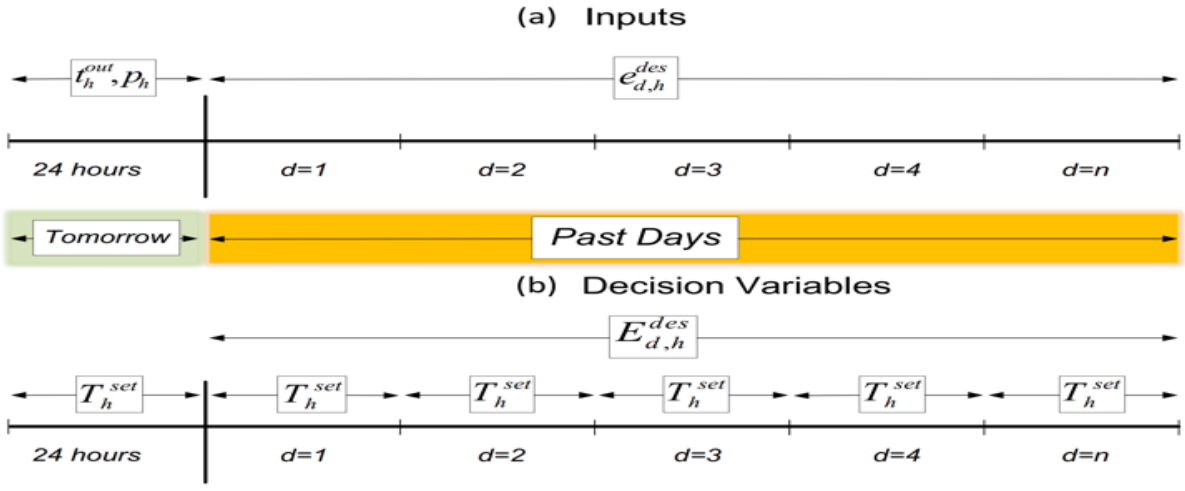

Figure 2. Horizon of inputs and variables

$$E_{d,h}^{\text{in}} \leq \left(1 - C_{d,h}\right) \cdot e^{\max} \tag{15}$$

Taken together, these constraints force the model to choose the correct operating mode for each interval *h* of each simulated day *d* by choosing appropriate values for $C_{d,h}$ and $M_{d,h}$. The four possible choices of $C_{d,h}$ and $M_{d,h}$ are enumerated in Table 2, along with the constraints that take effect for each combination. During each interval on each simulated day, the model must choose the single pair of values for $C_{d,h}$ and $M_{d,h}$ that make the constraints feasible, given the setpoint, starting temperature and energy demand for that interval.

Table 2. Possible operating modes for water heater

$C_{d,h}$ value	0	1	0	1
$M_{d,h}$ value	0	0	1	1
operating mode	Normal	Coasting	Max Power	Coast + Max Power
constraint (12)	$T_{d,h}^{\text{tank}} \geq T_h^{\text{set}}$	$T_{d,h}^{\text{tank}} \geq T_h^{\text{set}}$	no effect	no effect
constraint (13)	$T_{d,h}^{\text{tank}} \leq T_h^{\text{set}}$	no effect	$T_{d,h}^{\text{tank}} \leq T_h^{\text{set}}$	no effect
constraint (14)	$E_{d,h}^{\text{in}} \geq 0$	$E_{d,h}^{\text{in}} \geq 0$	$E_{d,h}^{\text{in}} \geq e^{\max}$	$E_{d,h}^{\text{in}} \geq e^{\max}$
constraint (15)	$E_{d,h}^{\text{in}} \leq e^{\max}$	$E_{d,h}^{\text{in}} \leq 0$	$E_{d,h}^{\text{in}} \leq e^{\max}$	$E_{d,h}^{\text{in}} \leq 0$
Notes	tank temperature exactly reaches setpoint with energy input in allowed range	tank temperature at or above setpoint with no heat added	tank temperature at or below setpoint with maximum heat added	not possible due to last two constraints; will never be selected

The temperature shortfall $T_{d,h}^{\text{short}}$ for interval *h* of simulated day *d* is equal to the amount by which the tank temperature $T_{d,h}^{\text{tank}}$ falls short of the minimum usable temperature $t^{\min}$, i.e., $\max\left(0, t^{\min} - T_{d,h}^{\text{tank}}\right)$. This expression cannot be included directly within one linear constraint. The first constraint to simulate $\max\left(0, t^{\min} - T_{d,h}^{\text{tank}}\right)$ is:

$$T_{d,h}^{\text{short}} \geq t^{\min} - T_{d,h}^{\text{tank}} \tag{16}$$

This constraint, combined with the nonnegativity constraint on $T_{d,h}^{\text{short}}$, forces $T_{d,h}^{\text{short}}$ to be assigned a value greater than or equal to $\max\left(0, t^{\min} - T_{d,h}^{\text{tank}}\right)$. However, We need the temperature shortfall to be exactly equal to $\max\left(0, t^{\min} - T_{d,h}^{\text{tank}}\right)$. Which mean to be zero when $T_{d,h}^{\text{tank}}$ is greater than the $t^{\min}$ and when the difference of these is positive, the result should become exactly equal to $t^{\min} - T_{d,h}^{\text{tank}}$. Since we don't want these value to be negative, we have to use 'greater or equal' in equation (16). Otherwise, we will get an infeasible answer

if equality is used. To force the MILP to set $T_{d,h}^{\text{short}}$ exactly equal (not greater or equal) for positive values of $T_{d,h}^{\text{short}}$, the following four constraints are added to the model:

$$T_{d,h}^{\text{short}} \leq t^{\min} - T_{d,h}^{\text{tank}} + \left(1 - B_{d,h}\right) * t^{\text{big}} \tag{17}$$

$$T_{d,h}^{\text{short}} \leq B_{d,h} * t^{\text{big}} \tag{18}$$

$$B_{d,h} * t^{\text{big}} \geq t^{\min} - T_{d,h}^{\text{tank}} \tag{19}$$

$$\left(1 - B_{d,h}\right) * t^{\text{big}} \geq T_{d,h}^{\text{tank}} - t^{\min} \tag{20}$$

Equation (19) and (20) define what value $B_{d,h}$ Can have. When there is a shortfall, $B_{d,h}$ must be on (1) based on (19) and when there is no shortfall, $B_{d,h}$ Must be off (0) based on equation (20). Then, when there is a shortfall ($B_{d,h}$=1) combination of (17) and (16) forces $T_{d,h}^{\text{short}}$ to be exactly to $t^{\min} - T_{d,h}^{\text{tank}}$. When there is no shortfall ($B_{d,h}$=0), equation (18) forces the $T_{d,h}^{\text{short}}$ to be zero ($T_{d,h}^{\text{short}}$ Is a positive variable). Table (3) shows the various state of constraints based on the value of $B_{d,h}$.

Table 3. Possible working mode for shortfall evaluator

$B_{d,h}$ value	0	1
Operating mode	No shortfall	shortfall
Constraint (17)	Relaxed constraint	$T_{d,h}^{\text{short}} \leq t^{\min} - T_{d,h}^{\text{tank}}$
Constraint (16)	$T_{d,h}^{\text{short}} \geq t^{\min} - T_{d,h}^{\text{tank}}$	$T_{d,h}^{\text{short}} \geq t^{\min} - T_{d,h}^{\text{tank}}$
Constraint (18)	$T_{d,h}^{\text{short}} \leq 0$	Relaxed constraint
Notes	Combination of constraint (18) and $T_{d,h}^{\text{short}}$ being a positive variable, results $T_{d,h}^{\text{short}} = 0$	Combination of constraint (17) and (16), results $T_{d,h}^{\text{short}} = t^{\min} - T_{d,h}^{\text{tank}}$

The energy shortfall is defined as the amount of thermal energy that would need to be added to hot water withdrawn by users to compensate for the temperature shortfall, if any. From equation (60) in the Appendix, this is calculated as

$$E_{d,h}^{\text{short}} = e_{d,h}^{\text{des}} \frac{T_{d,h}^{\text{short}}}{\left(t^{\min} - t_h^{\text{in}}\right)} \tag{21}$$

Intuitively, the energy shortfall is the same fraction of the desired energy input as the temperature shortfall is of the desired temperature increase.

The amount of energy withdrawn from the tank during interval *h* of simulated day *d* is equal to the desired amount of energy minus the energy shortfall, if any. As defined in equation (56) of the Appendix, this gives the relationship:

$$E_{d,h}^{\mathrm{w}} = e_{d,h}^{\mathrm{des}} - E_{d,h}^{\mathrm{short}} \tag{22}$$

Finally, we require that setpoints are within the allowed range for the water heater:

$$T_h^{\mathrm{set}} \leq t^{\max} \tag{23}$$

1.4 Solution Method

In the previous section, the development of the model was explained. In this section, we discuss the general solution algorithm for solving MILP and the quality of solution that CC-WH can achieve. The family of MILP problems is part of NP-hard problems. Until today, no method has been found to solve these problems in 'polynomial time.' However, practical algorithms have been developed to solve or find bounded optimal solutions in a reasonable amount of time. The main algorithm that is used to solve MILPs is Branch and Bound [56] (BnB), which has been developed is 1960. To interpret the results of CC-WH, first, we introduce concepts such as upper/lower bound, gap, and the relative gap in the next sections.

1.4.1 Upper and Lower Bound

In the BnB, the MILP first is solved as a Linear Programming problem (relaxed problem). i.e., by considering all variables, including integer variables as continuous variables. Based on the initial relaxed problem, the BnB creates two linear sub-problem by putting an extra constraint on each branch. Then each sub-problem is turned to two more sub-problems and so on. This action is called branching or creating the tree. The constraint that is added to each sub-problem is basically to force each relaxed integer variable from the parent branch to get an integer value. E.g., if an integer variable (X) had a value such as 3.3 in a relaxed LP problem, its corresponding sub-problems for that variable will add $X \geq 4$ and $X \leq 3$ constraints to each of the two sub-problems. This forces the corresponding integer variable in the relaxed LP sub-problem to have an integer value. This act is continued for all integer variables. This creates a graph of possible answers where the BnB has to explore through them for the optimal integer answer.

The result of the integer answer cannot be lower than the relaxed LP answer. Therefore, the result of the relaxed LP answer will give us the lower bound. The lowest-cost integer answer is called the upper bound. The BnB continually tries to find a lower cost integer answer. Whenever a new integer answer is obtained; If it has a lower cost than the previous upper bound in a minimization problem, the upper bound will be updated to the new value. However, if the new cost has a higher value than the previous upper bound, it will be discarded.

1.4.2 Updating Lower and Upper Bound

at each step, the algorithm starts with the branch that has the lowest relaxed LP cost. Through the search in the branches for lower cost relaxed LP sub-problem, three scenarios could happen to the relaxed LP problem: 1- it is infeasible. 2- it has a higher cost than the upper bound. 3- it has a lower cost than the upper bound. Whenever the first or second scenario happens, the BnB discard that branch and removes it from the search area. If the third scenario happens, it goes again through the same procedure similar to its parent branch until no integer variable is left. If the cost of the lowest branch (it will be an integer answer) is lower than the upper bound, the upper bound will be reduced to the new value.

When the work on the current lowest-cost relaxed LP sub-problem is finished (either through reaching the first or second scenario or reaching to the lowest level branch), the BnB goes to the next lowest-cost relaxed LP sub-problem (increasing lower bound). The process of increasing the lower bound and decreasing the upper bound is continued until they met, or the upper bound reaches to a certain proximity of the lower bound. The measure for the proximity of the answer is called the gap which is introduced in the next section.

1.4.3 Gap and the Relative Gap

The difference between the lower and upper bound is called gap (absolute gap). By dividing the absolute gap by the upper bound, the relative gap is obtained. Most of the available solvers have the corresponding setting for each of these gaps. In this work, we set the relative gap in CPLEX to obtain our desired results.

In MILP, the number of branches increases exponentially when the number of integer variables increases linearly. This causes gigantic possible search areas for the BnB algorithms. However, other complementary algorithms had been developed to boost the performance of BnB. Today, commercially available software such as GURUBI and CPLEX use these algorithms and can solve problems with considerable size with good accuracy in a reasonable amount of time. For example, the branch and cut [57] algorithm can tighten the LP relaxation and therefore removing many infeasible branches from the search space. Also, heuristic [58] algorithms are used to find feasible integer results faster than pure BnB algorithm in the early stages of optimization.

Most of the time, the commercially available solvers such as CPLEX can find a good integer answer (upper bound) in the early stage of optimization. Nevertheless, it will keep exploring through the branches for a better upper bound answer (less likely to happen) while the lower bound is increased. In other words, the solver finds an acceptable answer in the beginning stage of optimization, but it will keep searching to guaranty that this answer is in the acceptable gap. However, that is not a strict rule, and many parameters, such as the shape of the problem, can yield unorthodox behavior. To further analyze the CC-WH behavior, we conduct a test on the speed and accuracy of the result that CC-WH can find, which is provided in the sensitivity analysis section.

1.5 Results

In this section, we evaluate the performance of the proposed method using (1) a perfect forecast and (2) an uncertain, stochastic forecast. The goal of the first approach is to assess the performance of WH-MILP method against other methods under similar conditions. In this case, all inputs such as price, consumption pattern and outside temperature are known in advance and are the same for all models.

In the second part, the stochastic behavior of WH-MILP is evaluated. Here, it is assumed that every input is known except the consumption pattern, which is considered a random variable. In this case, we only have access to consumption patterns from the previous 60 days. The goal is to find the best thermostat setpoints based on known inputs and past days'

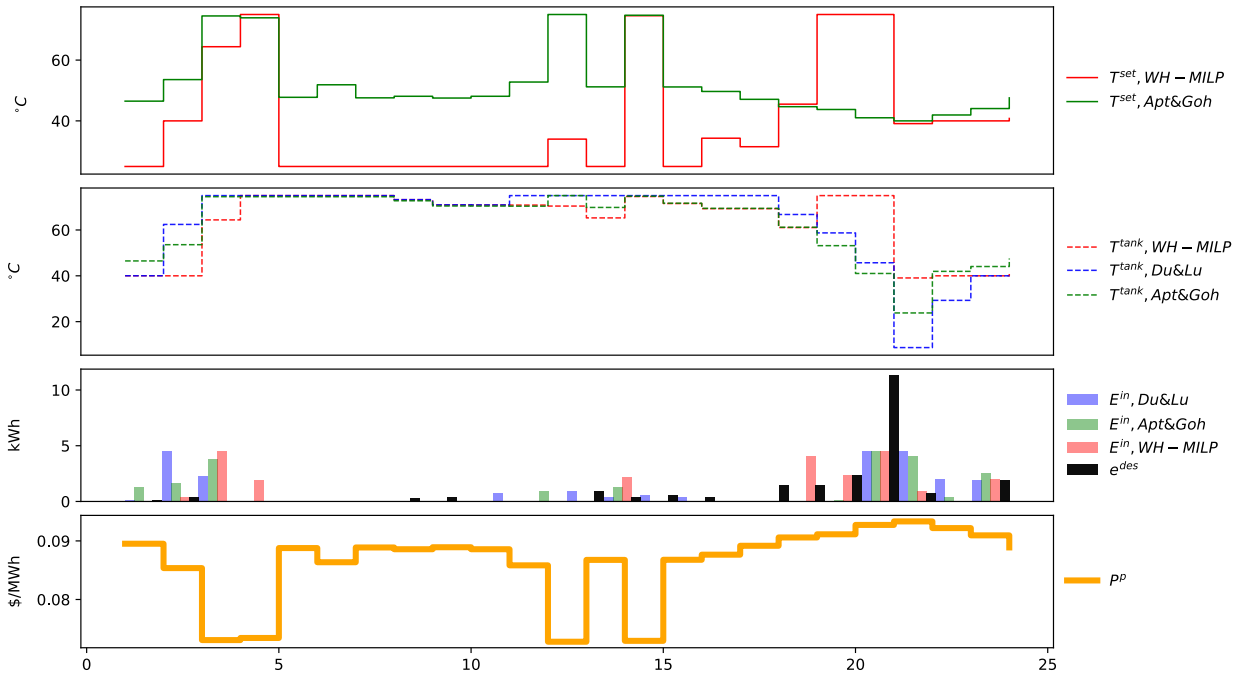

Figure 3. Perfect forecast result for one day

consumption pattern. All test are performed based on consumption patterns from the US Department of Energy's DHW [Domestic Hot Water] Event Schedule Generator [59].

1.5.1 Perfect Forecast Mode

The hot water consumption pattern and price of electricity are the main elements used to plan energy input for a water heater. This paper is in the category of dynamic pricing methods for the next 24 hours. In this section we compare our WH-MILP method against a method that only relies on tomorrow's price of electricity from Apt and Goh [29], which we refer to as the 'Apt&Goh' method. We also compare the WH-MILP to a more advanced method that considers both consumption pattern and price of electricity by Du and Lu [47], which we refer to as the 'Du&Lu' method. Finally, we include results for a fixed-setpoint method, where the water heater thermostat is set to fixed setpoint at all times, such as 60 degrees Celsius. This is the standard method used by existing water heaters (where owners make an implicit cost-comfort tradeoff when they choose any particular fixed setpoint).

1.5.1.1 Apt&Goh Method

The Apt&Goh method tries to take advantage of cheap electricity hours. The control variable is temperature setpoint. In this method, the temperature setpoint is the mirror of the price vector, rescaled to range between a minimum and maximum allowed temperature. Whenever the price is at its minimum, the temperature is set to its maximum and vice versa. Equation (24) shows how the temperature setpoint is updated based on price of electricity for each hour.

$$T_h^{\text{set}} = t^{\max} - \frac{\left(p_h^{\text{p}} - p^{\text{p,min}}\right)}{\left(p^{\text{p,max}} - p^{\text{p,min}}\right)} * \left(t^{\max} - t^{\min}\right) \quad (24)$$

Figure 3 shows the behavior of a simulated water heater over one sample day, using the three methods discussed in this section. The green traces correspond to the Apt&Goh method. The first section of Figure 3 shows the temperature setpoint found from equation (24). The second part shows what the actual temperature would be, if the withdrawal pattern shown in black in the third section occurs. The fourth section shows the electricity price for that specific day.

The Apt&Goh method can have some savings by warming up water in cheap hours. However, by being insensitive to consumption pattern, it may lose the chance to lower the cost or avoid underheated water. For example, consider a situation where a large amount of consumption is expected at 7 PM but since the price of electricity was high in previous hours between noon till 7 PM (lower than price of 7 PM), this algorithm sets the temperature setpoint to the lowest temperature. Then, when a large consumption happens at 7 PM, the water heater has to consume a lot of energy at 7 PM to keep up with consumption in a relatively expensive hour. In contrast, a smarter algorithm that takes advantages of price and consumption pattern could heat water to a higher temperature between 4-6 PM and then coast during the 7 PM hour, saving money relative to the Apt&Goh method. Furthermore, if the water heater allows temperatures to fall to the minimum allowed temperature, and then users withdraw water faster than the heater can reheat it, they will receive underheated water. For example, if the expected consumption pattern for 7 PM is 8 kWh but the rated power of the water heater is 4.5 kWh and the actual temperature is at its minimum, the user will encounter a 3.5 kWh of energy shortfall. However, a smarter method could warm up water in the previous hours even though those hours were part of expensive hours. This would lower energy shortfall and electricity price at the same time. One of the goals of development of the WH-MILP algorithm is taking advantage of these events which decrease both the electricity bill and the chance of having cold water. Another problem with responding to the price instantly is losing the chance of heating at the cheapest time. For example, if the price is decreasing to its minimum in three steps, the temperature setpoint is increased to its maximum in three steps. This causes heating to occur each time the setpoint is raised, which happens before the lowest prices are reached. A smarter algorithm could skip the intermediate setpoint steps, and instead wait to heat only at the cheapest time.

1.5.1.2 Du&Lu Method

In the Du&Lu method, the control variable is a vector of energy inputs for the next day (in contrast to temperature setpoints for Apt&Goh and WH-MILP). The goal of this method is to inject energy to the water heater exactly equal to the sum of expected required energy for tomorrow across all intervals. This strategy can save energy by avoiding extra heating and also avoid underheated water. The Du&Lu method sorts the price of electricity ascendingly, then heats water in the cheapest hours while considering a temperature deadband

constraint (if heating water in a cheap hour causes the temperature to go above the maximum allowed temperature, it will stop heating even though it is a cheap hour; alternatively, if it is an expensive hour but temperature is below the minimum, the water heater adds energy to the water).

The Du&Lu algorithm is recursive. It finds an energy input setpoint for the first interval first, then based on the decision made in the previous step, it finds setpoints for the next step and so on.

Here is the Du&Lu algorithm:

Step (0): Find total required energy for the day from first interval to the last interval:

$$E_1^{\text{total}} = \sum_{h=1}^{24} e_h^{\text{des}} \tag{25}$$

Step (1): Find how many intervals are needed to inject the required energy, where $e^{\max}$ is the rating power of EWH.

$$\text{Index\_Threshold} = {E_h^{\text{total}}}/{e^{\max}} \tag{26}$$

Step (2): Sort prices from current step *'h'* to the last step ascendingly.

Step (3): Tag sorted prices as 'cheap' or 'expensive': if the index of sorted price is below the 'Index_Threshold' then tag them as cheap hour. Otherwise, tag them as expensive.

Step (4): If step '*h*' tag is 'cheap', then turn the EWH on with full capacity ($E_h^{\text{in}} = e^{\max}$). If it then violates maximum temperature, only allocate enough energy ($0 \le E_h^{\text{in}} \le e^{\max}$) to just reach the maximum temperature. If step '*h*' is tagged expensive, keep the EWH turned off. I.e., ($E_h^{\text{in}} = 0$) and if temperature falls below minimum based on expected consumption pattern (e_h^{des}), then only give enough energy ($0 \le E_h^{\text{in}} \le e^{\max}$) to keep it at minimum temperature. The total allocated energy from first interval up to the step '*h*' is called: $E_h^{\text{allocated}}$ which is equal to equation (27):

$$E_h^{\text{allocated}} = \sum_{i=1}^{h} E_i^{\text{in}} \tag{27}$$

Step (5): Find how much more energy is required to be added in the later steps:

$$E_{h+1}^{\text{total}} = E_h^{\text{total}} - E_h^{\text{allocated}} \tag{28}$$

Step (6): return to step (1) and recalculate Index_Threshold and find E_{h+1}^{in} for the next step.

Results from the Du&Lu method are shown in blue in Figure 3. There is no blue line in the first section of the Figure 3 since this method uses energy input as control variable (third section), not temperature.

Unlike the Apt&Goh method, which is blind to user consumption, this method can take advantage of the total required energy for the future hours and plan for energy input based on the cheapest hours. However, this method has some disadvantages. First it assumes energy loss is negligible by referring to [29] in order to avoid considering the dependence of total expected required energy to actual temperature and ambient temperature. However, we know that the total energy loss throughout the day is dependent on the actual temperature of the whole intervals. However, this algorithm starts scheduling recursively from step one (does not know yet what the actual temperature would be for the following steps); therefore, does not have an accurate energy loss estimation even though this loss might be very small for most cases. But, if the ambient temperature is very low, the energy loss could not be considered negligible.

The second issue arises when a big portion of withdrawal happens only in one interval. Being insensitive to each individual interval could not only cost more electrical cost but also could leave more underheated water in comparison to an algorithm that is sensitive to each individual interval. To make it clear, assume the following scenario happens for a given day. In that day, the total required energy is 15 kWh for the whole day. However, 12 kWh of this energy is required at only one interval. Assume this burst of withdrawal happens at 9 PM. Also, assume that the previous hours (for example between 4-8PM) were tagged as expensive; and cheap hours start at 10 PM. The way Du&Lu algorithm will respond in this scenario is this: it will wait until 10 PM to start warming up water since the only important factor is the total required energy for the whole day, not the required energy for each specific interval.

Following this decision, the temperature would be kept low before 9 PM. However, when the burst starts at 9 PM, the EWH will be forced to work with the full capacity to provide the demand while it would fail to do that since the nominal capacity of EWH is much lower (usually around 4.5 kWh) than the required energy (12 kWh) which will result in a huge underheated water (about 7.5 kWh). What could have been done was to warm up the water in the afternoon (even though cheaper hours existed to do that) to be ready for the burst. Furthermore, if electricity price at 9 PM were higher than the previous hours (for example more than the price of intervals between 4-8PM), the forced to work with full capacity EWH would even cost more electricity while it could do the heating in relatively cheap hours at previous intervals. In short, it is only able to pre-heat for the whole day not for each specific interval. However, an algorithm that is sensitive to each specific interval could sense this situation and warm up water in relatively expensive hours to avoid underheated water and high electric cost at the next intervals. In short, we need an algorithm that has vision. i.e., it could see how much energy is needed on each hour while looking at the price to choose the best setpoints. WH-MILP addresses all these issues.

1.5.1.3 WH-MILP Method

The proposed method in this paper considers the price and consumption for each individual interval for the whole day. One important aspect of this method is that it gives the user the option to select their preference based on their need by selecting penalty factor. If the penalty factor is high, the cost for energy shortfall becomes very high. Therefore, the MILP algorithm avoids having shortfall and keeps temperature strictly between temperature deadband and takes advantage of cheap hours considering consumption pattern. In this case, it can behave exactly like the Du&Lu method. However, since it is sensitive to each individual interval consumption pattern, it can find better answers than Du&Lu method if there are burst consumption on some intervals.

Consider these two cases when 10 kWh of energy withdrawal is expected ahead. Case (1) has 9, and 1 kWh of withdrawal and case (2) has 5 and 5 kWh of withdrawal at 6 PM and 10 PM respectively for both cases. The way Du&Lu respond to these two is the same since it is only sensitive to the total required energy, causing huge underheated water in the first case. However, WH-MILP will pre-heat in case (1) to be ready for the situation. The ability to pre-heat for each individual hour and doing it optimally (by having linear programming cost function that considers both user preference and electricity cost at the same time) is another advantage of WH-MILP over Du&Lu and many other works.

Furthermore, the Du&Lu and Apt&Goh assume that withdrawal happens throughout the interval. However, we picked a more conservative approach by assuming that withdrawal happens at the start of each interval in a very short time. i.e., there is no time for adding the energy which will cause more temperature drop and underheated water in comparison to methods that assume withdrawal happens smoothly throughout the intervals. Also, despite Du&Lu, energy loss is not zero for each interval as it is shown in equation (11).

Table 4. Comparison of simulated methods

	CC_WH	Du&Lu	Apt&goh
Simplicity	✓	✓✓	✓✓✓
Considering Withdrawal	✓	✓	✗
Pre-heating	✓	✓	✗
Ready for a large burst of withdrawal	✓	✗	✗
Considering withdrawal uncertainty	In stochastic mode	✗	✗
Comfort-mode	Cost-based	Dead-band	Dead-band
Efficiency in execution	✓	✓✓	✓✓✓

On the other hand, if users would rather to reduce costs than providing perfect service during expensive-to-serve times, they can do so by reducing the penalty factor. For example, if there is a long period of high prices and minimal usage, letting the tank cool below the minimum acceptable temperature instead of reheating it up to minimum temperature can save significant amounts of money while creating relatively little inconvenience. Letting temperature to fall below minimum at times when the chance of withdrawal is low is a unique advantage of WH-MILP to other algorithm in the literature (they all strictly keep temperature above minimum even though the chance of withdrawal might be close to zero).

The WH-MILP method is shown in red in Figure 3. This simulation is done for high value of penalty factor ($p^s = \$2/\text{kWh}$). This means that it is very costly to have any shortfall at all. In this case, WH-MILP will strictly try to keep the actual temperature between temperature deadband (between min and max temperature) while also minimizing the electric cost. As shown in Figure 3 the results for Du&Lu and WH-MILP are similar when the penalty factor is high. This shows WH-MILP could be as good as Du&Lu (with high penalty value).

1.5.1.4 Electric Cost vs. Comfort with Perfect Forecast

This section studies the performance of aforementioned methods on US Department of energy [59] hot water consumption pattern data for a 365 day period. For all four methods, we calculate total energy consumption for the year as well as energy shortfall based on

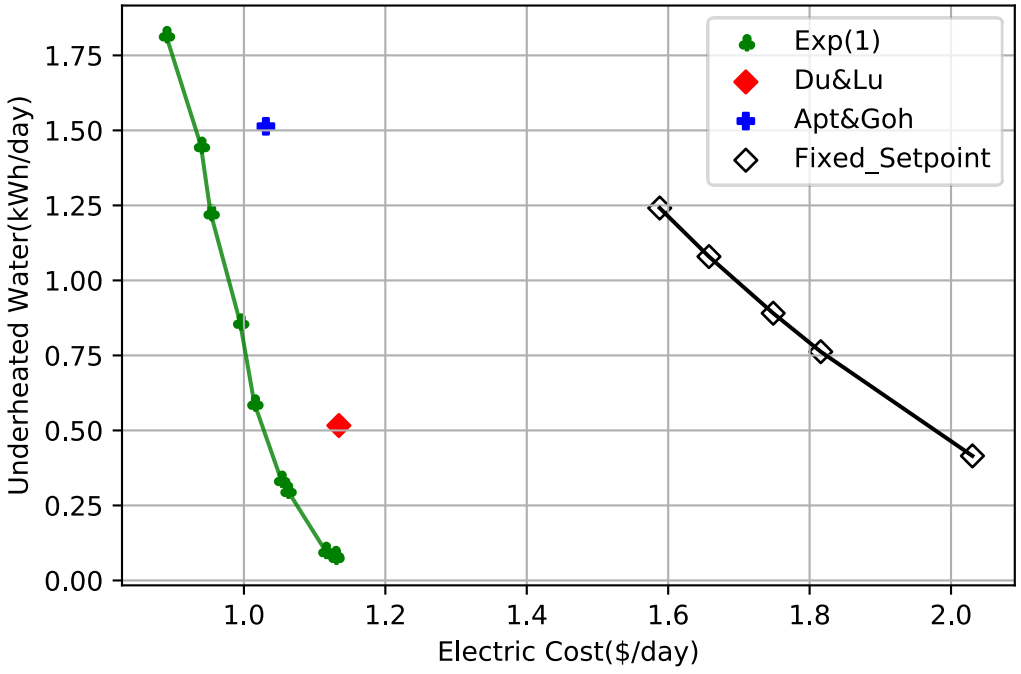

Figure 4 Perfect forecast results

equation (60) in the appendix. Water heater control can be regarded as a dual-objective optimization problem that seeks to minimize both of these. We simulate the WH_MILP for 10 values of penalty factor based on equation (29):

$$p^s \in \{0.09, 0.1, 0.11, 0.12, 0.14, 0.16, 0.18, 0.5, 0.7, 2\} \quad (29)$$

The Fixed-setpoint method is evaluated with setpoints of 40, 43, 47, 50 and 60 degrees Celsius. The results are shown in

. This shows that all methods can have significant improvements relative to the Fixed-setpoint approach (lower cost and less underheated water at the same time). The Apt&Goh method tends to find results that cost around 10 percent less than the Du&Lu method. However, the amount of expected underheated water is 3 times more (0.5 kWh/day against 1.5 kWh/day). The results found by the WH-MILP method for all values of penalty factor are lower for both electric cost and underheated water. This shows that WH-MILP outperforms

both of these methods. Furthermore, WH-MILP is flexible. i.e., it can find results based on user preference by changing the value of the penalty factor. Table (5) shows the percentage of electricity saving of WH-MILP against other methods with similar chance of underheated water. For example, Fixed-setpoint method (set on 60 Celsius) will cost around 2.40$/day with 0.4 kWh/day of underheated water. With equal underheated value on the WH-MILP curve, it will only cost around 1.08$/day which is about 55 percent cheaper than Fixed-setpoint method (set on 60 Celsius). WH-MILP is also 11 and 10 percent cheaper than Apt&Goh and Du&Lu respectively with the same amount underheated water.

Table 5. Comparison of WH-MILP against other methods with equal underheated water

	Fixed ($60^{\circ}C$)	Du & Lu	Apt & Goh
Underheated water (kWh/day)	0.4	0.5	1.5
Electric cost ($/day)	2.4	1.14	1.02
WH-MILP electric cost with equal underheated water ($/day)	1.08	1.02	0.9
WH-MILP cost savings (%)	**55**	**10**	**11**

1.5.2 Stochastic Optimization

The previous section benchmarked the performance of WH-MILP against other methods in the same conditions, with perfect foresight of hot water consumption for each day. In this section, we assess the performance of WH-MILP over a full year with uncertain usage.

The advantage of a stochastic based method is that it let us make decisions that is not possible to make when a single point forecast based on average is used. e.g., if there is a 10% chance of a 4 kWh withdrawal and 90% chance of zero consumption, then the system may need to keep either 4 kWh or 0 kWh available, depending on user preferences. While a single point forecast method such as [40] cannot make such a decision (if it uses the average, it will make a decision based on 400 Wh of consumption for that interval). Therefore, finding a common setpoint that works for multiple possible patterns is much better than finding a vector of setpoints that only is good for the average of multiple patterns. One of the key contributions of this paper is the use of a probabilistic forecast for hot water usage (i.e., a collection of withdrawal patterns from a set of previous days D).

A unique advantage of the stochastic behavior of WH-MILP that no other algorithm presents in the literature is considering dependency between usage in different hours. Other stochastic methods model each interval as an independent random variable. While in reality intervals of consumption are dependent to the previous interval. E.g., if one is taking a shower at 7 PM, the chance of taking a shower again at 8 PM is almost zero for a single resident house. To solve this, WH-MILP feeds the model with D day of withdrawal pattern (each pattern is a vector of withdrawal for each day) rather than feeding it with 24 distribution of withdrawals obtained by finding average and variance of each interval using the past D days which will destroy the correlation between intervals.

To evaluate the effectiveness of stochastic behavior of WH-MILP, The model in equation (9) is tested with different length of $|D|$ samples. So, we first assess how performance changes by solving for different numbers of sample days up to 60 (for longer times, usage patterns

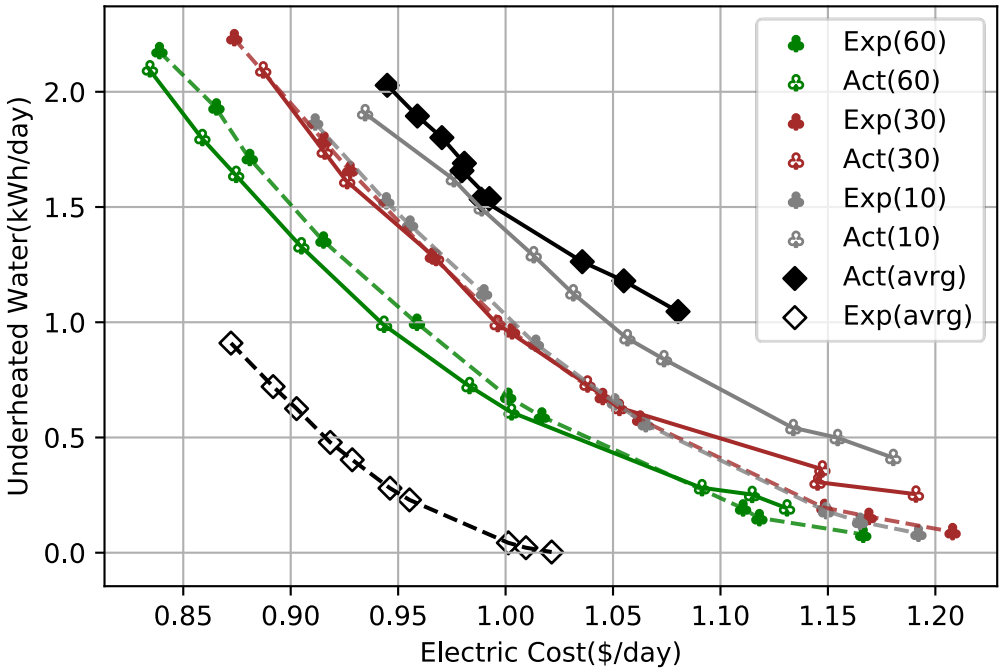

Figure 5 Stochastic optimization results

are more likely to change and computation becomes increasingly difficult). We also test the performance of WH-MILP when using a single sample day equal to the average of usage on the previous 60 days. That is, we solve equation (9) for 10, 30, 60, and the mean of 60 days lookback.

By solving equation (9), we obtain the expected cost for that given day and $\boldsymbol{T}^{\text{set}}$ based on the available forecast. Then we apply the $\boldsymbol{T}^{\text{set}}$ vector to the actual consumption pattern to find the actual cost for that day. For example, for $|D| = 10$, we want to find the expected and actual cost when tomorrow is day 46 of the year. The algorithm solves equation (9) based on consumption pattern of days 45 (today), 44 (yesterday), 43, …, 35. This gives the expected cost for day 46. To find the actual cost of day 46, the obtained $\boldsymbol{T}^{\text{set}}$ From solving equation (9) based on consumption pattern of 45, 44, 43, …, 35 is applied to the actual consumption pattern of day 46. The closer the actual and expected results, the more accurate the algorithm.

the average of all "tomorrow" days is reported as the average performance of the algorithm (both "expected" and "actual"). This process is repeated for different numbers of lookback days and different penalty factors to assess their performance over the course of the same year.

Table 6 error and runtime comparison

	Mean	10	30	60
RMS	3.97	0.74	0.28	0.23
Run Time	2 sec	23 sec	5.7 min	18 min

Figure 5 shows the performance of the model when using 10, 30 and 60 day lookbacks, and when using the mean of the previous 60 days as a single point forecast. This figure shows the expected and actual cost for 10 values of the penalty factor. Table 6 shows the RMS error between the actual and expected cost for 10, 30, 60, and mean of 60 days optimizations.

The 60-day lookback model finds better solutions than the 30-day model, i.e., it is able to reduce the cost of service for a given level of comfort (amount of underheated water). This appears to be because the 60-day model is better able to identify times when hot water use is unlikely and avoid heating water for those times. Both of these have fairly accurate estimates of their own performance. When it runs, the 10-day lookback model expects to have similar performance to the 30-day model, but then actually has about 5 percent worse performance when the setpoints are actually applied. This appears to be due to "surprises," where actual usage differed from the small sample the model used for prediction.

This effect is even more pronounced when using a point forecast consisting of the average usage vector for the previous 60 days. The average-usage model expected to perform very well, but actually performed worst of all the models when the setpoints were applied. This model also had the largest difference between expected and actual performance. This appears to occur for two reasons: (1) the average-usage model overfits to the single forecast vector instead of preparing for a diverse collection of usage vectors, and (2) the average-usage vector has small pulses each hour, which can be served by keeping the tank temperature just above $t^{\min}$, but actual usage may come in much larger pulses, which require a larger thermal reserve to avoid delivering underheated water or being forced to reheat during an expensive time.

The results indicate that extending the lookback period improves the performance of the model. In addition, they show that it is important for water heater setpoints to be scheduled based on a range of realistic usage vectors rather than a single point forecast, even one that minimizes RMSE relative to actual usage vectors (i.e., the mean usage vector).

However, one major defect of WH-MILP is its run time length. For example, the average run time for the 60-day lookback model is about 18 minutes on a single core CPU machine. In future work, we plan to develop reduced models that can provide similarly good solutions in a shorter time.

1.5.3 Sensitivity Analysis

Among all parameters that can affect the performance of CC-WH; There are only two parameters that are more important: the lookback days and the relative gap. In section 1.4 the relative gap was introduced. In this section the effect of changing lookback days and relative gap on the quality of the solution and time of optimization will be evaluated.

1.5.3.1 Effect of changing lookback days

In regard to the lookback parameter, in an ideal scenario, the difference between the average expected and actual cost would be zero. As can be seen in Table 6, the longer the lookback, the closer the actual and expected cost would be. Since the actual and expected results for 60-day lookback are almost converged, it is not expected that longer lookbacks have a better result. In other words, when the model is optimized on a diverse set of withdrawal patterns that its average expected and average actual cost converges, adding more lookbacks days will not add to the diversity of samples and only increased the optimization time.

1.5.3.2 Effect of changing Relative Gap

Another critical parameter in CC-WH is the relative gap. As mentioned before, the absolute gap is the difference between the actual integer solution of the problem (upper bound) with the possible lowest-cost (lower bound) which is the result of LP relaxation; and relative gap is obtained by dividing absolute gap by the upper bound. In the search between branches to find the lowest integer solution, the BnB repeatedly updates the bounds until they converge. The BnB continually tries to find the lowest-cost integer answer (decreasing upper bound) and increasing the lower bound (by investigating through the sub-branches of the problem to see if a low-cost LP answer can lead to a low-cost Integer result). When the bounds converge, the algorithm had found the optimal integer result. In this paper, CPLEX by IBM was used as the optimizer.

To investigate the effect of the optimization gap, we averaged the result of 15 samples of 20-day lookback models while the relative gap was changed from 10 percent to 0 percent. The time limit of the optimization time was 500 seconds. As can be seen in Table 7, the result for the zero gap is about 0.9 percent better than the result of a 10 percent gap. However, the average optimization time of zero gap models is about 13.8 times longer (if the time limit were more, the difference would have been much longer than that). For our models, we picked a conservative optimality gap of 6 percent. However, the results show that we could easily pick 7 or 8 percent without deviating much from the optimal results. The reason for that is that the solver can usually find near optimal integer answer at an early stage of optimization with the help of heuristic algorithms. However, to guaranty that the obtained answer is optimal or near optimal (within the gap range) it keeps searching through all possible low-cost LP relaxed subproblems until no branch is left or lower bound is increased enough so the relative gap becomes within the desired range which is a costly process.

Table 7. Sensitivity on MILP Relative Gap on CPLEX

Gap (%)	0	2	4	6	8	10
Cost ($)	1.0876	1.0880	1.0893	1.0895	1.0920	1.0974
Time (s)	428	149	126	75	41	31

1.5.4 Realtime performance of CC_WH

In the previous section, we showed that the 60-day lookback CC-WH model has almost the best performance that CC-WH can have. However, the question is how good is the best imperfect foresight result in comparison to the time when the model has perfect foresight (best performance). To answer this question, we compared the result of CC-WH in (perfect mode) with the actual performance of the 60-day CC-WH model from Figure 5. As can be seen in Figure 6, The performance of the 60-day lookback model is slightly worse than the perfect foresight result. This shows that the 60-day CC-WH model is finding results that, on average, is very close to the time that it has access to the perfect foresight about withdrawal pattern. This also reaffirms the results from the previous section.

Table 8. Realtime comparison of CC_WH with conventional water heater

	Fixed ($40^{\circ}C$)	Fixed ($60^{\circ}C$)	Du & Lu	Apt & Goh
Underheated water (kWh/day)	1.03	0.26	0.83	0.42
Electric cost ($/day)	1.35	1.42	1.28	1.2
CC_WH electric cost with equal underheated water ($/day)	0.95	1.12	0.98	1.06
CC_WH cost savings (%)	**29**	**21**	**31**	**13**

Also, we investigate the performance of Du&Lu under uncertainty while it has access to the same data that CC-WH has (the last 60-day withdrawal pattern). It is assumed that no other information is given to the CC-WH and Du&Lu to improve their predictions. The Du&Lu uses point forecast to make its decision. Therefore, the mean of the last 60-day look back is the best possible prediction for a method that relies on point forecast. Therefore, the performance of Du&Lu while the prediction is the average of the last 60-days withdrawal pattern was evaluated. As can be seen in

Table 8. the CC-WH has 31 percent more savings in comparison with Du&Lu under the uncertainty of withdrawal on average.

The fix-setpoint model and Apt&Goh do not rely on withdrawal patterns for decision making. Therefore, their performance will be the same as the result that is shown in figure 4. As can be seen, this method has 21 Percent saving in comparison to the Fixed setpoint method on 60 degrees, which is shown in Table 8. Also, if someone keeps their Electric Water heater setpoints to the lowest setpoint (we assume minimum usable temperature is $40^{\circ}C$), then CC_WH can have 29 percent lower cost against them with the same level of comfort. Looking into figure 6, we can see that CC-WH is not only better in case of perfect foresight, it also beats all other algorithms when imperfect foresight about withdrawal pattern is available.

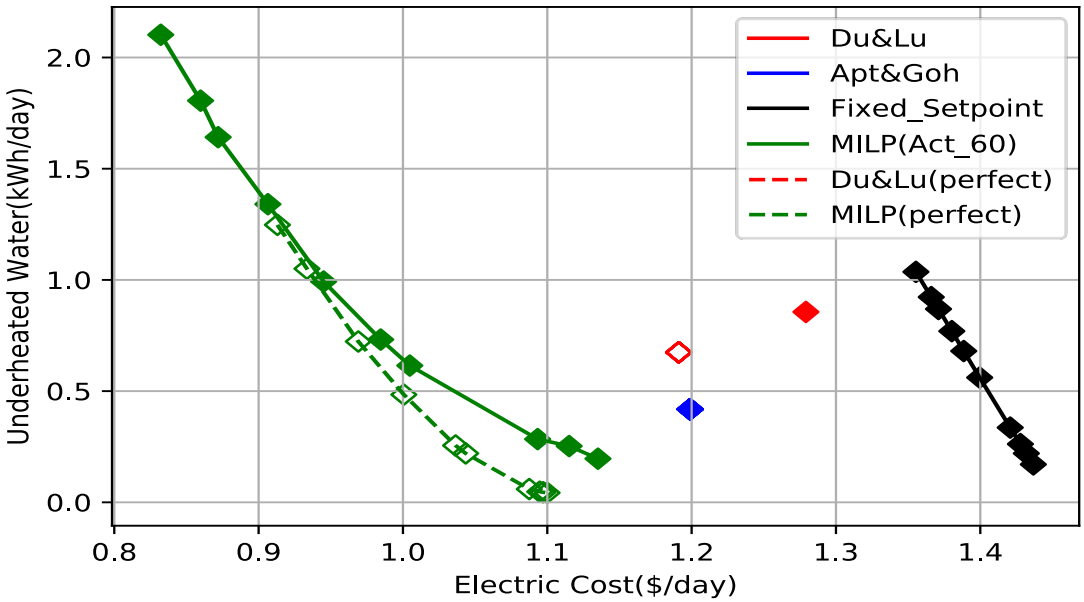

Figure 6. Realtime comparison results

1.6 Nomenclature

Table 9. Nomenclature

Indices	
D	set of historical days, indexed by *d*.
I	set of standard intervals used to divide up each day, usually indexed by *h*.
Constants	
$t^{\min}$	minimum usable temperature by the user.
$t^{\max}$	maximum allowed temperature.
t^{big}	an arbitrarily big temperature e.g., 200 °C.
r^{loss}	normalized heat loss rate per interval (1 hour).
v^{tank}	volume of the water heater tank (liters).
c^{liter}	specific heat of water (kWh of electricity required to raise 1 liter by 1°C).
c^{tank}	the number of degrees that temperature of the water heater would be raised for each kWh of input energy (°C/kWh); given by $c^{\text{tank}} = v^{\text{tank}} c^{\text{liter}}$.
p^{s}	shortfall penalty ($/kWh).
$e^{\max}$	maximum energy input.
w_d	weight of historical day *d* in optimization.
p_h^{p}	power price for interval *h* of the coming day ($/kWh).
t_h^{amb}	ambient temperature (°C) for interval *h* of the coming day.
t_h^{in}	inlet temperature for interval *h* of the coming day. Assumed to be known in advance.
$v_{d,h}^{\text{hist}}$	historical volume withdrawn (liters). The volume of hot water that was used during interval *h* on day *d*.
$e_{d,h}^{\text{des}}$	desired energy withdrawal. The amount of heat that would need to be added to water withdrawn during interval *h* to satisfy users, if household water usage follows the pattern from historical day *d*. Calculated from logged inlet and outlet temperatures and $v_{d,h}^{\text{hist}}$.
$\boldsymbol{e}_d^{\text{des}}$	vector of all the values of $e_{d,h}^{\text{des}}$ on day *d*.
$\boldsymbol{E}^{\text{des}}$	random variable representing possible withdrawal vectors; $\boldsymbol{e}_d^{\text{des}}$ vectors are realizations of this variable.
Decision variables (calculated by model)	
T_h^{set}	thermostat setpoint (°C) for interval *h* of the coming day.

$\boldsymbol{T}^{\mathrm{set}}$	vector of all the values of T_h^{set} on the coming day.
$E_{d,h}^{\mathrm{in}}$	the amount of heating energy that would be used for interval h of each past day d, if the new thermostat setpoints T_h^{set} had been used.

Chapter 2

PV Self-Consumption with EWH

2 Increasing PV Self-Consumption Using Electric Water Heater Thermal Capacity

2.1 Introduction

With the improvement in semiconductor technology, solar panels are becoming cheaper and cheaper day by day. However, solar energy is only available in the day with an unpredictable pattern, making it a non-dispatchable source [60]. One issue that stops the widespread installation of solar panels is the duck-curve [1]issue [61] as shown in Figure 9. In the middle of the day, when solar energy production is at its maximum rate, the total energy production could exceed the total consumption leading to a negative net load in the power system [62]. The negative net load causes numerous issues in the power system, including over-voltage in the grid, increased ramp cost [63], [64]. These issues cause the power systems to reduce buyback plan rates every year. Therefore, it makes the PV self-consumption to be more economical for the user in the future.

One way to increase PV self-consumption is by using larger energy storage units. However, batteries are expensive, and their efficiency reduces over time. One of the promising, supplementary approaches to overcome these issues is increasing PV self-consumption using Demand Response (DR) in home management systems, as is shown in Figure 7. In this method, the energy usage of home appliances is shifted to the middle of the day. DR can shift consumption to off-peak hours or reduce consumption on peak hours in response to electricity price through price-based control (PBC) or direct command from power system utility through direct load control (DLC) method [7].

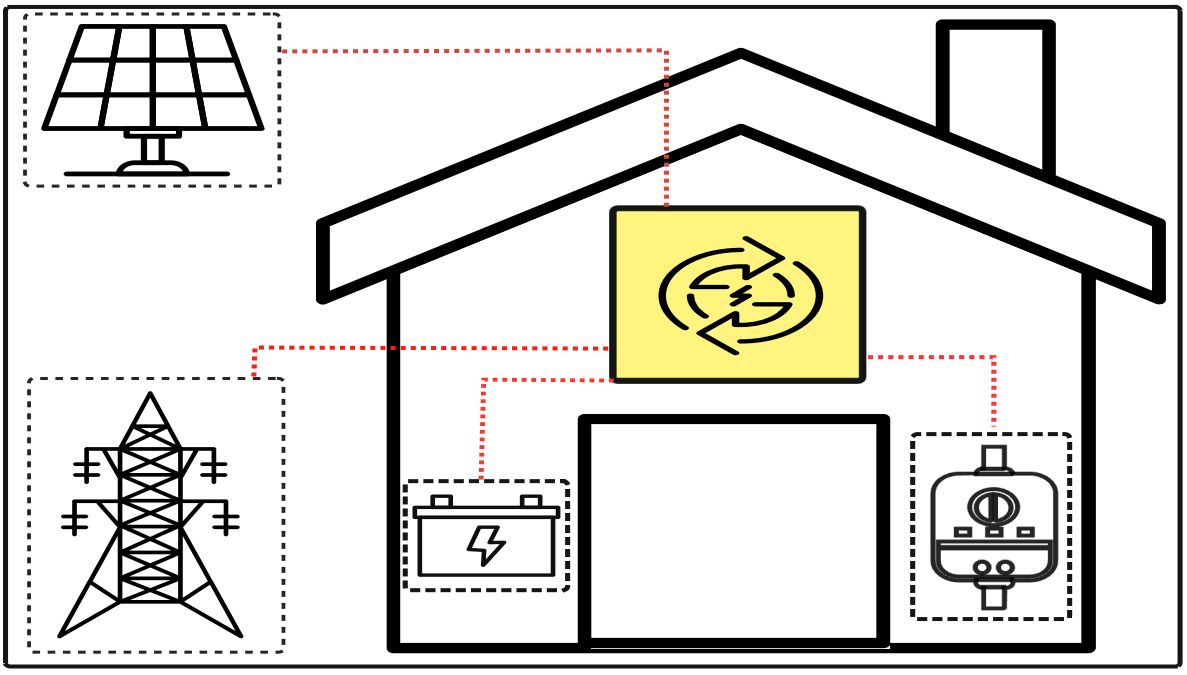

Figure 7 Home Management System

[1] Licensed with permission from the California ISO. Any statements, conclusions, summaries or other commentaries expressed herein do not reflect the opinions or endorsement of the California ISO.

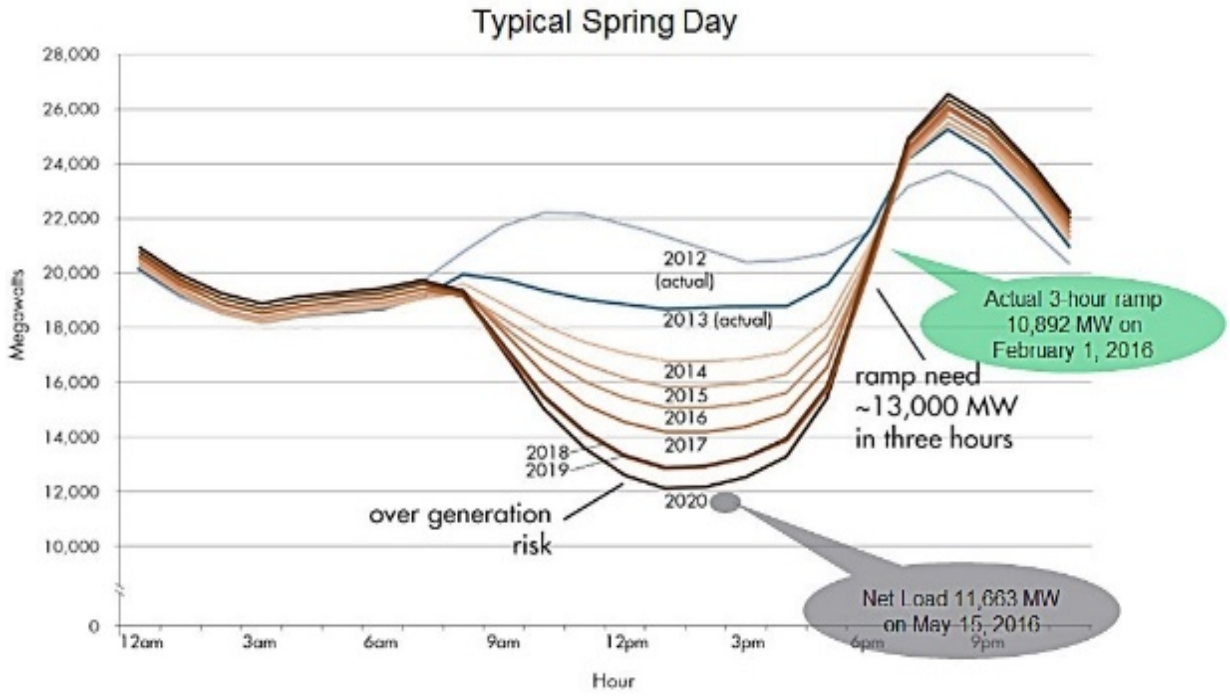

Figure 9 Duck Curve Load Pattern

Under PBC, the power utility propagates time-varying price signals to end-users to motivate them to shift their consumption from expensive hours (peak hours or low renewable generation) to cheap (off-peak or renewable abundant times. i.e., mid-day for solar) hours. Not only can PBC reduce end-user bills, but also it has advantages for power systems such as peak shedding, lowering operational cost, and increased system stability [11].

The dynamic pricing policy is still a matter of discussion in the literature. Different type of dynamic pricing has been used for different purposes such as Day-ahead pricing (DAP), real-time pricing (RTP), critical-peak pricing (CPP) and time-of-use (TOU) pricing[37]. The DAP forecast the price 24 hours ahead to the costumers. Under the DAP the user can schedule their consumption and enjoy the benefits of longer planning time in contrast to RTP when the user can only have access to the price of the next one or two intervals. This feature of DAP enables the large household

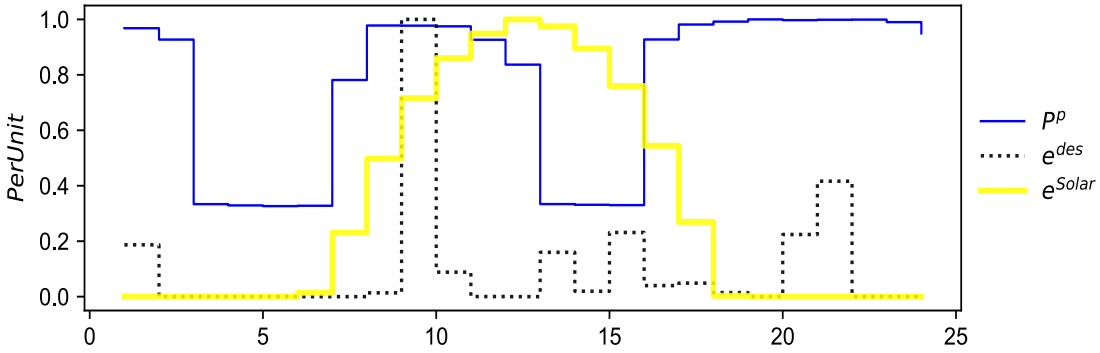

Figure 8 main input parameter with perfect foresight

consumer of energy such as EWH and HVAC to shift their energy input away from the times that the user uses energy. Therefore, EWH can behave as a virtual energy source when energy is cheap (low price) or is free energy (renewable energy).

EWH is an important load, featuring several advantages for DR. It is a relatively large consumer of household energy, consuming around 17 [65] percent of total household energy usage, most of which occurs during peak hour periods [66]. It has a large thermal storage capacity, which could be used as virtual electricity storage. I.e., the working temperature of an EWH can range between 40 and 85 degrees Celsius without affecting user comfort. Furthermore, it has good insulation, enabling it to preserve and shift energy usage more than other appliances.

[67] performs an economic optimization for two separate applications for batteries. Namely, PV self-consumption and demand-load shifting using genetic algorithms. Then they compare under which condition the use of batteries is more cost-efficient and analyzed the trade-off between self-consumption and demand-load shifting. [68] proposed a Mixed Integer Linear Programming (MILP) model, which they call “solar Plus” for scheduling an optimized operation of domestic water heater and air conditioner considering PV and energy storage under dynamic pricing. [69] propose a Model Predictive Control (MPC) method with a horizon of 12 intervals for the forecast hot water consumption for scheduling EWH to maximize PV self-consumption using Linear Programming (LP). Sichilalu et. At [70] work on optimal control model of heat pump water heater while it is supplied by various energy sources such as PV, wind, diesel under TOU electricity tariffs using MILP. [71] propose a data-driven model for scheduling EWH with the goal of maximizing PV self-consumption using reinforcement learning. The proposed model learns occupancy and predicts PV production.

A good EWH scheduling algorithm must take advantage of cheap electricity prices to preheat water while considering user consumption patterns for the upcoming hours. This algorithm must plan to store solar energy in a water heater as much as possible in the middle of the day. However, to store energy, the water heater should have a relatively low temperature. But not very low to cause dissatisfaction.

The implementation of such an algorithm can reduce the electricity bill by taking advantage of cheap electricity hours and free solar energy in the middle of the day while minimizing the chance of under heated water by considering user consumption. By storing energy in the middle of the day, EWH can store solar energy, which will reduce the need for a big battery in solar-equipped households. Also, it can reduce the number of charge and discharge of the battery, leading to increased expected battery life, which will decrease the operation cost of a household solar system.

Considering the need for DR methods that can increase PV self-consumption and the need for price-responsive household instruments, this paper proposes a method that can increase PV Self-consumption under DAP pricing. Furthermore, the proposed method improves user comfort under a unique method that defines user thermal comfort based on the undelivered amount of energy rather than a strict limit of the working temperature of EWH. Implementing such an algorithm has no trade-off. i.e., improving only one quality, while another quality is reduced. This algorithm can

reduce operational cost, implementation cost, and underheated water at the same time by taking advantage of solar production, cheap DAP hours, and user consumption pattern.

2.2 Method

In this section, the problem will be formulated as a MILP problem. First, the cost function is introduced, and then the constraints of the problem. A short description of variables and inputs is introduced in Table 11 . The problem is formulated under the Day-ahead pricing tariff (DAP). The forecasts such as ambient temperature, user withdrawal pattern, and sun radiation energy is assumed to be perfect for this problem. All the variables are indexed over intervals of tomorrow where $\boldsymbol{T}^{\mathrm{set}} \in \mathbb{R}^{24}$ is the decision variable. The per-unit value of the main input of the problem, e.g., solar radiation energy, energy withdrawal, and DAP price profile, are shown in Figure 8.

2.2.1 Objective

The objective of the problem is to find electric water heater setpoints T_h^{set} such that it minimizes electric cost and user discomfort at the same time by utilizing the cheapest energy source (solar) or cheapest DAP intervals for heating or preheating water. In this model, solar energy is model as an energy source with zero cost. Therefore, the cost function will be as formula (1):

$$\min_{\substack{\boldsymbol{T}^{\mathrm{set}} \in \mathbb{R}^{24} \\ \boldsymbol{x}_d \in \mathbb{R}^n}} \sum_{h \in I} p_h^{\mathrm{p}} E_h^{\mathrm{in}} + p^{\mathrm{s}} E_h^{\mathrm{short}} \tag{1}$$

The p_h^{p} is the DAP tariff for the next day during each interval (hour). The p^{s} is the penalty incurred to the total cost for each kilowatt of undelivered energy to the user ($/kWh). It has the same unit as the price. In this work, the p^{s} is considered constant for all intervals. However, one can change it based on different times of the day to get a different satisfaction level for each hour. If it is kept low, it means that the user is willing to risk having more cold water for having a higher chance of cost-saving. In other words, changing p^{s} from low to high force the algorithm to find optimal answers on the Pareto front that find answers with higher savings/chance of having cold water in one end of the Pareto and the reverse on the other side of the Pareto. The $p^{\mathrm{s}} E_h^{\mathrm{short}}$ is the amount of undelivered amount of energy to the user due to cold water. Therefore, the algorithm tries to minimize the user electric cost and amount of undelivered energy (discomfort).

2.2.2 Constraints

The constraints force the decision variables to take the right values that are consistent with the behavior of an actual EWH. They are grouped into four categories. Each group represents a section of the behavior of EWH. The thermodynamic constraint represents what will happen to the state of EWH temperature when energy is added or withdrawn. Working modes of EWH defines three different behavior of EWH in regard to the $\boldsymbol{T}^{\mathrm{set}}$. Temperature and energy shortfall are to model the user comfort. The solar constraints model solar energy effect on EWH. In addition to the constraints below, all decision variables are constrained to be non-negative (≥0).

2.2.2.1 Thermodynamic Model

The T_h^{tank} state depends on its previous state of temperature, i.e., $T_{(h-1)}^{\text{tank}}$ Ambient temperature and added/removed energy (withdrawn) from EWH. The following constant which was presented in [59] is used to model the thermodynamic behavior of EWH.

$$T_h^{\text{tank}} = T_{(h-1)}^{\text{tank}} + \frac{\left(E_h^{\text{total}} - E_h^{\text{w}}\right)}{c^{\text{tank}}} - r^{\text{loss}} \cdot \left(T_h^{\text{tank}} - t_h^{\text{amb}}\right) \quad (2)$$

2.2.2.2 Working states of EWH

In this work, the thermostat setpoints are separate from the actual temperature of EWH. This is especially useful when the model is solved for more than one-day lookback, as we did in our previous work [72]. Three different situations could happen based on the relation between $\boldsymbol{T}^{\text{set}}$ and actual temperature of the EWH: Coasting mode (when the setpoint is above tank temperature, which means no need to add any energy to the tank, $C_h = 1$, $M_h = 0$). The Max-power mode (where the desired optimal setpoint is so high that it can't reach it but EWH should work with its maximum capacity, $C_h = 0$, $M_h = 1$). The normal Mode (when reaching the desired setpoint is attainable, and the energy input will be between zero and maximum power, $C_h = 0$, $M_h = 0$). The following constraints force the model to take the right values for these three states:

$$T_h^{\text{tank}} + M_h \cdot t^{\text{big}} \geq T_h^{\text{set}} \quad (3)$$

$$T_h^{\text{tank}} \leq T_h^{\text{set}} + C_h \cdot t^{\text{big}} \quad (4)$$

$$E_h^{\text{total}} \geq M_h \cdot (e^{\max} + e_h^{solar}) \quad (5)$$

$$E_h^{\text{total}} \leq (1 - C_h) \cdot (e^{\max} + e_h^{solar}) \quad (6)$$

The combination of these four constraints forces the model to take the right value whether EWH can reach the desired setpoint or not. The C and M variables are binary. Combination of them can create four different states for these constraints. Out of these four, three of them is used to model three different states of EWH. The fourth one is simple infeasible ($C_h = 1$, $M_h = 1$).

2.2.2.3 Temperature and Energy Shortfall

The user comfort in this work is modeled as a cost of an undelivered amount of energy rather than a strict constraint on minimum temperature. i.e., despite other methods where there is a hard limit on the minimum temperature, solar-EWH can let the temperature drop below the minimum, but it incurs discomfort cost to the objective function. This is especially useful on days when a large burst of withdrawals happens.

$$T_h^{\text{short}} \geq t^{\min} - T_h^{\text{tank}} \quad (8)$$

In cases when a large burst of withdrawal happens, a large temperature drop (more than the difference of max minus min temperature) will happen. Models based on a strict limit on minimum temperature would have an infeasible answer for these cases.

Cost-based comfort is also better when a user needs to find its optimal point in the cost-comfort Pareto front. i.e., to change comfort level in constraint-based models, the user can only lower to minimum temperature. This leads to under heated water most of the time when energy is expensive since EWH sees no problem lowering the minimum temperature. On the other hand, if we let the temperature to fall below minimum (when energy is very expensive or huge burst of withdrawal happens) EWH tries to avoid very low temperature unless it has a significant saving or no energy withdrawal is predicted in the coming hours (low temperature won't cause dissatisfaction since EWH is not expected to be used). These reasons make cost-based treatment of comfort to be more desirable than constraint treatment.

The following model nonlinear behavior of discomfort. The key is the T_h^{short}. If the temperature is above, the is no dissatisfaction. Therefore, the T_h^{short} must be zero. If the temperature is fallen below minimum, the T_h^{short} will be proportional to the distance between minimum and actual temperature. This nonlinear behavior is modeled using the following four constraints.

$$T_h^{\text{short}} \leq t^{\min} - T_h^{\text{tank}} + (1 - B_h) * t^{\text{big}} \tag{9}$$

$$T_h^{\text{short}} \leq B_h * t^{\text{big}} \tag{10}$$

$$B_h * t^{\text{big}} \geq t^{\min} - T_h^{\text{tank}} \tag{11}$$

$$(1 - B_h) * t^{\text{big}} \geq T_h^{\text{tank}} - t^{\min} \tag{12}$$

As mentioned before, the comfort is the amount of undelivered energy. According to [72], energy shortfall is the amount of thermal energy that would be needed to be added to the water so that the user will not feel discomfort. is calculated by the formula (13):

$$E_h^{\text{short}} = e_h^{\text{des}} \frac{T_h^{\text{short}}}{\left(t^{\min} - t_h^{\text{in}}\right)} \tag{13}$$

Therefore, the amount of actual energy that is used is equal to the amount of energy that has been used minus the undelivered amount of energy.

$$E_h^{\text{w}} = e_h^{\text{des}} - E_h^{\text{short}} \tag{14}$$

Also, the tank temperature must always be kept below the maximum allowed temperature.

$$T_h^{\text{set}} \leq t^{\max} \tag{15}$$

2.2.2.4 Solar Constraints

The available solar energy just below the solar radiation for each hour. Constraint (14) enforces this rule to the model. Also, the available energy for EWH comes from two sources: the electrical source and the solar source. This rule shows itself in the constrain.

$$E_h^{\text{total}} = E_h^{\text{solar}} + E_h^{\text{input}} \tag{14}$$

$$E_h^{\text{solar}} \leq e_h^{\text{solar}}$$

The cost of using an electric source is defined by the price vector. On the other hand, solar energy is free. Therefore, the algorithm prioritizes using solar to the electrical source.

2.3 Results

In this section, we study the performance of solar-EWH given the deterministic price, withdrawal, and solar radiation pattern. This section studies the performance of solar-EWH in the span of 24-hour intervals. Here, we show what will happen to the state of temperature, energy input, battery state, self-absorption, based on the decision that the model makes (temperature setpoints) given the deterministic inputs where the per-unit values of the important inputs (solar radiation, user withdrawal, and price) are shown in figure 10. that are fed to the models. i.e., user withdrawal, ambient temperature, solar energy production, etc.,

Figure 10 shows the state of all variables given the inputs mentioned above based on the decision that the EWH made. The first section of figure 10 shows the state of actual temperature based on the result of optimization, which is the Thermostat setpoint (second section of figure 10). the third section is pertinent to energy inputs and variables. Where the dotted black and yellow shows the desired energy and available solar energy inputs respectively. The orange and light brown colors represent the solar energy and grid energy inputs decision variables, respectively. The fourth section of figure 10 shows the Day-ahead price input.

In this work, the minimum temperature that the user doesn't feel discomfort is considered 40 degrees Celsius. i.e., without mixing hot and cold water, the user is satisfied with the temperature. As it can be seen, the initial temperature of the day is around 38 degrees Celsius. However, if no usage is expected during the intervals when the temperature is below 40 degrees, the user will not feel any discomfort [ref ours]. Therefore, the algorithm can skip adding unnecessary energy addition when solar energy is not available or the price of electricity is high without affecting user comfort.

As can be seen, the main energy withdrawals happen in the morning and afternoon peak. These peaks are between 8-10 am and 5-10 pm, respectively. The first energy withdrawal of the day happens at 8 am. The right decision to provide this need must consider multiple factors, so the cheapest plan is provided while user comfort is satisfied. As it can be seen, 8 am is rather an expensive interval. Also, there is not enough solar energy available to provide this energy. Therefore, the algorithm peaks the cheapest interval before 8 am, which is at 4 am. At 4 am, the solar-EWH just adds enough energy so that this energy and all of the upcoming available solar energy can provide just enough energy to the user so that the actual temperature (first section of figure 10) is reached 40 degrees, which is means the user will not feel dissatisfaction. Therefore, in short, to provide morning peak energy, the solar-EWH: 1- uses all available solar energy. 2- avoids adding energy from the grid at 8 am since it is an expensive interval. 3- after using all solar energy, it provides the rest of the needed energy by preheating the water. As it is shown in section 3 of figure 10, this interval is 4 am for the given inputs. The rest of the morning energy needs at 9 and 10 am are totally provided by solar energy, and no energy from the grid is added to the EWH.

In the middle of the day (11 am to 2 pm) no energy usage is expected. Therefore, no energy is added (not from solar source nor from the grid). Therefore, energy falls below 40 degrees Celsius. However, any algorithm that forces the EWH temperature to be strictly above the minimum will lose this change of saving energy.

The afternoon energy withdrawal pattern happens between 5-10 pm. At these intervals, the price of energy is high. Therefore, a good scheduling strategy would preheat the water to make it ready for the afternoon peak. At the same time, preheating should not be far from consumption since it will cause energy to lose. As it is shown in figure 10, the solar-EWH starts preheating water at 14 pm, so that just right before the afternoon peak (16 pm), the temperature is reaching the maximum possible temperature (80 degrees in this work). However, as mentioned before, the preheating did not start sooner, so that reaching the maximum temperature would have happened sooner than interval 16th. Since it just would have increased energy losses.

TABLE 10 SELF-ABSORPTION DATA

Available Solar	needed energy	Percent of self-absorption	Total Cost Reduction
$\sum e_h^{solar}$	$\sum e_h^{\mathrm{des}}$	$\sum E_h^{\mathrm{solar}} / \sum e_h^{solar}$	$\sum E_h^{\mathrm{solar}} * p_h^{\mathrm{p}}$
48 Kw	25 Kw	52 %	$1.49

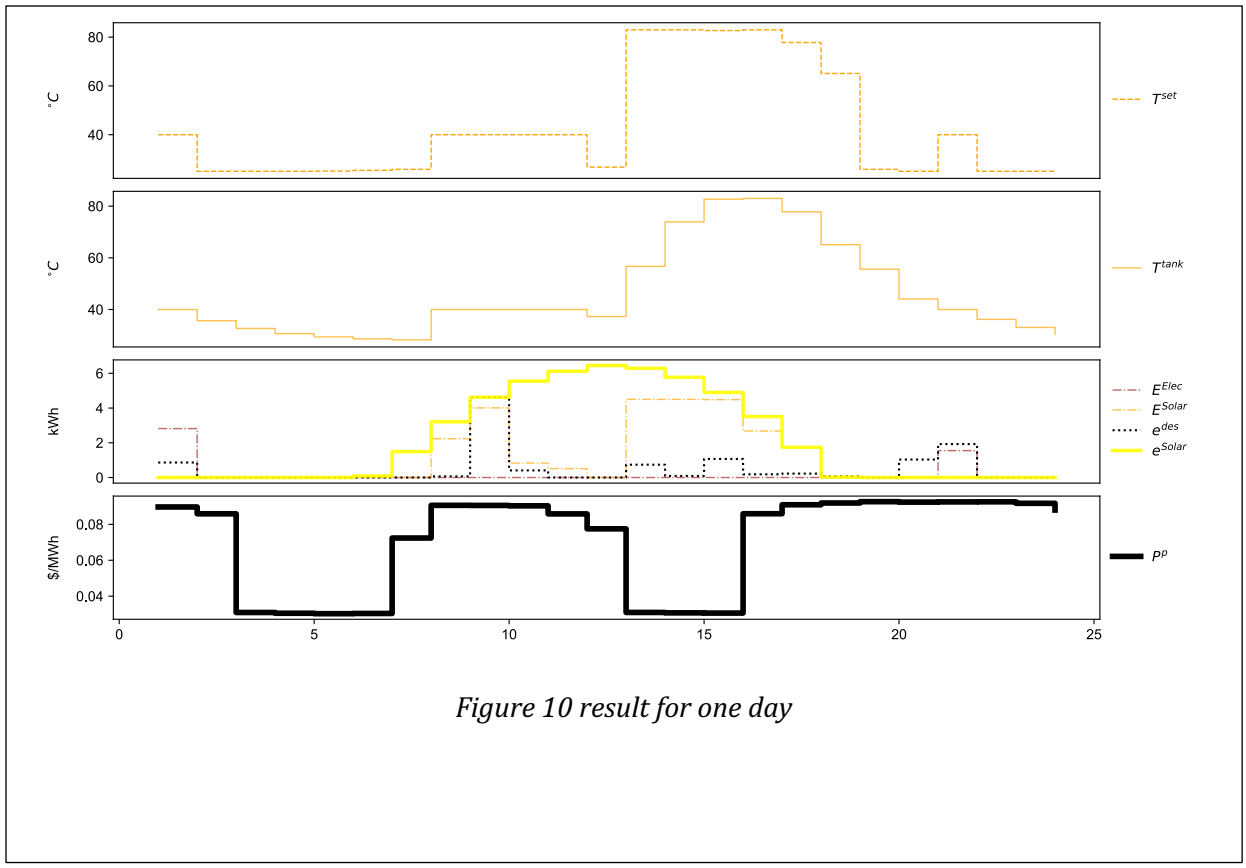

Figure 10 result for one day

The rest of the energy need of the day after 19 pm is provided by the energy grid while it added only enough energy to the water so that hot water with minimum acceptable is provided to the user.

2.3.1 PV self-absorption

Table 10 shows the summary of the energy consumption pattern. During the given day, 48 Kw of energy was radiated on the solar panels during the day. Without a DR program that can increase the PV self-consumption, given that the peak of household energy usage is usually in the morning and afternoon, only a small portion of this energy would have been used directly by the appliances. However, by using the solar-EWH plan, the EWH used 25 Kw out of 48 Kw available solar. Meanwhile, by using this free source of energy, the household could save $1.49. This plan showed it for these specific inputs, i.e., solar radiation, price, hot water withdrawal, it could use 52 percent of the whole available

2.4 Conclusion

in this paper, a new comprehensive control strategy for control of EWH for minimizing electric cost and user discomfort is provided while at the same time, it lets the EWH perform the auxiliary task of acting as a high-capacity solar energy absorber. The proposed method not only can reduce the operation cost of a household but also it can reduce the installation cost since it would need a smaller battery and inverter but also it can reduce the operational cost by preferring solar energy over grid energy and also by choosing cheap intervals over expensive ones by preheating hot water.

Solar-EWH can increase PV self-consumption using the thermal energy storage capacity of EWH. The problem is model as MILP optimization model that takes advantage of cheap electricity price, available solar energy while providing the user with the satisfactory service that is expected from an EWH.

2.5 Nomenclature

TABLE 11 LIST OF MODEL PARAMETERS

Constants	
$t^{\min}$, $t^{\max}$	Minimum and maximum usable temperature.
t^{big}	an arbitrarily big temperature e.g., 200 °C.
$\mathrm{r}^{\mathrm{loss}}$	normalized heat loss rate per interval (1 hour).
$\mathrm{c}^{\mathrm{tank}}$	the number of degrees that temperature of the water heater would be raised for each kWh of input energy (°C/kWh)
p^s	Shortfall penalty ($/kWh).
e^{max}	Maximum energy input.
e_h^{solar}	available solar energy available in each interval
p_h^{p}	Power price for interval h of the coming day ($/kWh).
t_h^{amb}	ambient temperature (°C) for interval h of the coming day.
t_h^{in}	inlet temperature for interval h of the coming day. Assumed to be known in advance.
e_h^{des}	desired energy withdrawal. The amount of heat that would need to be added to water withdrawn during interval h to satisfy users.
Decision variables (calculated by model)	
T_h^{set}	Thermostat setpoint (°C) for interval h of the coming day.
T_h^{tank}	Temperature of the water heater during interval h.
T_h^{short}	Temperature shortfall (°C) during the interval. This is the amount by which the tank temperature would fall short of minimum usable temperature (if any), if the setpoints T_h^{set} were used with hot water usage.
E_h^{in}	the amount of heating energy that would be used for interval h, if the new thermostat setpoints T_h^{set} had been used.
E_h^{w}	Amount of energy (in kWh) withdrawn from the tank during interval h, due to hot water usage.
E_h^{short}	Energy shortfall (kWh) during interval h. This is the amount of additional heat that would need to be added to hot water used by the household in order to correct the temperature

	shortfall (if any), i.e., the amount of heat that is "missing" from the hot water supply.
E_h^{solar}	A portion of available solar energy in interval h that is consumed to the EWH
E_h^{total}	The total energy that is added to the EWH in interval h which is a combination of grid and solar energy.
C_h, M_h	binary variables indicating whether the water heater is in "coasting" or "maximum power" mode during interval h.
B_h	Binary variable controlling nonlinear behavior of T_h^{short} during interval h. i.e., $\max\left(0, t^{\min} - T_h^{\text{tank}}\right)$.

2.6 Appendix

This appendix derives several relationships between historical hot water usage, hot water usage on simulated days, and the thermodynamic behavior of the water heater. These are used as the basis for several equality constraints in the water heater model, defining the values for some key decision variables.

Suppose that during interval *h* on historical day *d*, the household used a volume of mixed hot and cold water $v_{d,h}^{\text{mixed}}$, and desired this volume of water at a temperature of $t^{\min}$. (Our standard assumption in this work is that customers are satisfied with water at a temperature of $t^{\min}$ and unsatisfied with temperatures below that; future work may investigate different desired temperatures for different end uses, and different degrees of dissatisfaction for deviations from these temperatures.) Then the total desired thermal energy of the mixed water is given by

$$e_{d,h}^{\text{des,tot}} = c v_{d,h}^{\text{mixed}} t^{\min}, \tag{45}$$

where *c* is the specific heat per liter of water (shortened from c^{liter} used in the main body of this proposal). We neglect the weak temperature dependency of *c*. The right side of equation (45) can be written as a sum of the thermal energy in the cold water and hot water that were mixed to supply this usage, plus any shortfall that may have occurred due to underheated water:

$$e_{d,h}^{\text{des,tot}} = e_{d,h}^{\text{cold}} + e_{d,h}^{\text{hot}} + e_{d,h}^{\text{short}} = c v_{d,h}^{\text{cold}} t_{d,h}^{\text{in}} + c v_{d,h}^{\text{hist}} t_{d,h}^{\text{out}} + c v_{d,h}^{\text{hist}} t_{d,h}^{\text{short}}, \tag{46}$$

where $v_{d,h}^{\text{cold}}$ is the volume of cold water used, $v_{h,d}^{\text{hist}}$ is the amount of hot water used, and $t_{d,h}^{\text{short}}$ is the temperature shortfall, defined as $t_{d,h}^{\text{short}} = \max\left(0, t^{\min} - t_{d,h}^{out}\right)$. Other terms are defined in the main body of this proposal. Note that we assume that if $t_{d,h}^{\text{short}} > 0$, customers would desire to have the same volume of water, with the shortfall corrected.

Substituting $v_{d,h}^{\text{cold}} = v_{d,h}^{\text{mixed}} - v_{d,h}^{\text{hist}}$ gives

$$\begin{aligned} e_{d,h}^{\text{des,tot}} &= c\left(v_{d,h}^{\text{mixed}} - v_{d,h}^{\text{hist}}\right) t_{d,h}^{\text{in}} + c v_{d,h}^{\text{hist}} t_{d,h}^{\text{out}} + c v_{d,h}^{\text{hist}} t_{d,h}^{\text{short}} \\ &= c\left[\left(v_{d,h}^{\text{mixed}} - v_{d,h}^{\text{hist}}\right) t_{d,h}^{\text{in}} + v_{d,h}^{\text{hist}}\left(t_{d,h}^{\text{out}} + t_{d,h}^{\text{short}}\right)\right] \\ &= c\left[v_{d,h}^{\text{mixed}} t_{d,h}^{\text{in}} + v_{d,h}^{\text{hist}}\left(t_{d,h}^{\text{out}} + t_{d,h}^{\text{short}} - t_{d,h}^{\text{in}}\right)\right]. \end{aligned} \tag{47}$$

Our water heater model considers scenarios where the user has the same desire for hot water on the coming day as on day *d*, but the cold water temperature is now t_h^{in} and the water heater uses new setpoints $T_{d,h}^{\text{set}}$, resulting in outlet temperature $T_{d,h}^{\text{tank}}$ and shortfall $T_{d,h}^{\text{short}}$. In this case, the user would still desire the same energy service, and the desired energy content of the water would again equal the sum of the thermal energy in the cold water and hot water, plus any shortfall that occurs:

$$e_{d,h}^{\text{des,tot}} = E_{d,h}^{\text{cold}} + E_{d,h}^{\text{hot}} + E_{d,h}^{\text{short}} = c V_{d,h}^{\text{cold}} t_h^{\text{in}} + c V_{d,h}^{\text{w}} T_{d,h}^{\text{tank}} + c V_{d,h}^{\text{w}} T_{d,h}^{\text{short}}, \tag{48}$$

Note that most of the terms in this equation are capitalized, indicating that they are dummy decision variables which depend on the setpoints chosen for the water heater. We have also introduced the new variables $V_{d,h}^{\text{cold}}$ (volume of cold water used), $V_{d,h}^{\text{w}}$ (volume of hot water used) and $T_{d,h}^{\text{short}} = \max\left(0, t^{\min} - T_{d,h}^{\text{tank}}\right)$ (temperature shortfall). All the variables in this equation reflect conditions that *would* occur tomorrow with setpoints $T_{d,h}^{\text{set}}$ if water usage matches day d.

Substituting $V_{d,h}^{\text{cold}} = v_{d,h}^{\text{mixed}} - V_{d,h}^{\text{w}}$ gives

$$\begin{aligned} e_{d,h}^{\text{des,tot}} &= c\left(v_{d,h}^{\text{mixed}} - V_{d,h}^{\text{w}}\right)t_h^{\text{in}} + cV_{d,h}^{\text{w}}T_{d,h}^{\text{tank}} + cV_{d,h}^{\text{w}}T_{d,h}^{\text{short}} \\ &= c\left[\left(v_{d,h}^{\text{mixed}} - V_{d,h}^{\text{w}}\right)t_h^{\text{in}} + V_{d,h}^{\text{w}}\left(T_{d,h}^{\text{tank}} + T_{d,h}^{\text{short}}\right)\right] \\ &= c\left[v_{d,h}^{\text{mixed}}t_h^{\text{in}} + V_{d,h}^{\text{w}}\left(T_{d,h}^{\text{tank}} + T_{d,h}^{\text{short}} - t_h^{\text{in}}\right)\right]. \end{aligned} \tag{49}$$

Combining equations (45) and (49) gives

$$cv_{d,h}^{\text{mixed}}t^{\min} = c\left[v_{d,h}^{\text{mixed}}t_{d,h}^{\text{in}} + v_{d,h}^{\text{hist}}\left(t_{d,h}^{\text{out}} + t_{d,h}^{\text{short}} - t_{d,h}^{\text{in}}\right)\right], \tag{50}$$

and solving for $v_{d,h}^{\text{mixed}}$ gives

$$v_{d,h}^{\text{mixed}} = v_{d,h}^{\text{hist}}\frac{t_{d,h}^{\text{out}} + t_{d,h}^{\text{short}} - t_{d,h}^{\text{in}}}{t^{\min} - t_{d,h}^{\text{in}}}. \tag{51}$$

Combining equations (49) and (47) gives

$$v_{d,h}^{\text{mixed}}t_h^{\text{in}} + V_{d,h}^{\text{w}}\left(T_{d,h}^{\text{tank}} + T_{d,h}^{\text{short}} - t_h^{\text{in}}\right) = v_{d,h}^{\text{mixed}}t_{d,h}^{\text{in}} + v_{d,h}^{\text{hist}}\left(t_{d,h}^{\text{out}} + t_{d,h}^{\text{short}} - t_{d,h}^{\text{in}}\right),$$

so

$$V_{d,h}^{\text{w}}\left(T_{d,h}^{\text{tank}} + T_{d,h}^{\text{short}} - t_h^{\text{in}}\right) = v_{d,h}^{\text{hist}}\left(t_{d,h}^{\text{out}} + t_{d,h}^{\text{short}} - t_{d,h}^{\text{in}}\right) + v_{d,h}^{\text{mixed}}\left(t_{d,h}^{\text{in}} - t_h^{\text{in}}\right). \tag{52}$$

Substituting equation (51) into equation (52) gives

$$\begin{aligned} V_{d,h}^{\text{w}}\left(T_{d,h}^{\text{tank}} + T_{d,h}^{\text{short}} - t_h^{\text{in}}\right) &= v_{d,h}^{\text{hist}}\left(t_{d,h}^{\text{out}} + t_{d,h}^{\text{short}} - t_{d,h}^{\text{in}}\right) + v_{d,h}^{\text{hist}}\frac{t_{d,h}^{\text{out}} + t_{d,h}^{\text{short}} - t_{d,h}^{\text{in}}}{t^{\min} - t_{d,h}^{\text{in}}}\left(t_{d,h}^{\text{in}} - t_h^{\text{in}}\right) \\ &= v_{d,h}^{\text{hist}}\left(t_{d,h}^{\text{out}} + t_{d,h}^{\text{short}} - t_{d,h}^{\text{in}}\right)\left[1 + \frac{t_{d,h}^{\text{in}} - t_h^{\text{in}}}{t^{\min} - t_{d,h}^{\text{in}}}\right]. \end{aligned} \tag{53}$$

We now define

$$e_{d,h}^{\text{des}} \equiv c \cdot V_{d,h}^{\text{w}} \cdot \left(T_{d,h}^{\text{tank}} + T_{d,h}^{\text{short}} - t_h^{\text{in}}\right) = c \cdot v_{d,h}^{\text{w}} \cdot \left(t_{d,h}^{\text{out}} + t_{d,h}^{\text{short}} - t_{d,h}^{\text{in}}\right)\left[1 + \frac{t_{d,h}^{\text{in}} - t_h^{\text{in}}}{t^{\min} - t_{d,h}^{\text{in}}}\right] \tag{54}$$

The term $e_{d,h}^{\text{des}}$ can be thought of as the desired heat content of the hot water supply, relative to the inlet temperature ($e_{d,h}^{\text{des,tot}}$ was the desired heat relative to absolute zero). This equation is used to define the $e_{d,h}^{\text{des}}$ parameter in the water heater model.

The energy shortfall $E_{d,h}^{\text{short}}$ is the amount of energy that would need to be added to the hot water withdrawn by users to compensate for the temperature shortfall, if any. That is,

$$E_{d,h}^{\text{short}} = cT_{d,h}^{\text{short}}V_{d,h}^{\text{w}} \tag{55}$$

We next make the definition

$$E_{d,h}^{\text{w}} \equiv e_{d,h}^{\text{des}} - E_{d,h}^{\text{short}} = e_{d,h}^{\text{des}} - cT_{d,h}^{\text{short}}V_{d,h}^{\text{w}}. \tag{56}$$

The term $E_{d,h}^{\text{w}}$ is the amount of heat that would be withdrawn from the water heater during interval h of the coming day, if water usage matches day d. The relationship between $E_{d,h}^{\text{w}}$ $e_{d,h}^{\text{des}}$, and $E_{d,h}^{\text{short}}$ in the water heater model is fixed via an equivalent constraint.

Substituting the first half of equation (54) into t he second half of equation (56) gives,

$$\begin{aligned} E_{d,h}^{w} &= cV_{d,h}^{w}\left(T_{d,h}^{tank} + T_{d,h}^{short} - t_h^{in}\right) - cT_{d,h}^{short}V_{d,h}^{w} \\ &= cV_{d,h}^{w}\left(T_{d,h}^{tank} - t_h^{in}\right). \end{aligned} \tag{57}$$

We can now derive an equation for the change in the tank temperature from one interval to the next, i.e., a discrete-time model of the water heater's thermodynamics. First, we write the equation for conservation of energy between intervals, assuming all activities are concentrated at the start of the interval. Total thermal energy in the tank at the end of interval h on day d is equal to thermal energy at the end of the prior interval, plus energy added via the heating element, plus the change in energy due to replacing withdrawn hot water with cold water, minus thermal losses to the surrounding environment:

$$c^{\text{tank}}T_{d,h}^{\text{tank}} = c^{\text{tank}}T_{d,(h-1)}^{\text{tank}} + E_{d,h}^{\text{in}} + cV_{d,h}^{\text{w}}(T_{d,h}^{\text{tank}} - t_h^{\text{in}}) - r^{\text{loss}}c^{\text{tank}}\left(T_{d,h}^{\text{tank}} - t_h^{\text{amb}}\right)$$

Dividing this by c^{tank} and substituting $cV_{d,h}^{w}\left(T_{d,h}^{tank} - t_h^{in}\right) = E_{d,h}^{w}$ from equation (57) gives

$$T_{d,h}^{\text{tank}} = T_{d,(h-1)}^{\text{tank}} + \frac{\left(E_{d,h}^{\text{in}} - E_{d,h}^{\text{w}}\right)}{c^{\text{tank}}} - r^{\text{loss}} \cdot \left(T_{d,h}^{\text{tank}} - t_h^{\text{amb}}\right). \tag{58}$$

This relationship is included in the water heater model via an equivalent constraint.

Finally, we derive one additional relationship that is useful for the water heater model. Solving equation (54) for $V_{h,d}^{\text{w}}$ gives

$$V_{d,h}^{\text{w}} = \frac{e_{d,h}^{\text{des}}}{c\left(T_{d,h}^{\text{tank}} + T_{d,h}^{\text{short}} - t_h^{\text{in}}\right)} = \frac{e_{d,h}^{\text{des}}}{c\left(t^{\min} - t_h^{\text{in}}\right)}. \tag{59}$$

Substituting (59) into (55) gives

$$E_{d,h}^{\text{short}} = e_{d,h}^{\text{des}} \frac{T_{d,h}^{\text{short}}}{\left(t^{\min} - t_h^{\text{in}}\right)}. \tag{60}$$

This relationship is also included in the water heater model via an equivalent constraint.

Chapter 3

3 Market-Based Coordination of Price-Responsive Demand Using Dantzig-Wolfe Decomposition Method

3.1 Introduction

power systems structure is rapidly changing. Every day, new renewable and non-renewable Distributed Generation (DG) is being added to the power systems. Utility-scale storage systems and flexible and Demand Responsive (DR) loads are also added. Alongside the development of these technologies, the emergence of fast and reliable communication technologies such as 5G provided a two-way communication path between the generation and consumption sides in power systems. These changes created unprecedented challenges and opportunities in power systems[73], [74]. Control of demand alongside the generation side has been proposed to overcome these challenges. This objective has numerous advantages for the modern grids, such as balancing supply and demand, integrating larger portions of renewable energy, and auxiliary services such as frequency and voltage provisioning. Many different approaches have been proposed for the joint coordination of appliances in the literature[75]. Among these approaches, the collective coordination of price-responsive devices (PRD) is taking more momentum.

On top of the above advantages, the collective control of PRDs has numerous benefits for power systems, such as the incorporation of a larger share of renewables, stabilizing the grid by providing ancillary services such as voltage and frequency provisioning, peak shedding, and creating a market for unused renewable energy, and reducing generation cost [76]. One of the strategies to coordinate appliances is through central controllers[77], [78]. These approaches send the control signal to the appliances to achieve a specific objective, such as valley filling or generation cost minimization. In [79], [80], the authors proposed a solution for the valley filling problem. In these open-loop controllers, where no feedback (here the energy bid) is received from the end-users, may not necessarily be optimal for the end-user. E.g., the central controller asks users to change their consumption at a particular time. However, changing the energy plan forcefully is not desirable for the users.

Given that there was no effective communication method nor price or demand responsive appliances in the grid in the past, these approaches were beneficial. However, with the increased share of demand-responsive appliances such as batteries, EVs, and TCAs, not only a central control approach will lose the chance of optimal solutions, but also, due to the response to the price signals, an open-loop central control signal may yield solutions that are even worse compared to the time when only non-price responsive appliances exist. So, in short, a grid with a large share of price-responsive appliances can act like a double-sided knife. To overcome these undesirable outcomes, many studies proposed distributed coordination of flexible demands [81].

3.1.1 Paradigm of this work

in this paper, we develop a distributed market-based appliance coordination algorithm. The PRDs are modeled as privately rational individuals that try to minimize their local costs. The demand-responsive appliances consist of Electric Vehicles (EVs) as a sample of shiftable loads and Electric Water Heater (EWH) as a sample of Thermostatically Controlled Appliances (TCA). The appliances only communicate with an aggregator, whose only job is to gather information, execute the algorithm, and send back the price signal. The appliances do not share any information with each other, and we assume they do not have market power individually or create a coalition to manipulate the algorithm in their favor.

the main novelties of this work are:

(a) factor in private preferences for good service vs. cost reductions, (b) coordinate devices like EVs and customer-sited batteries that may have an all-or-nothing response to prices (and are likely to be on the margin often, so they are important to coordinate), and (c) can scale to incorporate any number of devices with any valid price response.

3.2 Related Works

This section reviews the methods that tackle device coordination problems where each individual response is important in the decision-making process. These methods have different objectives, such as generation cost minimization or valley filling. However, the results of these two objectives are closely correlated. I.e., pursuing an optimal answer for one objective will yield a near-optimal answer for the other objective. E.g., if one is pursuing to minimize the generation [82], the final aggregate load will get close to a flat line. In other words, the valleys are filled (near-optimal result for valley filling objective)[83]. While grid operators can have different objectives which could be closely correlated, as mentioned in [84], [85], the demand-responsive loads can be modeled in two different ways: 1- following the operator objective [86] (direct load control (DLC)). 2- following self-benefits [82] in a market-based fashion to bid their energy based on the price signal.

While pursuing the grid operator objective can have direct benefits for the operator (reduced generation costs), it can also have indirect benefits for the end-user as a form of discount or credit. However, while these indirect benefits could be beneficial, they may not be optimal for the end-user. This lack of optimality can prevent end-users from joining such programs.

Therefore, the market-based approaches are more appealing to the end-user since it gives them the ultimate benefit and freedom of choice. One of the leading chains of literature when it comes to distributed market-based coordination of appliances when appliances are modeled as self-benefiting and competing unit are based on the game theory framework [82], [83], [87]–[89].

The authors in [90] claim that intra-day and stationary coordination of appliances is not optimal. They prove that short-term scheduling (day-ahead) will be suboptimal in a longer time horizon. Therefore, they propose a scheme based on longer-horizon and nonstationary DSM where the billing and discomfort costs will reduce by up to 50% for the customers who adopt their plan.

[91] is based on Mean Field Game (MFG) approach. In the MFG methods, the individual response of the agents is not essential. However, the critical factor for decision-making is based on the overall agents (mean) response. Each appliance responds to the price signal in this method, and the appliance population is approximated as infinite. They showed that their model could reach ε-Nash equilibrium when a quadratic term is used in the cost function of appliances.

In [92] authors propose a distributed method using Mean Field Game (MFG) to schedule a large population of thermostatically controlled loads (TCLs). The price-responsive rational agents schedule their energy consumption and participate in frequency provisioning market.

Gan et al. [83] proposed a decentralized optimization model for valley-filling using the elastic energy need of EVs. they formulated a scheduling algorithm for EVs whose objective is to fill the

valley. The EVs respond to the control signal algorithm. The algorithm is solved iteratively until an optimal solution is obtained. The issue with this method is that it is not market-based. i.e., the appliances (here EVs) are supposed to follow the grid objective (valley-filling), not their benefit, i.e., minimizing their costs. Instead, the individual users follow the operator's objective, which is valley filling. While this could be advantageous for the users overall, it was not shown how each user would benefit from using this method, nor was it shown if the energy cost would decrease by using these approaches.

Ref. [89] proposed a distributed method to reach Nash equilibrium (NE) between self-serving plug-in electric vehicles (PEVs). To reach NE, the authors proposed an iterative algorithm where the PEVs respond to a price signal generated based on the average bid of all other PEVs in each iteration. The goal is to make the load pattern of each EV close to all other EVs. However, while it is assumed that EVs are cost-minimizing, it is not clear how they minimize the generation cost or user payments.

Ref. [93] proposes a decentralized algorithm for PEV control that finds a balance between generation cost and the cost associated with overloading and battery degradation. It was shown that under mild conditions, the algorithm converges to a socially accepted coordination between PEVs. An instantaneous billing scheme to shift the peak-time loads is proposed in[94]. The appliances are modeled as selfish units. The authors proposed different methods for different scenarios to reach NE. e.g., when loads are controlled, centralized, or distributed.

Rivera et al. [85] proposed a distributed optimization method for scheduling EVs based on the Alternating Direction of Multipliers (ADMM). They proposed a generic multi-objective optimization platform where the cost function is a weighted sum of aggregator and local user objectives. Using this generic platform, they solve the EV coordination problems with two different objectives. i.e., valley-filling and cost minimization. the size of the problem expands linearly with the increment in the size of the EV’s fleet. However, the proposed multi-objective is a weighted sum of end-user’s goals and the operator's goals. Therefore, based on the value of weights, an unfair bias could be enforced upon end-users or the operator.

Using the ADMM method proposed in [85], authors in [95] proposed a method for coordination of EV fleet where local objective optimally schedules EV’s charging session and on a higher level, the Macro Load Area Aggregator (MLAA) provides the DER with generation profiles. The method research Walrasian [96]equilibrium at its optimum.

As mentioned above, many of these approaches try to coordinate appliances based on different objectives where some claim their method could reach the equilibrium [82]–[84], [86] where the operator or the end-users want to change their consumption plans since the current condition is not optimal for them. While this method could be helpful, many users may not adopt it since it means one side needs to sacrifice their goal so the other side can reach their goals. However, the optimum point would be when neither side wants to change their generation/consumption plan. I.e., if a price is announced based on the marginal cost of generation to the customers based on the previous energy plan of the customers and customers do not want to change their consumption plan, we can say we reach to optimal point (Nash Equilibrium)

Depaola et. At [82] proposed iterative appliance coordination for price responsive appliances on a game theory framework. They proved that their method reaches the optimal point (Nash Equilibrium) in theory. They proved that at each iteration, the generation cost of electricity decreases. However, their method is very time-consuming since the price responsive appliances solve the problem one at a time and update the system's operator. This approach could be very time-consuming, especially if many PRDs exist in the network. To compensate for this issue, they proposed a faster semi-optimal algorithm, but the result slightly deviates from the equilibrium.

Mohsenian et al. [84] developed a games theoric approach between competitive resources. All the participants communicate with each other in the grid and are aware of each other's behavior. The goal is to reach Nash equilibrium between the users, which will be equivalent to reaching the global minimum when the objective is cost minimization. The issue with this method is that all users are connected to each other. This topology creates two issues:1) privacy: given that all users must know about the behavior of each individual, the privacy of each user is jeopardized. Also, it would open up more space for suspicious behavior, given that each user has access to more information. 2): The need for high bandwidth and more computation capacity. Sending each individual's data to all other users requires a costly infrastructure to send the data and a high bandwidth. At the same time, a delay on each connection link could reduce the speed of each iteration in the real world.

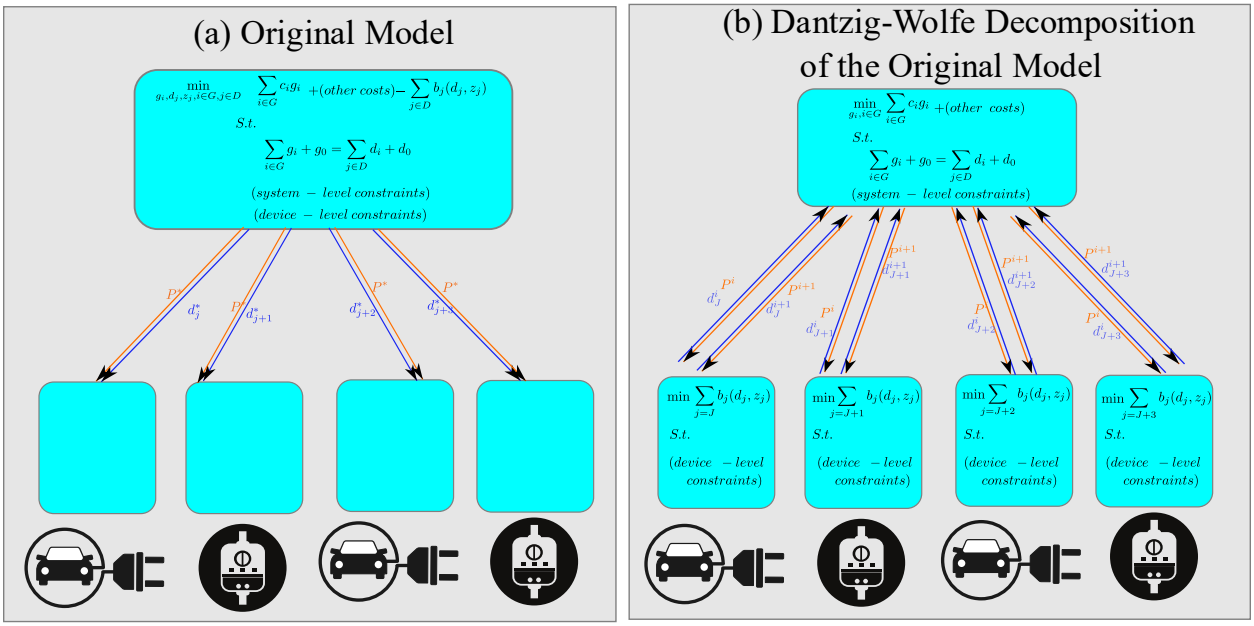

Figure 11(a) original unit commitment with PRD (solved at one step) (b) Dantzig-Wolfe decomposition of the original model (two iterations)

While the above approaches try to find the Nash equilibrium (optimal point) through game theory approaches, an alternative would be a comprehensive optimization problem containing the cost of electricity generation and the end-user PRD's local objective (that part of its cost of using

electricity). It must be noted that this is different from multi-objective optimization. If such a universal problem existed, there would be an optimal answer (optimal overall load profile or the corresponding price from the marginal cost of generating this optimal load schedule) where the generation costs and end-user's local objectives were minimized simultaneously. In such an optimization problem, the grid operator and the end-users did not want to change their consumption plans (because they are at the optimal point or Nash- Equilibrium). However, such a problem will be humongous and impossible to solve. Furthermore, the grid operator does not have all the information regarding the preference of each and every appliance at each house.

In this paper, we propose solving such a problem using the Dantzig-Wolfe (DW) decomposition method for the first time. DW [97] was first proposed to solve large-scale linear programming problems. It breaks the large problem into a master problem and some subproblems. Then the subproblems are solved independently in a separate computer, and report the primary results to the computer with the master problem. Figure 11 shows the summary of the main structure of this algorithm. This procedure is repeated in a loop until the optimal answer is obtained. While this structure was initially proposed to solve the linear programming problems faster, it has been used for distributed optimizations over time[98]. However, DW has never been used to solve unit commitments with PRD to coordinate them optimally. The structure of the above universal problem with unit commitment objectives and PRD's local objective makes it an ideal case to be solved with DW. Further information regarding the structure of the problem is provided in section 3.3.

In the proposed method, the PRD objective act as a subproblem of the DW, and the unit commitment objective act as the master problem. The solution to the master problem (unit commitment) would be the proposed load profile plan for each user and the corresponding price based on the marginal cost of electricity generation. The result of PRD's local objective is a load profile based on the proposed price from the master problem. This iterative procedure repeats until a point where the grid operator (which solved the unit commitment master problem) and the local PRDs (which solved subproblems) will not change their behavior (proposed price and load consumption) since the algorithm reached the optimal point.

Using DW to solve such a universal problem has numerous advantages 1) it is optimal. While it looks obvious, many appliance coordination algorithms that have been proposed above cannot find an optimal schedule for both sides of the market and one side needs to sacrifice for the other side. 2) it is fast. Since most of the optimization is done locally, the computation is high-speed. Also, at each iteration of the algorithm, the appliances solve the problem simultaneously. The simultaneous update is way faster than the algorithm that has been proposed in[82], [84] that one appliance solves the problem at the time. 3) it is private. The appliances only share information regarding their consumption plan with the grid operator. This approach also prevents a distrustful coalition between the appliances from changing the master problem result based on their benefits. This method is in contrast with the method proposed in [82], [84], where the information must be shared between all appliances. 4) it is a market-based algorithm. The utmost goal of this algorithm is to find the balance between supply and demand through a market. This paves the way for a larger corporation of distributed generations (including renewables) into the power system.

The chapter's structure is as follows: in capture 3.3, the fundamental principle of DW is explained. In capture 3.3.3, a simplified united commitment model for the grid operator and self-benefiting algorithms for appliances (EVs and EWHs) are proposed. Capture 3.4 discussed the results of implementing this algorithm.

3.3 Dantzig-Wolfe-Based Coordination Mechanism

3.3.1 Power System Operation with PRDs

Some key elements of the unit commitment problem for electric power systems with PRDs can be written as

$$\min_{\mathbf{g}_i, \mathbf{d}_j, \mathbf{z}_j, i \in G, j \in D} \sum_{i \in G} c_i(\mathbf{g}_i) + (\text{other costs}) - \sum_{j \in D} b_j(\mathbf{d}_j, \mathbf{z}_j)$$
$$\text{s.t.} \sum_{i \in G} \mathbf{g}_i + \mathbf{g}_0 = \sum_{j \in D} \mathbf{d}_j + \mathbf{d}_0 \tag{61}$$
$$(\text{and other system-level constraints})$$
$$(\text{and device-level constraints})$$

In this model, G is the set of all controllable power plants and D is the set of price-responsive devices. The main decision variables are the power output from plant i ($\mathbf{g}_i$), and the amount of power to be consumed by device j ($\mathbf{d}_j$). These are vectors with one element for each hour of the next day. $\mathbf{z}_j$ is a vector containing all the other decisions that must be made by device j, e.g., temperature or charge levels for each hour. Together, $\mathbf{d}_j$ and $\mathbf{z}_j$ constitute a complete operating plan for device j for the next day. The function c_i shows the cost of producing power in plant i. The function b_j shows the benefits to the owner of device j when it follows the specified operating plan, converted to dollar form, *i.e.*, the most the customer would be willing to pay to follow this plan. The only constraint shown is that the total generation scheduled for the next day, plus the noncontrollable generation $\mathbf{g}_0$ (e.g., distributed solar power) must equal the total demand from price-responsive devices plus the non-price-responsive demand $\mathbf{d}_0$.

For brevity, we have omitted numerous additional terms: costs for starting, stopping and running power plants; and constraints on minimum and maximum output levels for each plant; minimum up- and down-times; and transmission line loading during normal operation or contingencies [99]–[105]. These could be included in future work.

If we split problem (61) into a power production cost function $C(\mathbf{D})$ and a consumption benefit function $B(\mathbf{D})$ as follows:

$$C(\mathbf{D}) = \min_{\mathbf{g}_i, i \in GK} \sum_{i \in G} c_i(\mathbf{g_i}) + (\text{other system-level costs})$$
$$\text{such that} \sum_{i \in G} \mathbf{g}_i + \mathbf{g}_0 = \mathbf{D} + \mathbf{d}_0 \tag{62}$$
$$(\text{and other system-level constraints})$$

$$B(\mathbf{D}) = \max_{\mathbf{d}_j, \mathbf{z}_j, j \in D} \sum_{j \in D} b_j(\mathbf{d}_j, \mathbf{z}_j)$$
$$\text{such that } \sum_{j \in D} \mathbf{d}_j = \mathbf{D} \tag{63}$$
$$\text{(device-level constraints)}$$

then problem (61) becomes simply

$$\min_{\mathbf{D}} C(\mathbf{D}) - B(\mathbf{D}) \tag{64}$$

In other words, the system operator must find a consumption plan **D** that can be served at the lowest net cost, where net cost is defined as the system's production cost function $C(\mathbf{D})$ minus the customers' benefit $B(\mathbf{D})$.

3.3.2 Dantzig-Wolfe-Based Coordination Mechanism

For large power systems, it may be difficult to convey the details of the PRDs' benefit problems to a central coordinator, and even if the central coordinator had those details, the full unit commitment problem with millions of PRDs will likely be too large to solve on a single computer. In this paper, we instead present a distributed, iterative coordination mechanism based on Dantzig-Wolfe decomposition of the unit commitment problem, which relies on PRDs to calculate their own parts of this problem.

The unit commitment problem with PRDs has two properties that make this possible. First, the PRDs' local optimization problems can be separated from the main unit commitment problem, except for the requirement that total production equals total consumption. Second, the PRDs' private optimization problems are generally convex (often linear), e.g., choosing hourly consumption levels to fully recharge a battery overnight. These properties are true for the individual PRDs' optimization problems and also for the overall consumption benefit problem, which is the sum of all the independent problems for each PRD.

Dantzig-Wolfe decomposition is a well-known iterative technique for solving optimization problems of this form that are too large to represent directly on a single computer [97], [98], [106]–[108]. As such, it is a good choice for the unit commitment problem with millions of PRDs. Dantzig-Wolfe decomposition also comes with attractive guarantees: it provides a better solution with each iteration; convergence occurs in finite time with linear subproblems; at each iteration the difference between primal and dual objective values provides a measure of the distance from optimality; and if interrupted before convergence, it will always provide a feasible solution.

Dantzig-Wolfe decomposition relies on two facts about convex programs: (1) any feasible solution can be expressed as a convex combination (weighted average) of the extreme points of the program (i.e., the feasible region is all the space inside the convex hull of a collection of points known as the "extreme points" of the problem), and (2) the program's objective function (net cost) can

always be expressed as a convex combination of the objective value at the extreme points (i.e., the objective function is the convex hull of the objective values at those same points).

These facts allow us to reframe the consumption benefit function in terms of weights are applied to the extreme points of the consumption problem:

$$\begin{aligned} B(\mathbf{D}) = \max_{w_k} & \sum_{k \in K} w_k b_k \\ \text{s.t.} \quad & \mathbf{D} = \sum_{k \in K} w_k \mathbf{d}_k \\ & w_k \geq 0, \quad \forall\, k \in K \\ & \sum_{k \in K} w_k = 1 \end{aligned} \tag{65}$$

where K is the set of all feasible points, k is an index in K, $\mathbf{d}_k$ is the demand at point k, b_k is the value of the benefit function at that point, i.e., $b_k = B(\mathbf{d}_k)$, and w_k is the weight given to point k. With this in mind, we can rewrite problem (64) as the Dantzig-Wolfe master problem:

$$\begin{aligned} \min_{w_k:\, k \in K} & C(\mathbf{D}) - B(\mathbf{D}) = C\left(\sum_{k \in K} w_k \mathbf{d}_k\right) - \sum_{k \in K} w_k b_k \\ \text{s.t.} & \sum_{k \in K} w_k = 1 \end{aligned} \quad . \tag{66}$$

In this formulation, the master problem consists of constructing a consumption plan **D**—a convex combination of extreme points of the consumption problem—that can be served at the lowest net cost, where net cost is defined as the system's production cost function $C(\mathbf{D})$ minus the customers' benefit $B(\mathbf{D})$.

It is not usually possible to enumerate all the members of the set K. Instead, Dantzig-Wolfe decomposition builds up a subset K' that defines the feasible space near an optimal solution [97]. This subset is created by iterating between the master problem as shown in (66) and the demand-side sub-problem:

$$\min_{\mathbf{D}} \mathbf{p}^T \mathbf{D} - B(\mathbf{D}) \tag{67}$$

Here, **p** is a vector of hourly electricity prices. These are set equal to the marginal cost of serving additional load in the master problem (66) (e.g., dual values of the load-serving constraint) during the previous iteration. When the consumption subproblem (67) is solved with these prices, it finds the best possible consumption plan **D** at these prices. This solution must be at an extreme point of the consumption problem, so this provides another point $\mathbf{d}_k$ and benefit value $b_k = B(\mathbf{d}_k)$ to add to the set of extreme points K'.

This continues until there is no new extreme point that can improve the solution to problem, at which point the problem has converged on the optimal consumption plan [97]. If $B(\mathbf{D})$ is a linear program (or equivalent to one), then it has a finite number of extreme points, so convergence will

be achieved in finite time. On the other hand, nonlinear, convex programs are equivalent to linear programs with infinitely many extreme points. In this case, the solution will improve at each step, asymptotically approaching the optimum.

Consequently, the unit commitment problem with PRDs can be solved as follows. In each iteration, the master problem (66) chooses the best combination of all the previously reported demand vectors and offers tentative prices to the consumption subproblem; then consumption subproblem offers a demand vector that can be served at equal or lower net cost (cost minus benefit). Specifically,

1. The central coordinator makes an initial estimate of prices $\mathbf{p}_{(0)}$.
2. The consumption subproblem (67) is solved on a distributed basis:
    a. The central coordinator passes the price vector $\mathbf{p}_k$ to the PRDs.
    b. All PRDs solve their individual subproblems and return $\mathbf{d}_{jk}$ and b_{jk}. These are their consumption plan and an estimate of the benefit of this plan (i.e., the amount they'd be willing to pay to follow this schedule). For simplicity or privacy protection, the benefit can be specified with an arbitrary offset that is constant over all iterations.[2]
    c. The $\mathbf{d}_{j,k}$ and $b_{j,k}$ vectors from individual PRDs are summed to create a system-wide consumption plan $\mathbf{d}_k$ and benefit value b_k.
3. The central coordinator adds the new demand profile $\mathbf{d}_k$ with benefit value b_k to the set of extreme points K' and solves the master problem (66), choosing a new combination of previously reported extreme points. If an optimality threshold is reached, or if an iteration limit has been reached, then the process terminates. Otherwise, the objective and pricing have been slightly improved, and the central coordinator sets new prices $\mathbf{p}_{k+1}$ equal to the dual values of the load-serving constraints. Then the process returns to step 2.
4. At the end of the iterations, the system coordinator reports the final nonzero weights w_k to the PRDs (or possibly to the home or feeder coordinator). These are then multiplied by the load bids previously received from individual PRDs. These load levels are then assigned as the amount of power to be used by each PRD. If the problem converges, then these load vectors are optimal for individual PRDs and for the whole system at the final prices. If the process stops short of convergence, then the final price and load vectors are still known to be feasible and an improvement over the starting point, for both the system and the individual PRDs.

Importantly, this mechanism can choose any mixture of previous demand bids by the PRDs, rather than being confined to the exact load profiles that have been bid. With highly price-sensitive devices, this has significant advantages over approaches that attempt to find just the right price to induce the right demand: (1) If very price-sensitive PRDs such as EVs or customer-sited batteries

2 For devices where the direct benefit does not vary among all feasible operating plans (e.g., an electric vehicle that always charges fully regardless of prices), the benefit of any feasible plan could be reported as zero. For devices where the benefits vary from one plan to another, the value of the benefit function should change by the same amount.

are on the margin in multiple hours, they will arbitrage away any price differences; this occurs because even infinitesimal price differences between hours would cause large swings of load between those hours. Consequently, the efficient prices may be flat over the period when these devices are on the margin, and will fail to send a signal to achieve a particular shape of load (e.g., valley-filling or renewable-following). Instead, a quantity signal is also needed, such as the one provided here. (2) In practice, price-based coordination mechanisms often work by adjusting prices in small steps until supply and demand are balanced. However, that is not possible with infinitely price-sensitive devices, since even infinitesimal variations will cause all the load to swing in one direction or the other; this causes those methods to oscillate without converging on a single right price vector (and as noted above, even if they found the right price vector, that alone would not induce the right consumption vector). In our work, described below, the Dantzig-Wolfe mechanism performs well for highly-price-sensitive devices, choosing a mix of demand vectors from either side of the equilibrium point and quickly moving toward convergence.

It should also be noted that the consumption subproblem can naturally be divided into separate subproblems for each device. Then the main subproblem can be solved by passing the prices to all the individual devices, letting them solve their portion of the subproblem, and summing the load vectors and benefit values that they return. In a real-world implementation, this could allow for highly parallelized computation and efficient communication. For example, the master problem could be solved by a central coordinator, while nodal coordinators manage each distribution circuit, and home coordinators manage the individual PRDs within each home. Devices at each level of the hierarchy simply announce price vectors to the devices or coordinators below them and then sum the demand vectors and benefits that they receive back. This allows data to be condensed by several orders of magnitude at each level, so very little bandwidth is needed at each level (just enough to communicate with a few dozen elements at the next lower level). It is also worth noting that this technique can incorporate highly heterogenous PRDs without any modification, i.e., any device that has a convex (rational) response to prices.

3.3.3 Price Responsive Device (PRD) Models

In the literature, loads are categorized as non-shiftable, shiftable and thermostatically controlled appliances (TCA) [109]. non-shiftable (uninterruptible) are loads that are the one that energy must be delivered to them instantly. TVs or stoves are from the non-shiftable group. The interruptible are appliances that instant energy usage is not needed since either they have batteries or are needed once per day or week while urgent usage is not needed. EVs, dishwashers and driers are from this category. The TCAs are the ones where the energy consumption is a function of temperature (ambient temperature or user's desired temperature). The working temperature (desired) could be affected by the ambient temperature, or it could be affected by input/output of the energy through consumption or added energy from the heating/cooling elements respectively. In many works such as [84] only non-interruptible and interruptible loads are considered for the task of energy management. However, since non-shiftable loads have no response to any control command (either from direct load control or optimization), they could be removed from the problem without losing generality. Since it is not possible to show the dynamic response of all types of loads in one paper and the fact that their behavior is similar to some extent, EVs from shiftable loads and EWHs from

TCAs are selected to represent a sample of load profile. This section covers the self-benefiting model of PRDs that participate in the market bidding. i.e., the EWH and EV.

3.3.3.1 Electric Water Heater Model

The following shows a self-benefiting model of EWH that aims to minimize its cost. It is a day-ahead optimization implemented as a linear program based on the model developed in Section 1 and [76]. It is dual-objective, i.e., the model tries to find a balance between cost saving and discomfort. For this study, we assume perfect foresight of hot water requirements and optimize power consumption accordingly. In future work, we could consider an EWH that buys vectors of power as shown here, based on a stochastic forecast of hot water usage, as discussed in Section 1 and [76].

Equation (68) shows the dual-objective cost function which minimizes the cost from use of electricity and the discomfort cost (underheated water) that could happen from using this program.

$$\min_{\boldsymbol{E}^{\mathrm{in}} \in \mathbb{R}^{24}} \sum_{h \in I} p_h^{\mathrm{p}} E_h^{\mathrm{in}} + p^{\mathrm{s}} E_h^{\mathrm{short}} \tag{68}$$

Equation (69) models the thermodynamic behavior of EWH.

$$T_{d,h}^{\mathrm{tank}} = T_{h-1}^{\mathrm{tank}} + \frac{\left(E_h^{\mathrm{in}} - E_h^{\mathrm{w}}\right)}{c^{\mathrm{tank}}} - r^{\mathrm{loss}} \cdot \left(T_h^{\mathrm{tank}} - t_h^{\mathrm{amb}}\right) \tag{69}$$

In (70), the maximum energy that can be drawn from the grid is limited to the EWH energy input capacity.

$$E_h^{\mathrm{in}} \leq e^{\mathrm{max}} \tag{70}$$

Equation (71) and (72) model the temperature and energy shortfall respectively. They calculate the underheated water that would be caused by the plan.

$$T_h^{\mathrm{short}} \geq t^{\mathrm{min}} - T_h^{\mathrm{tank}} \tag{71}$$

$$E_h^{\mathrm{short}} = e_h^{\mathrm{des}} \frac{T_h^{\mathrm{short}}}{\left(t^{\mathrm{min}} - t_h^{\mathrm{in}}\right)} \tag{72}$$

After solving this problem, PRD number j reports its consumption vector during iteration k as $\mathbf{d}_{j,k} = [E_0^{\mathrm{in}}, E_1^{\mathrm{in}}, E_2^{\mathrm{in}}, \ldots, E_{23}^{\mathrm{in}}]$. It also calculates the benefit $b_{j,k}$ as being equal to the shortfall penalty times the quantity of hot water consumed (this may vary from one iteration to the next, as the plan adapts to different electricity prices). By definition, this is the amount that the customer would be willing to pay for the hot water they will receive, and by extension, for the power that will be used to produce this hot water.

3.3.3.2 Electric Vehicle Model

The electric vehicles follow a simple cost-minimizing algorithm. The user defines the hours that the EV can be charged (parking hours) in advance. These hours are defined through the maximum charging rate per hour. i.e., e_h^{max} for hour h. The e^{des} is the energy needed by end of charging

window (i.e., total energy needed in the day). Then, the role of the following cost-minimizing programming is to find the cheapest hours to pick to charge the vehicle.

The cost function is shown in equation (73). The objective is simply to minimize the user electricity cost.

$$\min_{\boldsymbol{E}^{\text{in}} \in \mathbb{R}^{24}} \sum_{h \in I} p_h^{\text{p}} E_h^{\text{in}} \tag{73}$$

In this equation, I is the set of all hours in the coming day and p_h^{p} is the (tentative) price for power during each of those hours, and E_h^{in} is the decision variable showing the amount of power to use for charging during each hour.

The charging window is modeled through the equation (74):

$$E_h^{in} \leq e_h^{max} \tag{74}$$

The total energy that is added to the battery through the charging window must be equal to the total energy needed. Equation (75) shows this constraint.

$$\sum_{h \in I} E_h^{\text{in}} = e^{\text{des}} \tag{75}$$

We use a simple algorithm to solve this linear program:

1. Select hours of the day when charging is possible ($e_h^{max} > 0$).
2. Sort these hours from lowest to highest price, then from early to late as a tie-breaker.
3. During each hour, starting with the first in the list, add enough charge to reach e^{des}, or charge at rate e_h^{max}, whichever is less.

After choosing the optimal charging plan, the EV model reports back the consumption vector $\mathbf{d}_{j,k} = [E_0^{\text{in}}, E_1^{\text{in}}, E_2^{\text{in}}, \dots, E_{23}^{\text{in}}]$. When using this algorithm, the EV always obtains a full charge, so the benefit to the EV is the same regardless of the charging plan. So the benefit $b_{j,k}$ is reported as zero for each EV during each iteration.

3.3.3.3 Aggregated Consumption Benefit Problem

For the Dantzig-Wolfe iteration described in this paper, the consumption subproblem (67) is regarded as a single problem encompassing all PRDs in the system. That is achieved simply by offering the same price vector $\mathbf{p}^p = \mathbf{p}_k$ to all the water heater and electric vehicle models, solving the model for each individual PRD, then summing the consumption plans for all the PRDs:

$$\mathbf{d}_k = \sum_{j \in J} \mathbf{d}_{j,k}$$

$$b_k = \sum_{j \in J} b_{j,k}$$

These are then reported to the central coordinator.

After the last iteration of the master problem, the final weights w_k from the master problem (66) are assigned back to the PRDs, based on each device's prior bids:

$$\mathbf{d}_j^* = \sum_{k=1}^{N} w_k \mathbf{d}_{j,k}$$

This could be done by reporting the weights to the devices themselves, or by having the home or circuit coordinator calculate $\mathbf{d}_j^*$ and report it to device j as the amount of power it has purchased.

With this assignment, the total power consumed by all PRDs matches the total expected/constructed in the system-level master problem:

$$\mathbf{D} = \sum_{k=1}^{N} w_k \mathbf{d}_k = \sum_{k=1}^{N} w_k \sum_{j \in D} \mathbf{d}_{j,k} = \sum_{j \in D} \sum_{k=1}^{N} w_k \mathbf{d}_{j(k)} = \sum_{j \in D} \mathbf{d}_j^* \tag{76}$$

This framework assumes that the PRDs all have convex responses to price, and it foregoes the option of assigning different weights to the extreme points (bids) elicited from the individual devices. In future work, we could incorporate devices with integer decisions (e.g., dishwashers or clothes washers that must run a full cycle once they start). One promising option for this would be to fine-tune the weights for individual PRDs at the feeder (neighborhood) level, requiring integer weights for the integer PRDs, and adjusting the weights for all the PRDs on the feeder so that the total for the feeder matches the total load requested by the system as closely as possible.

3.3.4 Power System Model

For this paper, we use a simple electricity production model. We ignore non-dispatchable generation $\mathbf{g}_0$ and non-price-responsive loads $\mathbf{d}_0$, so the load-balancing constraint of equation (62) becomes

$$\sum_{i \in G} \mathbf{g}_i = \mathbf{D} = \sum_{k \in K} w_k \mathbf{d}_k$$

We also assume that the system has a quadratic production cost, so that the minimum cost of producing an amount of power $\mathbf{D}$ from the available generators is

$$C(\mathbf{D}) = \sum_{h=1}^{24} a D_h^2 \tag{77}$$

where D_h is the element of the demand vector $\mathbf{D}$ for hour h.

These assumptions create a simple system with easily calculated marginal costs ($2aD_h$) each hour. However, the approach shown in this paper is general enough to apply to any convex supply side, e.g., a linear program where marginal costs are the dual values of the hourly load-balancing constraints.

3.3.5 Optimality Gap

By step N of the Dantzig-Wolfe iteration, the PRDs in the system have revealed the following extreme points (feasible consumption quantity vectors):

$$\mathbf{d}_k, \quad k \in K' = 1..N \tag{78}$$

where N is the number of iterations/bids we've done and $\mathbf{d}_k$ is the total consumption bid from all PRDs during step k. The benefit to the customers for each extreme point (the maximum they would be willing to pay for that vector, possibly shifted by a constant offset) is

$$b_k, \quad k \in K' = 1..N \tag{79}$$

where b_k is a scalar, the sum of all the benefits reported by the individual PRDs.

Then, any weighted combination of these bids is possible, because the feasible regions for the EV and EWH models are convex. So, the master problem constructs a consumption plan (load vector) that is a weighted sum of the previous bids:

$$\mathbf{D} = \sum_{k=1}^{N} w_k \mathbf{d}_k \tag{80}$$

where $\mathbf{D}$ is the constructed bid (vector, one element for each hour h).

The total benefit of this constructed bid is $B(\mathbf{D})$, where

$$B(\mathbf{D}) \geq B'(\mathbf{D}) = \sum_{i=1}^{N} w_k b_k \tag{81}$$

The central coordinator doesn't know $B(\mathbf{D})$ directly, but over multiple iterations, the reduced-form representation $B'(\mathbf{D})$ will converge to the true value of $B(\mathbf{D})$ [97]. As noted previously, this will occur in finite time if the PRD subproblems are linear programs (as they are for this paper), and will occur asymptotically if the PRD problems are convex but nonlinear [108].

Dantzig-Wolfe decomposition gives an optimality gap at each iteration, which can be seen as the difference between two measures: S^{best} (the best possible value of the objective function) and S^{known} (best objective value found so far).

During round k, the master problem minimizes $C(\mathbf{D}) - B'(\mathbf{D})$. The value of the objective function at this point is

$$S^{\text{known}} = C(\mathbf{D}_k) - B'(\mathbf{D}_k) \tag{82}$$

where $\mathbf{D}_k$ indicates the value of $\mathbf{D}$ selected by the master problem in round k.

S^{known} is a lower bound on the objective function because it is known to be achievable. $B'(\mathbf{D}_k)$ in the master problem is conservative. It is a weighted combination of points on the true $B(\mathbf{D})$ function, so it must be equal to or below the true $B(\mathbf{D}_k)$ with loads $\mathbf{D}_k$, since $B(\mathbf{D}_k)$ is convex. $C(\mathbf{D}_k)$ is also achievable because it is the actual production cost function.

After solving the master problem in round k, the central coordinator offers tentative prices $\mathbf{p}_k$ to the customers and they propose to buy a total amount of power each hour $\mathbf{d}_k$. They also report that this power gives them a benefit of b_k.

The subproblem solution $\mathbf{d}_k$ (with benefit b_k) is optimal, which means that all other values of $\mathbf{d}$ would give equal or worse objective values, i.e.,

$$B(\mathbf{d}) - \mathbf{p}_k \cdot \mathbf{d} \leq b_k - \mathbf{p}_k \cdot \mathbf{d}_k \tag{83}$$

for all $\mathbf{d}$, so

$$B(\mathbf{d}) \leq b_k - \mathbf{p}_k \cdot \mathbf{d}_k + \mathbf{p}_k \cdot \mathbf{d} \tag{84}$$

The master problem has solution $\mathbf{D}_k$, with production cost $C(\mathbf{D}_k)$ and incremental production cost $\mathbf{p}_k$, i.e., $\mathbf{p}_k$ is the gradient of $C(\mathbf{d})$ at $\mathbf{D}_k$. Since $C(\mathbf{d})$ is convex downward, it must lie above the plane that is tangent at this point, so

$$C(\mathbf{d}) \geq C(\mathbf{D}_k) + \mathbf{p}_k \cdot (\mathbf{d} - \mathbf{D}_k) \tag{85}$$

for all possible demand vectors $\mathbf{d}$.

Subtracting equation (84) from (85) gives

$$C(\mathbf{D}) - B(\mathbf{D}) \geq C(\mathbf{D}_k) - \mathbf{p}_k \cdot \mathbf{D}_k - b_k + \mathbf{p}_k \cdot \mathbf{d}_k \tag{86}$$

so

$$S^{\text{best}} = C(\mathbf{D}_k) - \mathbf{p}_k \cdot \mathbf{D}_k - b_k + \mathbf{p}_k \cdot \mathbf{d}_k \tag{87}$$

Then the optimality gap is

$$\begin{aligned} S^{\text{known}} - S^{\text{best}} &= C(\mathbf{D}_k) - B'(\mathbf{D}_k) - C(\mathbf{D}_k) + \mathbf{p}_k \cdot \mathbf{D}_k + b_k - \mathbf{p}_k \cdot \mathbf{d}_k \\ &= [b_k - \mathbf{p}_k \cdot \mathbf{d}_k] - [B'(\mathbf{D}_k) - \mathbf{p}_k \cdot \mathbf{D}_k] \end{aligned} \tag{88}$$

For this paper, we always performed 24 iterations and only used the optimality gap as an informative diagnostic. However, in future work, we could iterate until the gap is below a fixed limit or a fixed fraction of the direct costs $C(\mathbf{D}_k)$.

3.4 Results

3.4.1 Network structure and problem assumption

The structure of the power network is shown in Figure 12. This network serves eight households (a total of 16 appliances). All the loads are connected to the grid operator through a common line. Without losing the generality, it is assumed that all units are being fed through one distributed generator (DG) unit that feeds all the loads. Since the only source of energy is one dispatchable unit and no renewable energy that can affect generation cost, the marginal cost for all hours is the

same. Also, power quality constraints such as voltage and frequency regulations are not considered in this unit commitment problem, and the focus is on economic dispatch.

3.4.1.1 Load type:

In this work, it is assumed that the generator belongs to all consumers. This means the operator acts only as a coordinator and does not seek its own benefit. Each customer pays the operational cost of using the generator unit, which is equal to their consumption profile times the price that is proposed by the coordinator. Each household ONLY sends its bid to the coordinator, and no neighbor is aware of other individuals' consumption patterns.

Each household responds to the day-ahead price signal and sends the aggregate energy consumption of all devices. As mentioned above, the loads that can participate in the bidding process are both shiftable and TCA loads. To narrow the scope, EVs are selected among the shiftable loads, and electric water heaters are selected from the TCA loads. Therefore, in this work, each household responds to price signals to optimize the performance of its electric vehicle and electric water heater. All other loads (including other non-shiftable, shiftable, and TCAs) are removed from the load profile to simplify the problem.

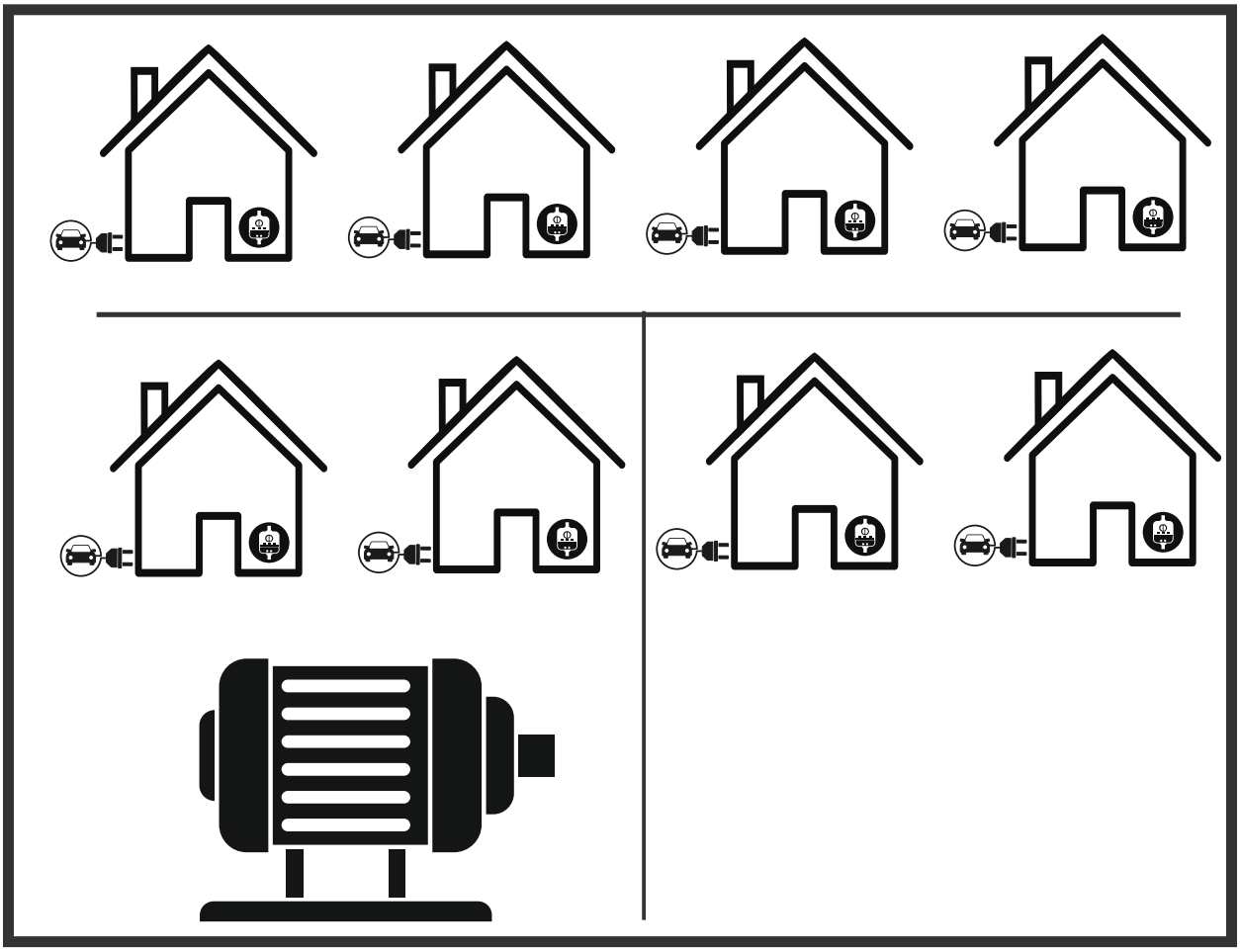

Figure 12Grid Structure

In this hypothetical scenario where the generation cost is equal for all hours (since no renewable energy generation exists) and only demand-responsive loads exist, the ideal aggregate load and price signal would be flat for all intervals. However, the current model could easily be changed to include non-interruptible loads of renewable energy sources.

3.4.2 Individual appliances respond to the price signal, and their benefit

As mentioned in the previous section, only two types of appliances are considered for this simulation. Also, it was mentioned that loads are categorized into three main types: 1-non-shiftable, 2-shiftable, and 3-TCAs. Non-shiftable loads don't respond to price, and their loads are fixed. Therefore, to simplify and focus to the claims of this paper, non-shiftable loads are removed from the load profile. In this section, we focus on the performance of an individual EV and EWH and show how they selfishly try to maximize their benefit by responding to the price signal by running the optimizations that are proposed in section 3.3.3.

3.4.2.1 EWH Response

Figure 13 shows the EWH response to the price signal that is sent from the coordinator at each round of optimization. Based on this price and prediction of user energy consumption, the EWH finds the optimal answer (self-benefiting). The energy usage that is the decision variable of EWH is sent to the aggregator as the energy bid on behalf of the EWH. The price signal is shown in black in the fourth section of the figure. At the same time, the EWH has a prediction for the energy withdrawal of the user. This prediction can come from analyzing historical data and using the machine learning method to obtain this prediction. The prediction in this work is considered perfect and is shown in the third section of the figure with dotted black lines. The main variables that are resulted from solving the optimization problem that was explained in section 3.3.3.1. Section one and two show the setpoint and actual temperature, respectively. Since the model is not stochastic, the setpoint and the actual temperature are the same for this section. The pink line in the third section represents the energy input that EWH plans to use. This is a variable that is sent to the coordinator after each round of solving the problem. A more detailed discussion of the EWH optimization model is provided in [76].

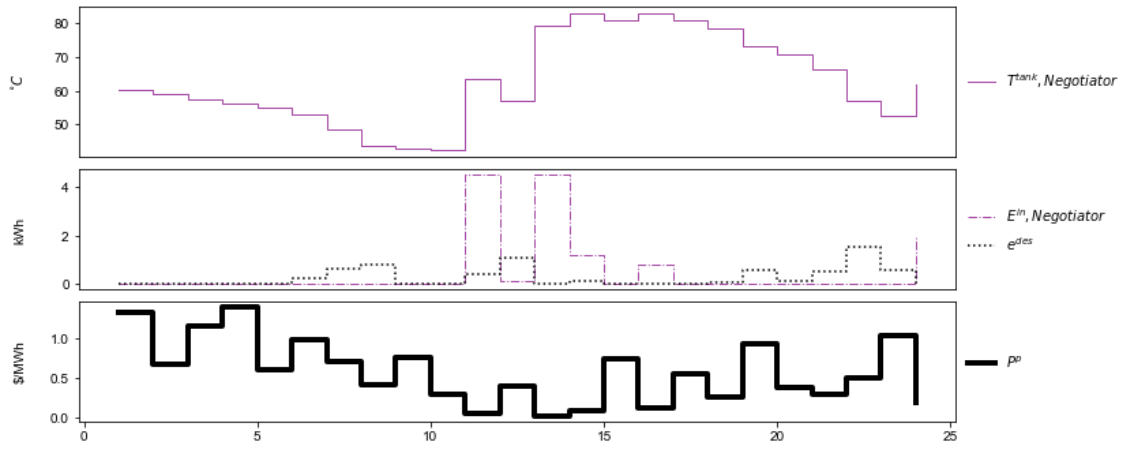

Figure 13 EWH response to the broadcasted price

3.4.2.2 EV Response

Figure 14 shows the response of the electric vehicle to the price signal. The gray bars show the amount of energy that the EV is able to absorb each hour. The times that availability is zero means that the vehicle is operational and can't be charged at those intervals. The blue bars show how much energy EV will absorb based on the result of the optimization that was explained in section 3.4.2.2. Similar to the EWH response, the energy input, which is the decision variable of EVs, is

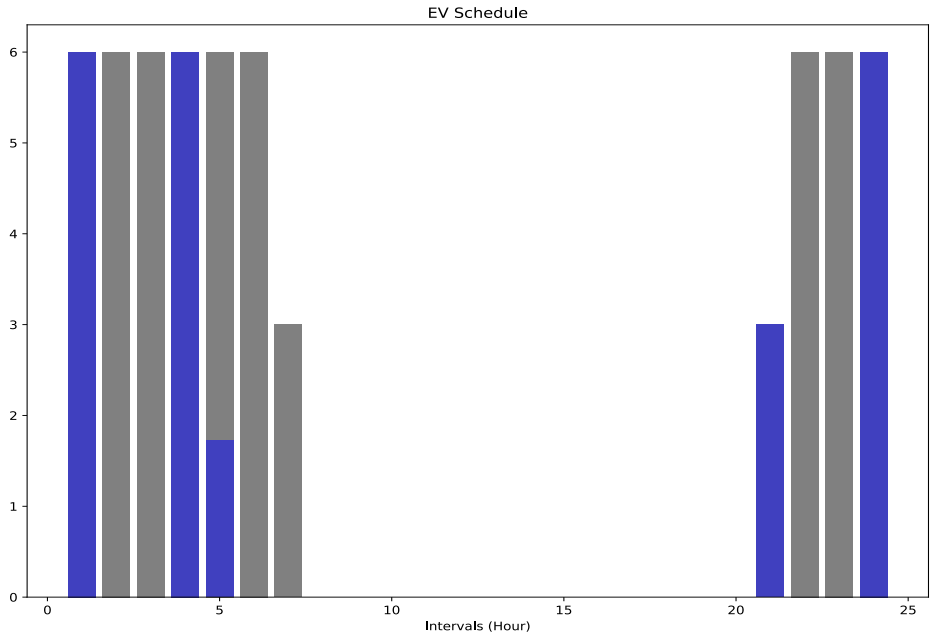

Figure 14 EV response to broadcasted price

reported to the coordinator as the energy bid of the EV. For example, this particular EV absorbed energy in full capacity in hours 1, 4, 21, and 24 and worked with one-third of its capacity at hour 5.

3.4.3 Price and Aggregate Demand Profile

in a problem where marginal cost is the same for all hours (since there is no renewable energy source for this problem) and there is no non-shiftable load, the ultimate ideal scenario for aggregate load and price profile is a flat line. i.e., the Peak to Average Ratio (PAR) is one. Therefore, to evaluate the performance of the DW algorithm, we must see how far from the flat curve the resulting aggregate load and price profile are from the flat lines.

Figure15 and Figure 16 show the price signal and aggregated load (in response to that price) at step 0 and the last step, respectively. i.e., each appliance solves its local self-benefiting optimizations in response to this price and reports back its scheduled energy usage as an energy bid. As it can be observed, the initial demand is accumulated only during specific hours (as mentioned before, only EVs and EWHs are used in this work). So, it means that the price generated by the expected marginal cost of electricity generation (which is based on energy consumption) will not represent the marginal cost of generation anymore. The reason is that the PRDs change their behavior to maximize their own benefit (which means they will shift their consumption to cheap hours). This accumulation causes a high generation cost for the hours that were initially

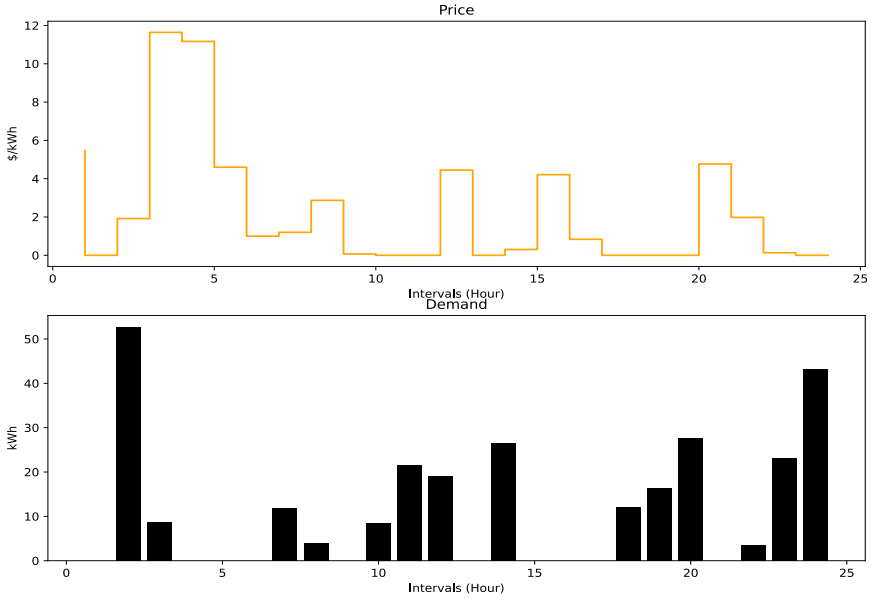

Figure15 initial load & price profile

expected to be sparsely used. As it can be seen, the initial price is high between 3-6 AM. This sparks a low energy consumption in these expensive hours. While a 54 KWh is recorded as a peak hour that causes a high. So, this response means that if the coordinator price generation is only based on the current expected energy consumption, the algorithm never converges, and a flip-flop response is observed.

However, this point is where the importance DW algorithm shows up. At each step of optimization, the DW finds the optimal point between the previously reported bits. For example, in the third step of the optimization, by using the interpolation between the first bid and second bit. This guarantees that the result of the third step is more optimal than the first two steps. This process is valid for other steps as well. For example, in the n^{th} step, the algorithm has access to the behavior of the model for the n-1 points. This means it can find an answer for the n^{th} step that is at least as good as the previous step or better. This algorithm is repeated until no further improvement happens in the system.

Figure 16 shows the price and aggregate demand when the iterative algorithm finishes the optimization. The PAR reduces significantly, and the peak load is reduced from 54 KW to 26 KW. It must be noted that all loads are price responsive in this simulation. In a more realistic scenario, where part of the loads is non-responsive to the price, the amount of PAR will be less than the time when all loads are price responsive. As shown in Figure 16, the PAR for the price signal reduces significantly from 4.7 to 2.6.

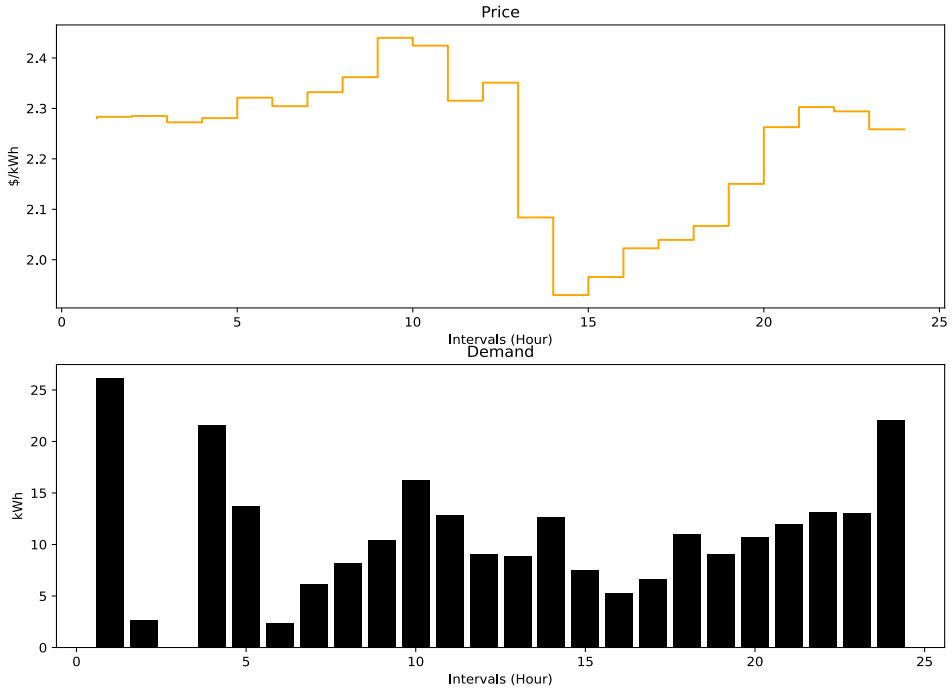

Figure 16 final load & price profile

3.4.4 Progress through iteration

As mentioned before, in each iteration, the price signal is sent from the coordinator to each appliance in each house. Then each device maximizes its own benefit by solving an optimization problem locally given the broadcasted price signal. When the optimization reaches a certain level, when the price signal is broadcasted, none of the appliances change their bid. This shows the network reached the global optimum or the Nash equilibrium. Figure15 shows the progress of the DW through iterations. In the initial iteration of iterations, the variation is high for both the price and aggregated demand. The PAR for the price and aggregate demand is around 4.7 at this point. As the iterations progress, the PAR and standard deviation (STD) reduce. At iteration 5 and after, the PAR reduces to approximately 1.1. however, this variation is significant enough to induce a response to the loads to change their consumption. At iteration 15, no changes happen to the response of loads to the price. i.e., the algorithm reaches a point where no appliance wants to change its consumption plan (definition of Nash Equilibrium). This shows the algorithm reached its main goal, which was to propose a price/energy bid to each individual user where they don't want to change their behavior. The optimality of the algorithm is discussed in the next section.

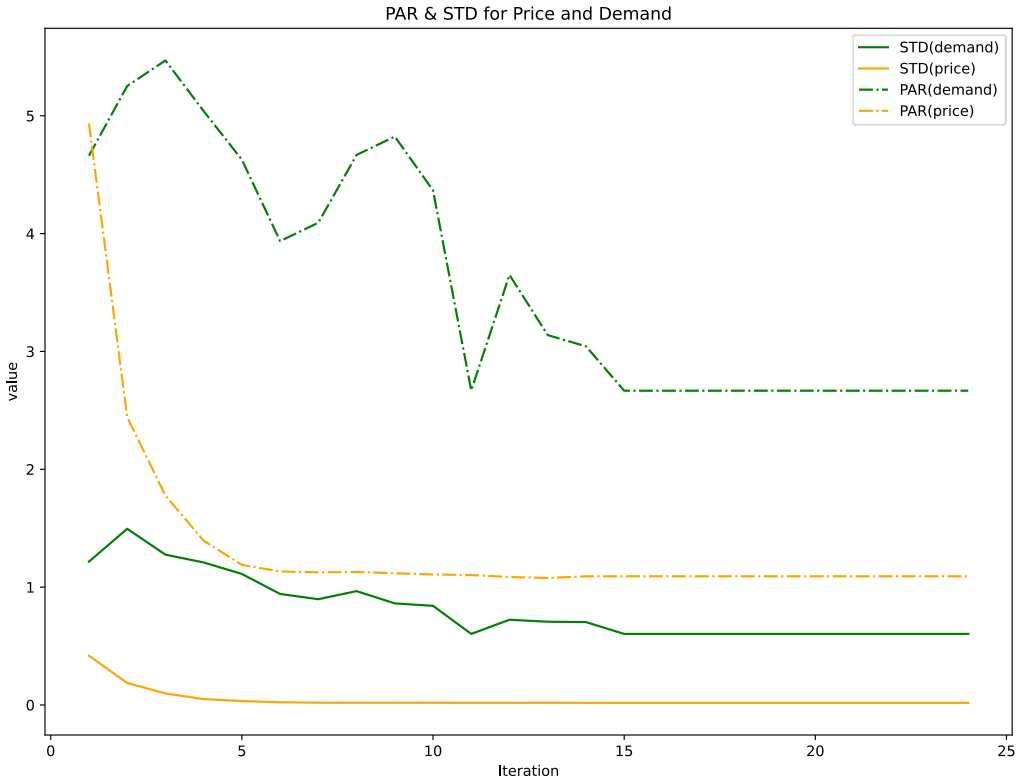

Figure 17 PAR & STD for price and aggregate demand

3.4.5 User Payment & Generation Cost & Optimality Gap

The generation cost and aggregate user payments are shown in Figure 18 in red and black, respectively. User payment is the sum of electricity price times the aggregate consumption for that interval. The generation cost is calculated using formula (77). As shown in Figure 18, generation cost and user payment are both high at the start of the algorithm. As the negotiation (iterations of the algorithm) goes forward, the cost of generation and user payment decreases. At this point, when the price signal is announced, none of the appliances change their consumption plans (they reach the Nash Equilibrium if we talk in terms of game theory). The gap, which is defined through formula (88), is shown in blue color in Figure 18. The gap shows the distance between the best possible answer and the best-known answer. As the algorithm progress, the algorithm updates the value of these two variables. At the later part of the optimization (iteration 15 for this specific simulation), the distance between these two variables (Gap) stays fixed, and no further improvement happens (optimal point). Alternatively, as was mentioned in the previous section, the algorithm reaches the Nash equilibrium at iteration 15.

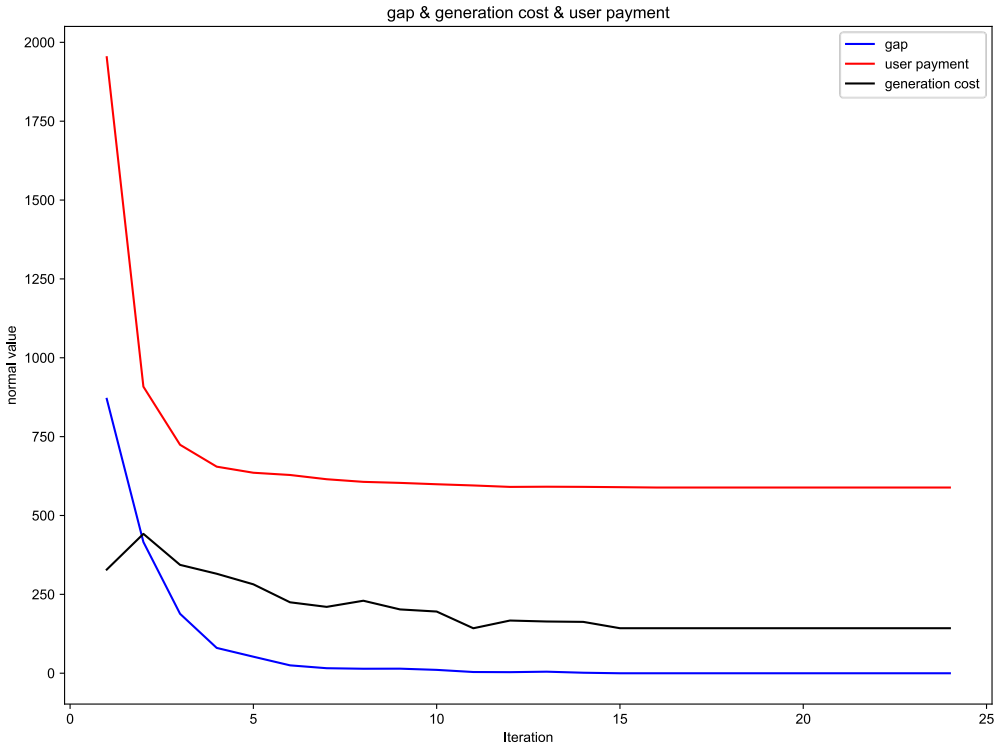

Figure 18 Gap & Generation cost & user Payment

3.5 Conclusion

In this work, a new price-based appliance coordination algorithm was proposed. This algorithm considered appliances and the operator as self-serving entities who try to maximize their benefit. This approach is on the path to having a market-based appliances coordination system where buyers and sellers can participate bid for energy. However, as of now, no mechanism has been implemented to achieve a balance between generation and consumption. A few market-based price-responsive demand coordination has been proposed in recent years based on the game theory framework. However, the potential of the Dantzig-Wolfe decomposition method in market-based coordination of appliances has never been investigated.

In this work, first, a universal large optimization model was proposed. Solving such a problem guarantees reaching an optimal point (or Nash equilibrium). However, solving such a large problem is impossible due to a lack of knowledge of the end user's behavior and preference at the

local level. Furthermore, even if such a knowledge (being aware of each user's preference) exists, solving such a massive problem will be computationally expensive (if not impossible).

However, the distributed nature of DF can tackle these two challenges. First, by breaking the universal problem into master (solved by the operator) and subproblems (solved by appliances), there will not be any need to know the preferences of each appliance. Instead, the appliances will only announce their energy usage as the energy bid to the operator. Second, due to the distributed behavior of the optimization, the algorithm will run very fast at iteration. Third, the way the algorithm is modeled guarantees convergence in limited iterations. Solving subproblems simultaneously and in a distributed fashion makes it possible to coordinate thousands of devices without losing speed.

In this work, a simple unit commitment with one generator was proposed. The next step for this project would be a more detailed unit commitment model with generation and transmission constraints in the optimization model. Given the efficiency and the speed of the proposed algorithm in this work, it will be possible to solve a large unit commitment problem with PRDs efficiently and optimally one day.

4 References

[1] A. J. Wood and B. F. Wollenberg, *Power generation, operation, and control*. John Wiley & Sons, 2012.

[2] F. E. R. Commission and others, "Federal Energy Regulatory Commission Assessment of Demand Response & Advanced Metering, Staff Report and Excel Data, December 29. 2008." 2008.

[3] Q. Qdr, "Benefits of demand response in electricity markets and recommendations for achieving them," *US Dept. Energy, Washington, DC, USA, Tech. Rep*, 2006.

[4] N. Ruiz, I. Cobelo, and J. Oyarzabal, "A direct load control model for virtual power plant management," *IEEE Transactions on Power Systems*, vol. 24, no. 2, pp. 959–966, 2009.

[5] A. Gomes, C. H. Antunes, and A. G. Martins, "A multiple objective approach to direct load control using an interactive evolutionary algorithm," *IEEE Transactions on Power Systems*, vol. 22, no. 3, pp. 1004–1011, 2007.

[6] C.-M. Chu, T.-L. Jong, and Y.-W. Huang, "A direct load control of air-conditioning loads with thermal comfort control," in *Power Engineering Society General Meeting, 2005. IEEE*, 2005, pp. 664–669.

[7] S. J. Darby, "Load management at home: advantages and drawbacks of some active demand side'options," *Proceedings of the Institution of Mechanical Engineers, Part A: Journal of Power and Energy*, vol. 227, no. 1, pp. 9–17, 2013.

[8] M. G. Lijesen, "The real-time price elasticity of electricity," *Energy Econ*, vol. 29, no. 2, pp. 249–258, 2007.

[9] P. Centolella, "The integration of price responsive demand into regional transmission organization (RTO) wholesale power markets and system operations," *Energy*, vol. 35, no. 4, pp. 1568–1574, 2010.

[10] K. Herter, "Residential implementation of critical-peak pricing of electricity," *Energy Policy*, vol. 35, no. 4, pp. 2121–2130, 2007.

[11] C. Triki and A. Violi, "Dynamic pricing of electricity in retail markets," *4OR: A Quarterly Journal of Operations Research*, vol. 7, no. 1, pp. 21–36, 2009.

[12] S. Caron and G. Kesidis, "Incentive-based energy consumption scheduling algorithms for the smart grid," in *Smart grid communications (SmartGridComm), 2010 First IEEE international conference on*, 2010, pp. 391–396.

[13] P. Samadi, A.-H. Mohsenian-Rad, R. Schober, V. W. S. Wong, and J. Jatskevich, "Optimal real-time pricing algorithm based on utility maximization for smart grid," in *Smart Grid*

Communications (SmartGridComm), 2010 First IEEE International Conference on, 2010, pp. 415–420.

[14] J. H. Yoon, R. Baldick, and A. Novoselac, "Dynamic demand response controller based on real-time retail price for residential buildings," *IEEE Transactions on Smart Grid*, vol. 5, no. 1, pp. 121–129, 2014.

[15] V. Kapsalis and L. Hadellis, "Optimal operation scheduling of electric water heaters under dynamic pricing," *Sustainable Cities and Society*, vol. 31, pp. 109–121, 2017.

[16] Z. Chen, L. Wu, and Y. Fu, "Real-time price-based demand response management for residential appliances via stochastic optimization and robust optimization," *IEEE Transactions on Smart Grid*, vol. 3, no. 4, pp. 1822–1831, 2012.

[17] Z. Chen and L. Wu, "Residential appliance DR energy management with electric privacy protection by online stochastic optimization," *IEEE Transactions on Smart Grid*, vol. 4, no. 4, pp. 1861–1869, 2013.

[18] P. Du and N. Lu, "Appliance commitment for household load scheduling," *IEEE transactions on Smart Grid*, vol. 2, no. 2, pp. 411–419, 2011.

[19] A. Sepulveda, L. Paull, W. G. Morsi, H. Li, C. P. Diduch, and L. Chang, "A novel demand side management program using water heaters and particle swarm optimization," in *Electric Power and Energy Conference (EPEC), 2010 IEEE*, 2010, pp. 1–5.

[20] R. Diao, S. Lu, M. Elizondo, E. Mayhorn, Y. Zhang, and N. Samaan, "Electric water heater modeling and control strategies for demand response," in *Power and Energy Society General Meeting, 2012 IEEE*, 2012, pp. 1–8.

[21] M. H. Nehrir, R. Jia, D. A. Pierre, and D. J. Hammerstrom, "Power management of aggregate electric water heater loads by voltage control," in *Power Engineering Society General Meeting, 2007. IEEE*, 2007, pp. 1–6.

[22] C. Diduch, M. Shaad, R. Errouissi, M. E. Kaye, J. Meng, and L. Chang, "Aggregated domestic electric water heater control-building on smart grid infrastructure," in *Power Electronics and Motion Control Conference (IPEMC), 2012 7th International*, 2012, vol. 1, pp. 128–135.

[23] P. Kepplinger, G. Huber, and J. Petrasch, "Autonomous optimal control for demand side management with resistive domestic hot water heaters using linear optimization," *Energy and Buildings*, vol. 100, pp. 50–55, 2015.

[24] N. Lu and S. Katipamula, "Control strategies of thermostatically controlled appliances in a competitive electricity market," in *Power Engineering Society General Meeting, 2005. IEEE*, 2005, pp. 202–207.

[25] S. H. Lee and C. L. Wilkins, "A practical approach to appliance load control analysis: a water heater case study," *IEEE Transactions on power apparatus and systems*, no. 4, pp. 1007–1013, 1983.

[26] D. Livengood and R. Larson, “The energy box: Locally automated optimal control of residential electricity usage,” *Service Science*, vol. 1, no. 1, pp. 1–16, 2009.

[27] F. C. Schweppe, M. C. Caramanis, R. D. Tabors, and R. E. Bohn, *Spot pricing of electricity*. Springer Science & Business Media, 2013.

[28] T. Ericson, “Direct load control of residential water heaters,” *Energy Policy*, vol. 37, no. 9, pp. 3502–3512, 2009.

[29] C. H. K. Goh and J. Apt, “Consumer strategies for controlling electric water heaters under dynamic pricing,” 2004.

[30] A.-H. Mohsenian-Rad and A. Leon-Garcia, “Optimal residential load control with price prediction in real-time electricity pricing environments,” *IEEE transactions on Smart Grid*, vol. 1, no. 2, pp. 120–133, 2010.

[31] M. A. A. Pedrasa, T. D. Spooner, and I. F. MacGill, “Coordinated scheduling of residential distributed energy resources to optimize smart home energy services,” *IEEE Transactions on Smart Grid*, vol. 1, no. 2, pp. 134–143, 2010.

[32] S. Tiptipakorn and W.-J. Lee, “A residential consumer-centered load control strategy in real-time electricity pricing environment,” in *Power Symposium, 2007. NAPS’07. 39th North American*, 2007, pp. 505–510.

[33] D. T. Nguyen and L. B. Le, “Joint optimization of electric vehicle and home energy scheduling considering user comfort preference,” *IEEE Transactions on Smart Grid*, vol. 5, no. 1, pp. 188–199, 2014.

[34] A. Belov, V. Kartak, A. Vasenev, N. Meratnia, and P. J. M. Havinga, “A hierarchical scheme for balancing user comfort and electricity consumption of tank water heaters,” in *Innovative Smart Grid Technologies Conference (ISGT), 2016 IEEE Power & Energy Society*, 2016, pp. 1–5.

[35] M. Ali, J. Jokisalo, K. Siren, A. Safdarian, and M. Lehtonen, “A User-centric Demand Response Framework for Residential Heating, Ventilation, and Air-conditioning Load Management,” *Electric Power Components and Systems*, vol. 44, no. 1, pp. 99–109, 2016.

[36] T. L. Zimmerman, S. F. Smith, and A. Unahalekhaka, “CONSERVE: Client side intelligent power scheduling,” 2011.

[37] V. Kapsalis and L. Hadellis, “Optimal operation scheduling of electric water heaters under dynamic pricing,” *Sustainable Cities and Society*, vol. 31, pp. 109–121, 2017.

[38] N. Pflugradt, J. Teuscher, B. Platzer, and W. Schufft, “Analysing low-voltage grids using a behaviour based load profile generator,” in *International Conference on Renewable Energies and Power Quality*, 2013, vol. 11, p. 5.

[39] C. Gouveia, J. Moreira, C. L. Moreira, and J. A. P. Lopes, “Coordinating storage and demand response for microgrid emergency operation,” *IEEE Trans Smart Grid*, vol. 4, no. 4, pp. 1898–1908, 2013.

[40] D. S. Management, C. Modeling, and T. W. Heaters, “Enhancing User Comfort Models for Demand Response Solutions for Domestic Water Heating Systems,” 2014.

[41] M. Ali, A. Safdarian, and M. Lehtonen, “Demand response potential of residential HVAC loads considering users preferences,” *IEEE PES Innovative Smart Grid Technologies Conference Europe*, vol. 2015-Janua, no. January, pp. 1–6, 2015, doi: 10.1109/ISGTEurope.2014.7028883.

[42] J. Xiao, J. Li, R. Boutaba, and J. W. K. Hong, “Comfort-aware home energy management under market-based Demand-Response,” *Network and service management (cnsm), 2012 8th international conference and 2012 workshop on systems virtualiztion management (svm)*, pp. 10–18, 2012.

[43] M. Motoki, M. Umeda, M. Fripp, and A. Kuh, “Approximate dynamic programming for control of a residential water heater,” in *2015 International Joint Conference on Neural Networks (IJCNN)*, Jul. 2015, pp. 1–8. doi: 10.1109/IJCNN.2015.7280735.

[44] T. T. Kim and H. V. Poor, “Scheduling power consumption with price uncertainty,” *IEEE Transactions on Smart Grid*, vol. 2, no. 3, pp. 519–527, 2011.

[45] P. Samadi, H. Mohsenian-Rad, V. W. S. Wong, and R. Schober, “Tackling the load uncertainty challenges for energy consumption scheduling in smart grid,” *IEEE Transactions on Smart Grid*, vol. 4, no. 2, pp. 1007–1016, 2013.

[46] X. Chen, T. Wei, and S. Hu, “Uncertainty-aware household appliance scheduling considering dynamic electricity pricing in smart home,” *IEEE Transactions on Smart Grid*, vol. 4, no. 2, pp. 932–941, 2013.

[47] P. Du and N. Lu, “Appliance commitment for household load scheduling,” *IEEE transactions on Smart Grid*, vol. 2, no. 2, pp. 411–419, 2011.

[48] P. Du and N. Lu, “Appliance commitment for household load scheduling,” *IEEE transactions on Smart Grid*, vol. 2, no. 2, pp. 411–419, 2011.

[49] I. Almutaz, A. Ajbar, Y. Khalid, and E. Ali, “A probabilistic forecast of water demand for a tourist and desalination dependent city: Case of Mecca, Saudi Arabia,” *Desalination*, vol. 294, pp. 53–59, 2012, doi: 10.1016/j.desal.2012.03.010.

[50] L. Paull, H. Li, and L. Chang, “A novel domestic electric water heater model for a multi-objective demand side management program,” *Electric Power Systems Research*, vol. 80, no. 12, pp. 1446–1451, 2010, doi: 10.1016/j.epsr.2010.06.013.

[51] Y.-Y. Hong, J.-K. Lin, C.-P. Wu, and C.-C. Chuang, “Multi-Objective Air-Conditioning Control Considering Fuzzy Parameters Using Immune Clonal Selection Programming,”

IEEE Transactions on Smart Grid, vol. 3, no. 4, pp. 1603–1610, 2012, doi: 10.1109/TSG.2012.2210059.

[52] J. R. Birge and F. Louveaux, *Introduction to stochastic programming*. Springer Science & Business Media, 2011.

[53] R. J. Serfling, *Approximation theorems of mathematical statistics*, vol. 162. John Wiley & Sons, 2009.

[54] A. J. Kleywegt, A. Shapiro, and T. Homem-de-Mello, "The sample average approximation method for stochastic discrete optimization," *SIAM Journal on Optimization*, vol. 12, no. 2, pp. 479–502, 2002.

[55] P. Constantopoulos, F. C. Schweppe, and R. C. Larson, "ESTIA: A real-time consumer control scheme for space conditioning usage under spot electricity pricing," *Comput Oper Res*, vol. 18, no. 8, pp. 751–765, 1991.

[56] E. L. Lawler and D. E. Wood, "Branch-and-bound methods: A survey," *Oper Res*, vol. 14, no. 4, pp. 699–719, 1966.

[57] P. Kesavan and P. I. Barton, "Generalized branch-and-cut framework for mixed-integer nonlinear optimization problems," *Computers & Chemical Engineering*, vol. 24, no. 2–7, pp. 1361–1366, 2000.

[58] M. Fischetti and A. Lodi, "Heuristics in mixed integer programming," *Wiley Encyclopedia of Operations Research and Management Science*, 2010.

[59] "DHW Event Schedule Generator | Department of Energy." https://www.energy.gov/eere/buildings/downloads/dhw-event-schedule-generator (accessed Jun. 24, 2019).

[60] D. A. Halamay, T. K. A. Brekken, A. Simmons, and S. McArthur, "Reserve Requirement Impacts of Large-Scale Integration of Wind, Solar, and Ocean Wave Power Generation," *IEEE Transactions on Sustainable Energy*, vol. 2, no. 3, pp. 321–328, Jul. 2011, doi: 10.1109/TSTE.2011.2114902.

[61] P. Denholm, M. O'Connell, G. Brinkman, and J. Jorgenson, "Overgeneration from Solar Energy in California. A Field Guide to the Duck Chart," Golden, CO (United States), Nov. 2015. doi: 10.2172/1226167.

[62] J. Olauson *et al.*, "Net load variability in Nordic countries with a highly or fully renewable power system," *Nature Energy*, vol. 1, no. 12, p. 16175, Dec. 2016, doi: 10.1038/nenergy.2016.175.

[63] L. Hirth, F. Ueckerdt, and O. Edenhofer, "Integration costs revisited – An economic framework for wind and solar variability," *Renewable Energy*, vol. 74, pp. 925–939, Feb. 2015, doi: 10.1016/J.RENENE.2014.08.065.

[64] E. Demirok, P. C. González, K. H. B. Frederiksen, D. Sera, P. Rodriguez, and R. Teodorescu, "Local Reactive Power Control Methods for Overvoltage Prevention of Distributed Solar Inverters in Low-Voltage Grids," *IEEE Journal of Photovoltaics*, vol. 1, no. 2, pp. 174–182, Oct. 2011, doi: 10.1109/JPHOTOV.2011.2174821.

[65] J. J. Shah, M. C. Nielsen, T. S. Shaffer, and R. L. Fittro, "Cost-Optimal Consumption-Aware Electric Water Heating Via Thermal Storage under Time-of-Use Pricing," *IEEE Transactions on Smart Grid*, vol. 7, no. 2, pp. 592–599, 2016, doi: 10.1109/TSG.2015.2483502.

[66] R. Diao, S. Lu, M. Elizondo, E. Mayhorn, Y. Zhang, and N. Samaan, "Electric water heater modeling and control strategies for demand response," pp. 1–8, 2012, doi: 10.1109/PESGM.2012.6345632.

[67] A. Pena-Bello, M. Burer, M. K. Patel, and D. Parra, "Optimizing PV and grid charging in combined applications to improve the profitability of residential batteries," *Journal of Energy Storage*, vol. 13, pp. 58–72, 2017, doi: 10.1016/j.est.2017.06.002.

[68] E. O'Shaughnessy, D. Cutler, K. Ardani, and R. Margolis, "Solar plus: Optimization of distributed solar PV through battery storage and dispatchable load in residential buildings," *Applied Energy*, vol. 213, pp. 11–21, Mar. 2018, doi: 10.1016/J.APENERGY.2017.12.118.

[69] F. Sossan, A. M. Kosek, S. Martinenas, M. Marinelli, and H. Bindner, "Scheduling of domestic water heater power demand for maximizing PV self-consumption using model predictive control," *2013 4th IEEE/PES Innovative Smart Grid Technologies Europe, ISGT Europe 2013*, pp. 4–8, 2013, doi: 10.1109/ISGTEurope.2013.6695317.

[70] S. Sichilalu, T. Mathaba, and X. Xia, "Optimal control of a wind–PV-hybrid powered heat pump water heater," *Applied Energy*, vol. 185, pp. 1173–1184, 2017, doi: 10.1016/j.apenergy.2015.10.072.

[71] O. De Somer, A. Soares, K. Vanthournout, F. Spiessens, T. Kuijpers, and K. Vossen, "Using reinforcement learning for demand response of domestic hot water buffers: A real-life demonstration," in *2017 IEEE PES Innovative Smart Grid Technologies Conference Europe (ISGT-Europe)*, 2017, pp. 1–7.

[72] F. Najafi and M. Fripp, "Stochastic optimization of comfort-centered model of electrical water heater using mixed integer linear programming," *Sustainable Energy Technologies and Assessments*, vol. 42, p. 100834, 2020.

[73] M. H. Albadi and E. F. El-Saadany, "A summary of demand response in electricity markets," *Electric power systems research*, vol. 78, no. 11, pp. 1989–1996, 2008.

[74] Q. Qdr, "Benefits of demand response in electricity markets and recommendations for achieving them," *US Dept. Energy, Washington, DC, USA, Tech. Rep*, vol. 2006, 2006.

[75] R. Teng and T. Yamazaki, "Load profile-based coordination of appliances in a smart home," *IEEE Transactions on Consumer Electronics*, vol. 65, no. 1, pp. 38–46, 2018.

[76] F. Najafi and M. Fripp, “Stochastic optimization of comfort-centered model of electrical water heater using mixed integer linear programming,” *Sustainable Energy Technologies and Assessments*, vol. 42, p. 100834, 2020.

[77] J. Peppanen and S. Grijalva, “Neighborhood electric vehicle charging scheduling using particle swarm optimization,” in *2014 IEEE PES General Meeting| Conference & Exposition*, 2014, pp. 1–5.

[78] M. R. V. Moghadam, R. Zhang, and R. T. B. Ma, “Demand response for contingency management via real-time pricing in smart grids,” in *2014 IEEE International Conference on Smart Grid Communications (SmartGridComm)*, 2014, pp. 632–637.

[79] Z. Ma, D. Callaway, and I. Hiskens, “Decentralized charging control for large populations of plug-in electric vehicles: Application of the Nash certainty equivalence principle,” in *2010 IEEE International Conference on Control Applications*, 2010, pp. 191–195.

[80] L. Gan, U. Topcu, and S. H. Low, “Stochastic distributed protocol for electric vehicle charging with discrete charging rate,” in *2012 IEEE Power and Energy Society General Meeting*, 2012, pp. 1–8.

[81] Y. Xu, W. Liu, and J. Gong, “Stable multi-agent-based load shedding algorithm for power systems,” *IEEE Transactions on Power Systems*, vol. 26, no. 4, pp. 2006–2014, 2011.

[82] A. de Paola, D. Angeli, and G. Strbac, “Price-based schemes for distributed coordination of flexible demand in the electricity market,” *IEEE Transactions on Smart Grid*, vol. 8, no. 6, pp. 3104–3116, 2017.

[83] L. Gan, U. Topcu, and S. H. Low, “Optimal decentralized protocol for electric vehicle charging,” *IEEE Transactions on Power Systems*, vol. 28, no. 2, pp. 940–951, 2012.

[84] A.-H. Mohsenian-Rad, V. W. S. Wong, J. Jatskevich, R. Schober, and A. Leon-Garcia, “Autonomous demand-side management based on game-theoretic energy consumption scheduling for the future smart grid,” *IEEE transactions on Smart Grid*, vol. 1, no. 3, pp. 320–331, 2010.

[85] J. Rivera, C. Goebel, and H. A. Jacobsen, “Distributed Convex Optimization for Electric Vehicle Aggregators,” *IEEE Transactions on Smart Grid*, vol. 8, no. 4, pp. 1852–1863, Jul. 2017, doi: 10.1109/TSG.2015.2509030.

[86] Z. Ma, D. S. Callaway, and I. A. Hiskens, “Decentralized charging control of large populations of plug-in electric vehicles,” *IEEE Transactions on control systems technology*, vol. 21, no. 1, pp. 67–78, 2011.

[87] P. Samadi, H. Mohsenian-Rad, R. Schober, and V. W. S. Wong, “Advanced demand side management for the future smart grid using mechanism design,” *IEEE Transactions on Smart Grid*, vol. 3, no. 3, pp. 1170–1180, 2012, doi: 10.1109/TSG.2012.2203341.

[88] A. de Paola, V. Trovato, D. Angeli, G. Strbac, and A. de Paola, "A Mean Field Game Approach for Distributed Control of Thermostatic Loads Acting in Simultaneous Energy-Frequency Response Markets."

[89] Z. Ma, D. S. Callaway, and I. A. Hiskens, "Decentralized charging control of large populations of plug-in electric vehicles," *IEEE Transactions on Control Systems Technology*, vol. 21, no. 1, pp. 67–78, 2013, doi: 10.1109/TCST.2011.2174059.

[90] L. Song, Y. Xiao, and M. van der Schaar, "Demand side management in smart grids using a repeated game framework," *IEEE Journal on Selected Areas in Communications*, vol. 32, no. 7, pp. 1412–1424, 2014.

[91] A. C. Kizilkale, S. Mannor, and P. E. Caines, "Large scale real-time bidding in the smart grid: A mean field framework," in *2012 IEEE 51st IEEE Conference on Decision and Control (CDC)*, 2012, pp. 3680–3687.

[92] A. de Paola, V. Trovato, D. Angeli, and G. Strbac, "A mean field game approach for distributed control of thermostatic loads acting in simultaneous energy-frequency response markets," *IEEE Transactions on Smart Grid*, vol. 10, no. 6, pp. 5987–5999, 2019.

[93] Z. Ma, S. Zou, L. Ran, X. Shi, and I. A. Hiskens, "Efficient decentralized coordination of large-scale plug-in electric vehicle charging," *Automatica*, vol. 69, pp. 35–47, 2016.

[94] H. Chen, Y. Li, R. H. Y. Louie, and B. Vucetic, "Autonomous demand side management based on energy consumption scheduling and instantaneous load billing: An aggregative game approach," *IEEE transactions on Smart Grid*, vol. 5, no. 4, pp. 1744–1754, 2014.

[95] A. Papavasiliou, S. S. Oren, and R. P. O'Neill, "Reserve requirements for wind power integration: A scenario-based stochastic programming framework," *IEEE Transactions on Power Systems*, vol. 26, no. 4, pp. 2197–2206, 2011.

[96] F. Gul and E. Stacchetti, "Walrasian equilibrium with gross substitutes," *Journal of Economic theory*, vol. 87, no. 1, pp. 95–124, 1999.

[97] G. B. Dantzig and P. Wolfe, "The decomposition algorithm for linear programs," *Econometrica: Journal of the Econometric Society*, pp. 767–778, 1961.

[98] G. Dantzig, *Linear programming and extensions*. Princeton university press, 2016.

[99] P. Beraldi, D. Conforti, C. Triki, and A. Violi, "Constrained auction clearing in the Italian electricity market," *Quarterly Journal of the Belgian, French and Italian Operations Research Societies*, vol. 2, no. 1, pp. 35–51, 2004.

[100] T. Alvey, D. Goodwin, X. Ma, D. Streiffert, and D. Sun, "A security-constrained bid-clearing system for the New Zealand wholesale electricity market," *IEEE Transactions on power systems*, vol. 13, no. 2, pp. 340–346, 1998.

[101] L. Wu, M. Shahidehpour, and T. Li, "Stochastic security-constrained unit commitment," *IEEE Transactions on power systems*, vol. 22, no. 2, pp. 800–811, 2007.

[102] M. Shahidehopour and Y. Fu, “Benders decomposition: applying Benders decomposition to power systems,” *IEEE Power and Energy Magazine*, vol. 3, no. 2, pp. 20–21, 2005.

[103] E. Ela and M. O’Malley, “Probability-weighted LMP and RCP for Day-ahead energy markets using stochastic security-constrained unit commitment,” 2012.

[104] A. Papavasiliou and S. S. Oren, “Multiarea stochastic unit commitment for high wind penetration in a transmission constrained network,” *Oper Res*, vol. 61, no. 3, pp. 578–592, 2013.

[105] F. D. Galiana, F. Bouffard, J. M. Arroyo, and J. F. Restrepo, “Scheduling and pricing of coupled energy and primary, secondary, and tertiary reserves,” *Proceedings of the IEEE*, vol. 93, no. 11, pp. 1970–1983, 2005.

[106] P. Wentges, “Weighted Dantzig-Wolfe decomposition for linear mixed-integer programming,” *International Transactions in Operational Research*, vol. 4, no. 2, pp. 151–162, 1997.

[107] M. E. Lübbecke and J. Desrosiers, “Selected topics in column generation,” *Oper Res*, vol. 53, no. 6, pp. 1007–1023, 2005.

[108] A. Grothey, “Decomposition methods for nonlinear nonconvex optimization problems,” Citeseer, 2001.

[109] M. C. Bozchalui, S. A. Hashmi, H. Hassen, C. A. Canizares, and K. Bhattacharya, “Optimal Operation of Residential Energy Hubs in Smart Grids,” vol. 3, no. 4, pp. 1755–1766, doi: 10.1109/TSG.2012.2212032.